12-15-2007

Dielectrophoretic characterization of ABO blood type, frequency and AC field strength of erythrocytes

Prashant Reuben Daggolu

DIELECTROPHORETIC CHARACTERIZATION OF ABO BLOOD TYPE, FREQUENCY AND AC FIELD STRENGTH OF ERYTHROCYTES

By

Prashant Reuben Daggolu

A Thesis
Submitted to the Faculty of
Mississippi State University
in Partial Fulfillment of the Requirements
for the Degree of Master of Science
in Chemical Engineering
in the Dave C. Swalm School of Chemical Engineering

Mississippi State, Mississippi

December 2007

DIELECTROPHORETIC CHARACTERIZATION OF ABO BLOOD TYPE,

FREQUENCY AND AC FIELD STRENGTH OF

ERYTHROCYTES

By

Prashant Reuben Daggolu

Approved:

_____	_____
Adrienne R. Minerick Assistant Professor of Chemical Engineering (Director of Thesis and Major Professor)	Mark Bricka Associate Professor of Chemical Engineering (Committee Member)
_____	_____
Bill Elmore Hunter Henry Chair, Associate Professor of Chemical Engineering (Committee Member)	Shane C. Burgess Director Life Sciences & Biotechnology Institute (Committee Member)
_____	_____
Rudy E. Rogers Professor / Graduate Co-coordinator Of Dave C. Swalm School of Chemical Engineering.	Glenn Steele Dean of James Worth Bagley College of Engineering

Name: Prashant R. Daggolu

Date of Degree: December 14, 2007

Institution: Mississippi State University

Major Field: Chemical Engineering

Major Professor and Director of Thesis: Dr. Adrienne R. Minerick.

Title of Study: DIELECTROPHORETIC CHARACTERIZATION OF ABO BLOOD TYPE, FREQUENCY AND AC FIELD STRENGTH OF ERYTHROCYTES

Pages in Study: 160

Candidate for degree of Master of Science

This research investigates the role of ABO blood type of erythrocytes in their dielectrophoretic response. The dielectrophoresis of erythrocytes of positive ABO blood types was studied at 5 V (peak to peak) and 1 MHz frequency AC field. The study revealed that the ABO blood type had an influence on the dielectrophoretic motion of the erythrocytes, particularly separating AB+ and O+ blood types. This is of particular significance since AB+ is a universal acceptor and O+ is a universal donor for blood transfusion purposes. The influence of field parameters, namely field strength and frequency of the AC field, was also studied for erythrocytes of positive ABO blood types. This research revealed that erythrocytes of each blood type respond differently at various frequencies and field strengths.

DEDICATION

I would like to dedicate this work to my mother Bharathi and father Francis Daggolu whose support and encouragement was of utmost importance during the course of this study. Also, I would like to extend this dedication to my brother Benjamin and sister Jerusha.

ACKNOWLEDGEMENTS

I would like to thank Dr. Adrienne Minerick, my major advisor for her valuable advice and guidance throughout this research work, I would like to thank Dr. Mark Bricka, Dr. Bill Elmore and Dr. Shane Burgess for their timely suggestions and also for serving on my committee.

I would like to thank *Longest Student Health Center* for supplying blood samples from volunteers necessary for this research. I would like to gratefully acknowledge all the volunteers who participated in this research by donating their blood.

TABLE OF CONTENTS

LIST OF TABLES

TABLE

LIST OF FIGURES

FIGURE

CHAPTER 1

INTRODUCTION

The rise of electrokinetics over the past decade as a separation technique has opened doors to new methods of quantitative analysis in medical applications. Dielectrophoresis , a subset of electrokinetics, shows potential as a useful tool in developing inexpensive, easy-to-use medical microdevices capable of streamlining emergency medical diagnosis. Blood typing is a simple, yet life-essential, diagnostic step needed in major emergency medical situations. This is because a blood donor's blood type must match the receiver's blood type or adverse immune responses can cause death in the recipient . After accidents, natural disasters, wars and terror attacks, blood transfusions comprise an essential and important facet of stabilizing victims and saving lives. Current blood typing technologies require a clinical environment, antibody assays for each blood type, and medical technological methodologies which are not portable to the site of an emergency [1]. This work analyzes a novel technique of using dielectrophoresis as a tool for distinguishing the positive blood types of the ABO blood type system (A+, B+, AB+, O+). A major portion of this chapter will be submitted for publication [2].

1.1 Human Blood

Blood is a highly specialized fluid connecting all the biological processes of the human body. It carries oxygen from lungs, nourishment from digestion, hormones to the body and disease fighting cells for the health of the body [3]. Blood is a fluid suspension with various components such as erythrocytes, white blood cells, platelets and plasma. Normally, 7-8% of the body weight is comprised of blood [4]. There is about 6 – 8 liters of blood in a normal adult [5].

1.1.1 Erythrocytes

Erythrocytes (Figure 1.1) are the most abundant cells comprising whole blood and in healthy individuals comprise 42 – 54% of the blood volume for adult males [6]. Their main function is to bind and carry oxygen from the lungs to the tissues in the body and remove CO_2 from the tissues for release in the lungs. The membrane of erythrocytes is composed mainly of proteins, lipids and polysaccharides. Erythrocytes are manufactured in bone marrow, do not have a nucleus, and have a life span of approximately 120 days in the human body [7]. These 6-8 microns diameter cells are biconcave in shape to maximize surface area for gas (O_2 and CO_2) transport across their membrane to the interior hemoglobin protein, which transiently binds the gases.

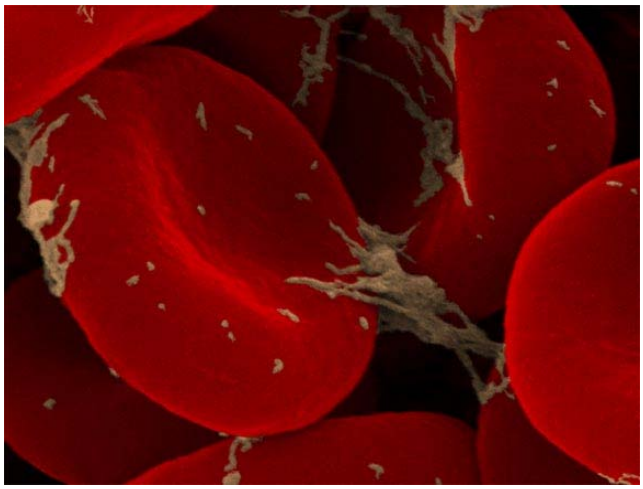

Figure 1.1 Scanning electron microscopy (SEM) images of Erythrocytes at 11000 times magnification [8]

1.1.2 Blood typing

There are 29 established blood typing systems [9]. These were discovered based on the relevance of the blood type to a specialized application. For example, ABO blood type is relevant to blood transfusion, and an improper transfusion based on ABO blood type could be fatal. Therefore, this system is the most important and widely applicable system. The present work limits its scope to ABO blood type system since the motivation for the work presented here is to develop science which could ultimately lead to a device for performing blood typing instantaneously for blood transfusion purposes.

1.1.3 ABO blood typing system

The ABO blood typing system is the most prominent of the blood typing systems due to its application in blood transfusion. An ABO incompatible transfusion could lead to intravascular hemolytic reactions which are among the top causes of transfusion related fatalities [10]. The ABO blood type system was discovered by Karl Landsteiner in 1901 while investigating the cause for blood transfusion fatalities [11]. He was awarded the Nobel Prize in Medicine in 1930.

In the ABO blood type system, there are three types of antigens which result in eight combinations of antigen expression on erythrocyte surfaces [12]. The A and B antigen differ by the type of modification made to an acceptor glycoconjugate, H glycoconjugate found on cell surface glycoproteins and glycol lipids [12, 13]. The A antigen terminates in an α 1,3–linked N-acetylgalactosamine while the B antigen terminates in an α 1,3–linked terminal galactose [14, 15]. O type blood cells have neither modification to the H glycoconjugate. According to the ABO blood typing system, there are 4 base blood types (Figure 1.2), A, B, O and AB, which is simultaneously shown in Table 1.1. The presence or absence of a third antigen, termed the Rhesus (Rh) factor, determines the positive and negative blood types [14]. The blood type is assigned a "+" or a "-"sign based on Rh presence or absence respectively. Also, there are complimentary antibodies in the blood plasma (A and B antibodies) which are the recognition helpers of the immune system. The antibody A is present in B type blood type plasma (both + and -) and antibody B is present in A blood type plasma (both + and -). O blood type plasma has both antibodies, and AB

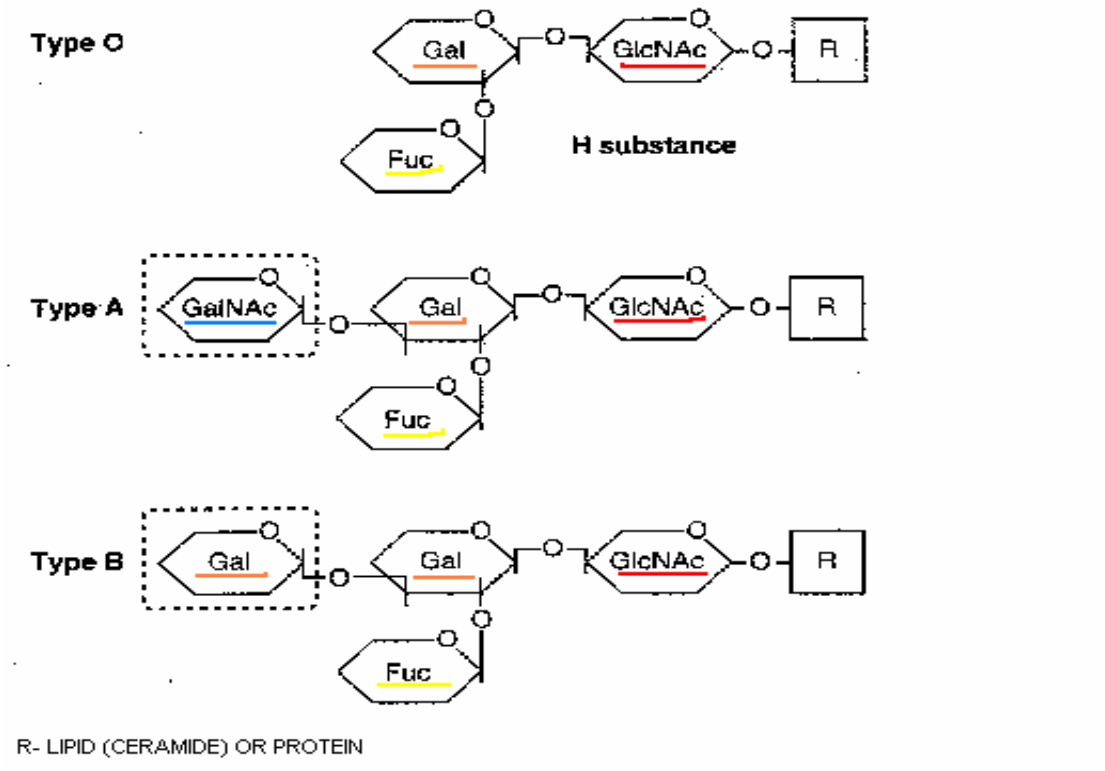

Figure 1.2 ABO antigen structures [15]

Table 1.1 Details of the ABO blood type system

Blood Type	Antigen	Antibody	Rh Antigen
A+	A	B	+
AB+	A,B	None	+
B+	B	A	+
O+	None	A,B	+
A-	A	B	-
AB-	A,B	None	-
B-	B	A	-
O-	None	A,B	-

has none. Since antibodies are free in the surrounding blood plasma and not bound to the cell surface, it is assumed that they do not affect dielectrophoretic-erythrocyte response and are neglected.

An inaccurate blood transfusion could be fatal due to blood coagulation. The blood of A type has anti – B antibodies in its serum, and blood of B type has anti- A antibodies in the serum. Hence, if an incompatible transfusion is done, the antibodies attack the antigen and blood coagulates [17]. While this is matter of concern during Blood transfusion, this attribute becomes useful when performing laboratory blood typing test.

Blood typing tests are performed in three steps. The first step is called 'ABO typing'. In this step, the whole blood from the sample is put in two wells, one containing anti-A and one containing anti-B antibodies [18]. If the blood coagulates in one of those wells then the blood is of corresponding type. If the blood does not coagulate in any of those wells then it is O type. The second step of blood typing is

called ‘back typing’. In this step, the serum of the sample blood is mixed with A and B type blood separately. This step helps in determining the blood type more accurately. In the final step, the sample blood is mixed with the blood of the same ABO type in the presence or absence of the Rhesus factor. This helps in determining the positive or negative blood type. If the blood coagulates with the Rhesus factor, then it is negative blood type; otherwise, it is positive [19, 20]. Based on the blood type which is determined with the above procedure, a proper blood transfusion is done. Table 1.2 illustrates ABO compatible blood transfusions [21]. The table also illustrates the occurrence of the blood types worldwide.

1.1.4 Other blood typing systems

As stated previously, there are 29 blood typing systems, which are summarized in table 1.3 [22]. These have various applications based on the antigens selected for demarcation of the blood type.

One of the important blood type systems other than the ABO system is the P blood type system. Landsteiner [23] and Levine et al [24] were the first to perform these experiments in the 1920s. This system is characterized by 3 different antigens. Five different blood types arise due to a combination of these antigens given in Table 1.4 [25].

The P blood type system has clinical significance. All the P antigens are modifications of a glycosphingolipid which are molecules resembling sphingomyelin,

Table 1.2 ABO compatible blood transfusions and the percentage occurrences of each ABO blood type worldwide

ABO blood type	% Occurrence	Can donate erythrocytes to:	Can receive erythrocytes from:
A+	34.3%	A+, AB+	A+,A-,O+,O-
A-	5.7%	A-.A+,AB-,AB+	A-,O-
B+	8.6%	B+,AB+	B+,B-,O+,O-
B-	1.7%	B+,B-,AB+,AB-	B-,O-
AB+	4.3%	AB+	ALL TYPES
AB-	0.7%	AB-,AB+	AB-,A-,B-,O-
O+	38.5%	O+, A+, AB+, AB+	O+,O-
O-	6.5%	ALL TYPES	O-

Table 1.3 Details of the 29 known blood type systems

Serial No.	Blood type	Symbol	Genes
1	ABO	ABO	ABO
2	MNS	MNS	GYPA,GYPB,GYPE
3	P	P1	
4	Rh	RH	RHD, RHCE
5	Lutheran	LU	LU
6	Kell	KEL	KEL
7	Lewis	LE	FUT3
8	Duffy	FY	DARC
9	Kidd	JK	SLC14A1
10	Diego	DI	SLC4A1
11	Yt	YT	ACHE
12	Xg	XG	XG, MIC2
13	Scianna	SC	ERMAP
14	Dombrock	DO	ART4
15	Colton	CO	AQP1
16	Landsteiner – Weiner	LW	ICAM4
17	Chido/Rodgers	CH?RG	C4A, C4B
18	H	H	FUT1
19	Kx	XK	XK
20	Gerbich	GE	GYPC
21	Cromer	CROM	CD55
22	Knops	KN	CR1
23	Indian	In	CD44
24	Ok	OK	BSG
25	Raph	RAPH	CD151
26	John Milton Hagen	JMH	SEMA7A
27	I	I	GCNT2
28	Globoside	GLOB	B3GALT3
29	Gill	GIL	AQP3

Table 1.4 P Blood type system: details of antigens in each type of the system.

Blood type	Antigen	Antibody
P_1	P_1,P,P^k	None
P_2	P, P^k	Anti – P_1
P^k_1	P_1, P^k	Anti – P
P^k_2	P^k	Anti – P_1, anti – P
P	None	Anti – P_1, anti – P, anti – P^k

but they have a sugar residue in place of a choline group [26]. Due to this, the P blood type system plays a role in susceptibility of a patient to infectious disease since some pathogens use glycosphingolipids as receptors [27]. Glycosphingolipids also act as coreceptors for Human Immuno Deficiency Virus (HIV) to enter the affected cell [28, 29]. This has lead to research into the possibility of using P^k analogues to inhibit HIV infection [30]. Parovirus B19 uses the P antigen as a co receptor for attacking the affected cells [31]. Parovirus B19 causes erythema infectiosum. Also this can cause serious problems in sickle cell anemia disease or chronic anemia diseases patients who are immuno compromised [32].

As seen from above, there are other blood types which are also quite significant but they do not have a significant role in blood transfusion. Hence keeping in view the ultimate goal of designing a medical microdevice for blood typing during

blood transfusion, the dielectrophoretic response of erythrocytes of only ABO blood type system was studied.

1.1.5. Properties of erythrocytes

Erythrocytes have a net negative charge based on their conventional linear electrophoretic behavior [9]. However, the surface charge of erythrocytes rapidly decreases if the blood is stored more than 6 days. Cell rigidity also increases over this time span, which could be related to the surface charge phenomena [33]. Blood age as well as the storage container can also influence its properties. It was found that hemolysis was less in cells stored in di (2-ethyl) hexylpthlate (DEHP) plasticized bags than in butryltrihexylcitrate (BTHC) plasticized bags [34].

1.2 Microdevices

Microdevices are devices which have components of micrometer scales. The use of microdevices is varied from applications in microelectromechanical systems (MEMS) to microfluidic, lab-on-a-chip devices for DNA analysis and cellular testing [35]. Microdevice design varies based on the application. The particular dielectrophoretic microdevice design used in this work was based on the microdevice fabricated for studying erythrocyte pearl chain formations by *Minerick et al* [36]. This microdevice has a perpendicular arrangement of 100 μm platinum electrodes in a hybriwell chamber secured to a microscope slide. Several other designs have also

been studied including spiral arrangement of electrodes for cell separations [37], interdigitated micro arrays [38, 39], pyramidal microdevice [40], trapezoidal electrode arrays [41], multi phase electrodes [42] and checker board arrangements of electrodes [43]. Microdevices in various forms are being developed to make complicated multi-step biological analysis simpler [44]. They are being developed into biosensors in conjunction with dielectrophoresis [45]. Microdevices have been designed for many applications involving bioparticle separations due to low sample sizes required in such devices and low costs [46 - 50]. Also the rise of new technology for implanting the electrodes in these devices both on a micro and nano scale has made it easier to make these devices [51, 52].

The use of medical microdevices could lead to inexpensive medical kits that can perform a variety of medical tests such as blood typing, pathogen detection and quantification to monitor blood diseases, efficacy of medicinal drugs and other medical diagnostic related procedures. Equipment used to perform medical tests like a standard hematology pane, which includes hematocrits (erythrocyte, platelet and white blood cell count), electrolyte balance, hemoglobin, etc., range from $5,500 to $9,500 [53]. Other tests like CD4, which tests for HIV, rely on flow cytometers that can cost from $30,000 to $150,000 [54]. The fees for individual tests on medical laboratory cytometers are above $50, with medical costs rising annually [55]. In contrast, the cost of microdevices is quite low. As manufacturing of microdevices is scaled up, the price per device drops and is expected to cost less than $6 each [56].

These microdevices could also find applications in identifying and quantifying the progression of acute as well as chronic diseases.

One example of a chronic disease is sickle cell anemia which affects 1 in 500 African Americans (1 in 12 carrying the sickle cell trait) [57, 58]. Diagnosis of sickle cell anemia requires over 4 ml of blood and is accomplished via linear gel electrophoresis. This requires a dedicated technician for over one hour in a medical laboratory and ranges in price from $69 - $175 each [59, 60]. From the patient's perspective, it takes 3 to 5 days to get results back from this test. Furthermore, the loss of 4 ml of blood exacerbates the patient's anemia. Medical microdevices can improve upon this by enabling point of care testing in less than 5 minutes, with only few drops of blood (~62 μl) while simultaneously eliminating technician error [61]. As sensitivity in these devices improves, quantitative output (as opposed to just positive or negative results) becomes possible; they have the potential to not only act as diagnostic tools, but also as monitoring devices for disease management. Specialized microdevices ideally will be user-friendly, rapid and cost effective diagnosis kits for a wide variety of medical applications.

The development of such medical microdevices requires employing techniques which need only small sample amounts to give quantitative results. They would also require methods which are easy to perform and do not require a skilled technician. Hence, dielectrophoresis becomes a potential technique for use in these devices due to operational simplicity and the requirement of just a few micro liters (62 micro liters) of blood for analysis.

Unlike conventional electrophoresis, dielectrophoresis employs AC electric fields which are much more suitable for biomedical applications due to reduced specimen sample sizes required. Also, this phenomenon utilizes the polarizability of particles. Hence, it is reasonable to expect that dielectrophoresis would play a major role in development of medical microdevices.

1.3 Dielectrophoresis

1.3.1 Theory

Dielectrophoresis is a phenomenon which results in movement of polarizable particles in a nonuniform AC electric field. The movement is due to a net force, F_{DEP}, resulting from transient polarization of particles [62] in a non-uniform electric field [63]:

$$F_{DEP} = 2\pi r^3 \varepsilon_m \alpha \nabla E^2 \tag{1.1}$$

The radius of the particle is denoted by r; ε_m is the medium permittivity; α is the real part of a frequency factor (termed the Clausius-Mossotti factor) and E is the electric field strength. It is useful to note that the force a particle experiences scales nonlinearly due to the electric field. The effective polarizability of the particle in a

suspending medium relative to the particles is given by 'α'. This is Clausius-Mossotti factor is frequency dependent and given by the following relation:

$$\alpha = \mathrm{Re}\left\{\frac{\tilde{\varepsilon}_p - \tilde{\varepsilon}_m}{\tilde{\varepsilon}_p + 2\tilde{\varepsilon}_m}\right\} \tag{1.2}$$

$\tilde{\varepsilon}$ denotes complex permittivity and the subscripts p and m denote particle and medium respectively. The complex permittivity $\tilde{\varepsilon}$ is given by $\tilde{\varepsilon} = \varepsilon - i\sigma/\omega$. The complex permittivity is a function of polarizability ε, electrical conductivity of the medium σ and the frequency of the field ω. The imaginary part (iσ/ω) is out of phase with the dielectrophoretic field and hence only the real part accounts for dielectrophoretic force.

Equation 1.1 is a generalized equation for dielectrophoretic force on spherical, homogenous particles. Cells are nonhomogenous complex biochemical entities with nonuniform distribution of insulating and conducting components. Hence, equation 1.1 can be seen as a reasonable approximation of the dielectrophoretic force on erythrocytes, but not a precise relation. Analytical dielectric modeling has been done to interpret the movement of biological cells in electric fields using either spheres or ellipses as approximations for their shapes [12]. However, erythrocytes are biconcave exhibiting a much more complicated geometry than can currently be solved analytically. This is an important area for improvement because it was shown that

correct cell geometrical parameters are critical for understanding permittivity of cell suspensions [13, 64, 65].

1.3.2. Types of dielectrophoresis

Transient polarization of particles results in their movement in an electric field that scales between two extremes depending on the exciting AC frequency. Herbert Pohl, in *Dielectrophoresis,* defined these two phenomenological extremes: positive dielectrophoresis and negative dielectrophoresis [63]. These two cases arise as a consequence of the polarizability of a uniform composition particle being greater or lesser than the polarizability of the medium in which it is suspended. If the polarizability of the particle is greater than that of the medium, then the electric field lines pass through the particle causing a polarization. A resultant force directs the particle to high electric field regions; this observed movement is positive dielectrophoresis. If the polarizability of the particle is less than that of the medium in which it is suspended, electric field lines divert around the outside of the particle causing an ion depletion at the particle poles and subsequent polarization. The resulting force directs the particle to the low field electrode and this is termed negative dielectrophoresis [59, 60]. However, various cell species demonstrate more complicated responses to the dielectrophoretic field due to their nonhomogenous structure and charge distribution [36]. This work examines these more complicated responses with a medically relevant system: erythrocytes expressing ABO blood type antigens.

1.3.3 Uses of dielectrophoresis

Dielectrophoresis has been studied in detail by researchers over last 20 years. In particular, the phenomenon was studied with regards to erythrocytes [39]; it was observed that A+ erythrocytes form pearl chains in a dielectrophoretic field. Dielectrophoresis is also studied to differentiate normal cells from leukemia cells [66], metastatic breast cancer cells [67] and malaria-infected cells [68]. Using a spiral electrode configuration, the dielectrophoretic movement of cells based on health was studied, and malarial cells were separated from healthy cells [38]. Dielectrophoresis has also been used to separate white blood cells from erythrocytes [63] and sample preparation for chip based hybridization assays in an integrated DNA/RNA system [39]. Furthermore, a special technique known as dielectrophoretic field flow fractionation was used to study differential analysis of human leukocytes [69]. Dielectrophoresis has been used in determining drug sensitivity [70 – 73], fusion of cells [74] and studying cardio myocyte hypertrophy [75]. This electrokinetics tool has also started to influence not only analysis of diseased cells but also detection of diseases like oral cancer [76]. Biophysical characteristics of membrane and cytoplasm of apoptotic cells [77] and multi-drug resistance were studied using dielectrophoresis [78]. Dielectrophoresis was found useful to study responses of cells to toxicants [79], concentrations of bacteria [80] and viruses [25] in solutions.

Dielectrophoresis has already become quite useful in analyzing medical samples, particularly for research purposes [81]. It was also used for nonbiological applications in colloid science. For example, dielectrophoresis was used in making

Au/aniline polymeric pairs [82, 83], separation of colloid polystyrene particles [84]. By tuning the frequency of the AC field, the nanoparticles can be manipulated using dielectrophoresis [85-88].

1.3.4 Derivation of dielectrophoretic force

Dielectrophoretic force causes the cells to move in a nonuniform AC field. This movement is mainly due to electric field strength, volume of the particle and frequency dependent Clausius-Mossotti factor. The dielectrophoretic force equation can be derived from the basic principles of electricity and dielectrics. The derivation was performed by Herbert Pohl and is presented below [62].

To do this, consider a particle of dipole moment 'p' which is separated by a distance 'l'. The dipole moment p is equivalent to a pair of charges +q and –q. Then, in accordance with the definition of dipole moment [62],

$$p = ql \tag{1.3}$$

The force exerted on the negative charge at the position r_- by the force E_e is $F_- = -qE_e(r_-)$. Similarly, the force exerted on the positive charge at the position r_+ by the force E_e is $F_+ = qE_e(r_+)$ (see Figure 1.3)[62].

Assume that the dipole is aligned in the +z direction. The field can be expressed in a Taylor's series expansion as [62]

$$E_e(r_+) = E_e(r_-) + l\frac{\partial E_e}{\partial z} + higher\ order\ terms \tag{1.4}$$

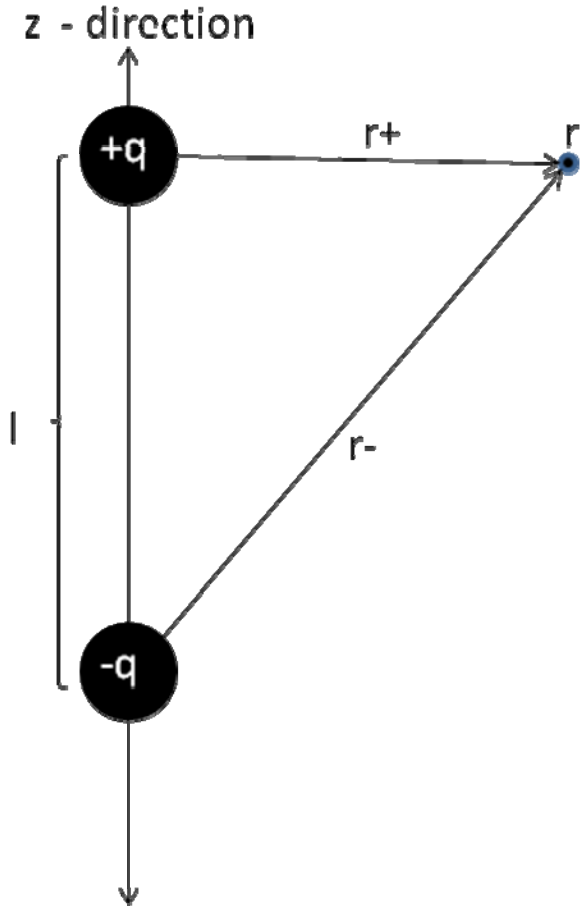

Figure 1.3 Pair of electric dipole charges aligned in z direction shown along with radius vectors

Since erythrocytes are about 7 microns in diameter, for such small dipoles, the higher order terms can be neglected. Hence,

$$F = F_{-} + F_{+} = q(E_{e+} - E_{e-}) = lq\frac{\partial E_e}{\partial z} = (p_z \frac{\partial}{\partial z})E_e \quad (1.5)$$

The above force expression is only for the case when dipole is oriented in a z direction. The expression of force in any direction can be recognized to be of the following form from the last term of the above expression. Including all the 3 dimensions,

$$F = (p_x \frac{\partial}{\partial x} + p_u \frac{\partial}{\partial y} + p_z \frac{\partial}{\partial z})E_e = (p \bullet \nabla)E_e \quad (1.6)$$

The expression $(p \bullet \nabla)E_e$ can be evaluated using the following well known vector equation [62].

$$(A \bullet \nabla)B = \nabla(A \bullet B) - (B \bullet \nabla)A - A \times (\nabla \times B) - B \times (\nabla \times A)$$

Hence,

$$(p \bullet \nabla)E_e = \nabla(p \bullet E_e) - (E_e \bullet \nabla)p - p \times (\nabla \times E_e) - E_e \times (\nabla \times p) \quad (1.7)$$

$\nabla \times E_e$ is called the 'Curl' of the electric field and it is equal to zero in the absence of a changing magnetic field. Hence $p \times \nabla \times E_e$ in Equation 1.7 is 0.

$$F = (p \bullet \nabla)E_e = \nabla(p \bullet E_e) - (E \bullet \nabla)p - (E_e \times (\nabla \times p)$$

(1.87

Since $p=\alpha E_e v$ [62],

$$F = \alpha(E_e \bullet \nabla)E_e v = (\alpha \nabla \left|E_e\right|^2 - \alpha(E_e \bullet \nabla)E_e - \alpha(E_e \times (\nabla \times E_e))v \quad (1.8)$$

Since $\nabla \times E_e = 0$,

$$F = \alpha(E_e \bullet \nabla)E_e v = (\alpha \nabla |E_e|^2 - \alpha(E_e \bullet \nabla)E_e)v$$

The above equation can be simplified to

$$F = \frac{1}{2} \alpha v \nabla |E_e|^2 \quad (1.9)$$

As seen from v in the above equation, the dielectrophoretic force depends upon the shape of the cell, or precisely, its volume. Generally, a sphere has been used to model the dielectrophoretic force for biological cells. Dielectrophoretic force equation for erythrocyte geometry is presented below.

Specific dielectrophoretic force equation for erythrocytes id presented here. Assume erythrocyte to be a sphere of radius 'r'. From standard text books [62], the induced moment, μ, for spherical particles due to external electric field, E_e, is given by:

$$\mu = 4\pi r^3 \varepsilon_m \alpha E_e = (\alpha v) E_e \quad (1.10)$$

Where ε_m, α, E_e are defined as before.

Canceling E_e and α,

$$v = 4\pi r^3 \varepsilon_m \quad (1.11)$$

Substituting this expression for volume of sphere into the generalized dielectrophoretic force equation (1.9),

$$F_{DEP} = 2\pi r^3 \varepsilon_m \alpha \nabla E_e^2 \quad (1.12)$$

While the dielectrophoretic force expression for spherical particles is less complicated, it is not accurate for erythrocytes. Erythrocytes are biconcave in shape with a slight depression in the center. They are 6 – 8 microns in diameter. If the average is taken to be 7 microns, then the spherical volume of the cell would be 179.5 cubic microns.

The spherical volume is calculated using the following equation:

$$V_s = \frac{4}{3}\pi r^3 \tag{1.13}$$

where V_s is the volume of sphere and r is its radius.

The mean cell volume of erythrocytes for a normal adult is considered to be 86 – 98 femtoliters (or cubic micrometers) a difference of volume of 81.5 - 93.5 cubic micrometers[89]. Hence the error in the force by taking spherical approximation is high. Another approach is taken for the calculation of dielectrophoretic force for erythrocytes and that is by approximating them to a torus. This is a better approximation of an erythrocyte than to that of a sphere because erythrocytes have a depression in the center which can be compared to the hole in the center of a torus and the biconcave nature of the erythrocyte to the bulged nature of the torus.

The volume of the torus is given by [90]:

$$V_t = 2\pi^2 Rr^2 \tag{1.14}$$

Where 'R' is the distance from the center of the torus to the center of the tube. and 'r' is the distance from the center of the tube to the outer edge of the tube.

In the case of the erythrocyte (R+r) = 3.5 microns, since the diameter is 7 microns. Then if R is set as 2 and the r as 1.5 then the volume of the torus is 88.73 cubic microns which is in the range of normal mean cell volume for adults. Also, these values would mean a center hole radius of just 0.5 microns.

Then for this geometry, the induced moment is given by the following equation,

$$\mu = (\alpha v)E_e = 6\pi^2 Rr^2 \varepsilon_m \alpha E_e \tag{1.15}$$

Substituting the above expression for volume in the generalized force equation (1.9),

$$F_{DEP} = 3\pi^2 Rr^2 \alpha \nabla E^2 \tag{1.16}$$

Equation 1.16 shows that the dielectrophoretic force of erythrocytes depend not only their outer radius but also the radius of their central depression. This equation represents a better approximation to the force equation based on a spherical geometry of erythrocytes.

1.4 Conclusion

This chapter discussed the benefits of dielectrophoresis, its use in microdevices for analytical purpose. Further discussion was done on the details of human blood with particular emphasis on ABO blood typing system. It was described how the present method of blood typing was lab centered and required trained personnel to perform it. It was shown in this chapter that a blood typing device based on dielectrophoresis could increase the convenience and decrease the cost of blood typing.

CHAPTER 2

PROJECT OVERVIEW

2.1 Project objectives

The main goal of the project is to develop and quantify the phenomenological dielectrophoretic response which would aid in manufacturing an electronic, easy-to-use blood typing instrument. Dielectrophoresis, due to its ability to detect slight changes in the properties of biological cells, its mild harmless force to the cells, and its already established applications in medical and biological analysis was chosen as a phenomenon to be studied for use in blood typing instrument. The dielectrophoretic behavior of the erythrocytes of the positive blood types (A+, B+, AB+ and O+) was studied. For all the studies conducted, the vertical and horizontal movement of erythrocytes in the electric field was analyzed. The specific objectives of the project are listed below.

- Study the dielectrophoresis of erythrocytes of positive blood types at 0, 20, 30, 50, 60, 90 and 120 seconds after field application. The field strength was maintained at 0.025 V_{pp} (volts peak to peak)/micron and frequency of the field was maintained at 1 MHz.

- Conduct the above experiments with the same blood on 3 different days. Experiments were conducted on days 0, 2 and 5. The experiments were repeated twice with fresh blood each time.
- Perform statistical analysis on the data to understand the significance of the vertical and horizontal movements of the cells.
- Perform regression analysis on the data to understand the trend of the behavior of the cells with time in the electric field.

- Study the dielectrophoresis of the blood types with field. The frequencies that were tested were 0.5, 1, 2, 3, 4 and 5 MHz. The field strength was maintained at 0.03 Vpp/micron. The experiments were repeated 3 times with fresh blood each time.
  - Perform statistical analysis of the data to analyze the effect of frequency on the dielectrophoresis of the erythrocytes.
- Study the influence of the electric field strength on the dielectrophoresis of erythrocytes.
  - Reproduce the above experiments 3 times at comparable field strengths, when possible.
  - Perform the least squares fit on the data obtained in order to understand the general trend of the dielectrophoretic movements of the erythrocytes with an increase in field strength.
- Simulate the dielectrophoretic field using COMSOL Multiphysics™ software to understand the effect of electrode shape on the electric field density

distribution. The field was simulated for 2 different distances between the electrodes and 3 different geometries of the electrode.

2.2 Project structure

In order to realize the objectives stated in the previous section, the project was structured as shown in the block diagram in Figures 2.1, 2.2 and 2.3. The main steps included design of experiments, experimentation, data analysis and statistical analysis.

2.3 Project hypothesis and experimental matrix

The main hypotheses are listed below and further explained in this section:

- Blood type antigens impact the dielectrophoresis of erythrocytes.
- Change in frequency of the AC field impacts the dielectrophoresis of erythrocytes based on their ABO blood type.
- Change in AC field strength impacts the dielectrophoresis of erythrocytes based on their ABO blood type.

The main objective of the study is to understand the effect of blood type of the erythrocytes on their dielectrophoretic movement. This was done by studying three main factors that could influence the dielectrophoresis. The first parameter studied is

Table 2.1 Project structure

STAGE NAME	MAJOR TASK	COMMENTS
I BACKGROUND WORK	1. Prepare Phosphate Buffer Saline (PBS) solution 2. Setup the AXIOCAM 4.0 to analyze image 3. Develop MATLAB program for analyzing the movement of erythrocytes 4. Develop experimental matrix for different studies	
II EXPERIMENTATION	1. Collection and storage of whole blood 2. Prepare the blood solution and rinse the microdevices 3. Load microdevice with blood solution and place it on the microscope table 4. Program the waveform generator to give 1MHz AC current for blood typing experiments 5. Adjust the voltage of the current from the waveform generator such that the field strength is 0.025 V_{pp}/micron 6. Run the experiment at specified parameters while video microscopy records images of cell movement	• Experiments were performed on days 0, 2, 5. • Frequency dependency was tested at 0.5,1,2,3,4,5 MHz • Field dependency was tested between 0.02 and 0.08 V_{pp}/micron • Video recorded every 10 seconds for 4 minutes.
III DATA ANALYSIS	1. Perform Image analysis using AXIOCAM 4.5 to give X/Y position of all the cells on each image 2. Process X/Y data using the developed MATLAB program to analyze the movement of cells 3. Simulate Dielectrophoretic field.	Images analyzed were those only at 0, 20, 50, 60, 90 and 120 seconds after field application
IV STATISTICAL ANALYSIS	1. Process data using EXCEL to calculate Averages and standard errors 2. Analysis of variance and multiple comparisons were performed on the data using SAS	

time, the time dependency of the hypothesis postulated was that the dielectrophoresis of erythrocytes. This section of research was called dielectrophoretic Blood typing.

each of the positive ABO blood types. The main This is discussed extensively in chapter 3 of this thesis. In this part of the work, the extent of dielectrophoretic movement of the erythrocytes with time was studied for ABO blood type antigen would impact the movement of erythrocytes in a dielectrophoretic field. This is because it is already shown in literature that dielectrophoresis can differentiate cells based on their biological properties. This was discussed in section 1.2.3. dielectrophoresis of erythrocytes was studied by analyzing their movement after 20, 30, 50, 60, 90 and 120 seconds of application of AC field and comparing with their initial position at time 0 seconds (before the application of field). The experiments were performed on Day 0 (the day the fresh blood was taken from a volunteer), Day 2 and Day 5. The frequency of the field was held constant at 1 MHz and field strength at 0.025 V/micron. The results are presented in chapters 3 and 6. Table 3.1 gives the experimental matrix for the "Dielectrophoretic Blood typing" part of research. The experiments were repeated twice for each day with fresh blood by repeating the matrix.

The second parameter studied is the frequency of the AC field. Here the erythrocyte cell movement was analyzed with varying frequencies (0.5, 1, 2, 3, 4 and 5 MHz). The cell movement was studied only at 120 seconds of field application along with their initial position at time 0 seconds (before the application of field). The

Table 2.2 Experimental matrix for blood typing part of research

Blood Type / Day	A+	B+	AB+	O+
0	5-3-06 6-7-06	5-11-06 10-8-04	6-22-06 6-22-06 run2	7-24-06 7-25-06
2	6-9-06 9-15-04	5-13-06 10-10-04	5-28-06 10-10-04	7-26-06 7-26-06 set2
5	6-5-06 9-18-04	6-12-06 6-12-06 set2	5-31-06 10-13-04	7-29-06 7-29-06 set2

The above table shows the dates of conducting experiments. Each experiment was analyzed for 0, 20, 30, 40, 50, 60, 90 and 120 seconds About 3 different donors for A+, 3 different donors for B+. 2 different donors for AB+ and 4 different donors for O+ were used

Table 2.3 Experimental matrix for frequency dependency part of research

Dataset \ Blood Type	A+	B+	AB+	O+
Set1	9-17-04	10-23-06	03-15-07	9-17-04
Set 2	03-03-07	03-03-07	05-17-07	5-17-07
Set 3	03-07-07	02-16-07	04-12-07	23-02-07

The above table shows the dates of experimentation. Each experiment consisted of testing 6 different frequencies (0.5, 1, 2, 3, 4 and 5 MHz). About 2 different donors for A+, 2 different donors for B+. 2 different donors for AB+ and 3 different donors for O+ were used

field strength was maintained at 0.03 V_{pp}/micron. All the experiments were conducted on Day 0 (the same day as the fresh blood was taken). The Clausius Mossotti factor which influences the dielectrophoretic force is influenced by the frequency of the field (see section 1.2.4).Hence it is hypothesized that the frequency of the field could influence the dielectrophoretic behavior of the erythrocytes and the impact of the ABO blood type on this influence was to be studied. An experimental matrix for this part of the research is presented in Table 3.2. The experiments were repeated 3 times with fresh blood each time. The results of this work are presented in chapters 4 and 6.

The last parameter studied is Field strength influence on dielectrophoresis of erythrocytes. The project hypothesis for this part of research is that the cell movement of erythrocytes is greater for greater field strengths. This is because the dielectrophoretic force is strongly influenced by field gradient (see Equation 1.13). The dielectrophoretic force equation is dealt in detain in section 1.2.4. In order to study the influence of field strength, experiments were designed to be conducted with varying field strengths between 0.02 and 0.08 V_{pp}/microns while keeping the frequency constant at 1 MHz. The field strength is defined as the ratio between the voltage and distance between the electrodes. Experiments were conducted by keeping the voltage constant at 6V and varying the distance between the electrodes. The target distance between the electrodes was between 100 microns and 200 microns. The target interval was 25 microns. Experiments were repeated 3 times with fresh blood each time. The cell movement was analyzed at time 0 (before the application of field) and 120 seconds after field application. The results of this study are discussed in

Table 2.4 Experimental matrix for field dependency part of research

Blood Type / Dataset	A+	B+	AB+	O+
Set 1	7-21-06	07-19-06	03-15-07	07-25-06
Set 2	2-27-07	03-30-07	03-28-07	02-08-07
Set 2	03-07-07	02-16-07	04-12-07	03-03-07

The above table shows the dates of experimentation in a matrix. About 2 different donors for A+, 2 different donors for B+. 2 different donors for AB+ and 3 different donors for O+ were used

chapters 5 and 6. Table 2.3 shows the experimental matrix used in this work. Adjusting the distance between the electrodes is a challenging task. Hence it was not possible to attain the field strength values shown in Table 2.3 precisely. The experiments were conducted in the range shown. The details about conducting the actual experiments are discussed in section 4.1.

2.4 Conclusion

This chapter outlined the basic structure of the project and explained the hypothesis of the research performed. It was discussed that the research was divided into blood typing, frequency dependence and field dependence sections. The central theme of the hypotheses was discussed to that ABO blood types would impact their dielectrophoretic behavior. The main objective of the work was to develop a study of quantification of the dielectrophoresis of erythrocytes.

CHAPTER 3

DIELECTROPHORETIC BLOOD TYPING

Dielectrophoresis of erythrocytes was tested for all the 4 different ABO positive blood types. The dependency of the response on the specific blood type of the erythrocyte was tested. The hypothesis tested is that the dielectrophoresis of erythrocytes depends on their ABO blood type (see chapter 2). The experiments were done 9 times for each blood type and analyzed. Analysis was done using a MATLAB program developed during the course of this research. The vertical and horizontal movements of the erythrocytes based on the blood types were quantified and tabulated via use of wedges which approximated the nonuniform electric field. The study showed that the dielectrophoresis of erythrocytes depends on ABO blood type. A major portion of this chapter will be submitted for publication [1].

3.1 Materials and methods

The parameters of relevance in this project were frequency of the AC field, electric field strength, time of field application, and time of blood storage. In this chapter, the study of dielectrophoretic response of erythrocytes by varying blood type alone is presented. The frequency was maintained at 1 MHz and the electric field strength was maintained at 0.025 V_{pp} /micron. The important steps in the process

were microdevice fabrication, experimentation (including blood sample preparation), image analysis, quantification, and correlation. Each of these will be discussed below.

3.1.1 Microdevice fabrication

The dielectrophoretic field was generated within a microdevice using 100 μm platinum electrodes positioned approximately 200 microns apart in a perpendicular configuration to create a nonuniform AC field. The microdevice was made by attaching a Hybriwell chamber (HBW 75, item # 10484908) to a glass microscopic slide creating a thin chamber (40 by 21 by 0.15 mm). Platinum wires for electrodes (100 microns OD, 99% pure, Goodfellow, PT005127/128) were placed perpendicular to each other (Figure 3.1) and the whole chamber was sealed by pressing the adhesive edges of the Hybriwell chamber onto the microscopic slide. The microdevice has two sample ports to draw fluids across as shown in Figure 3.1. The electrodes were wrapped in conductive foil so that alligator clips from a 33250A Agilent Waveform Generator could be attached. Independent programming of the generator results in a sinusoidal AC electric field in the chamber. The step wise procedure for custom microdevice fabrication is given in Appendix A.

3.1.2 Microsample preparation

Whole blood was drawn from voluntary donors via venipuncture by a certified phlebotomist into Benton Dickson, 4 mL vacuutainers. The blood was drawn from

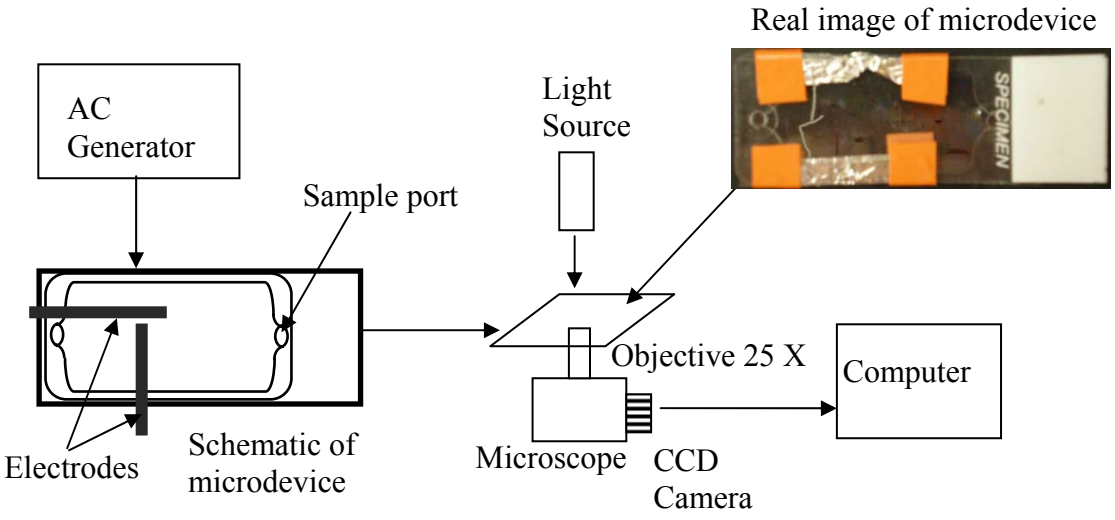

Figure 3.1 Schematic of the experimental set up for blood typing experiments.

Schematic illustrates the connections of the experimental system from AC generator to microdevice; microdevice to the microscope; microscope to the computer.

volunteers recruited via IRB approved procedures. Their gender, age and ethnicity varied. The fresh human blood samples were stored in 1.8 mg of K_2 EDTA anticoagulant per mL of blood in a refrigerator at 3˚C. Prior to conducting experiments, whole blood samples were diluted using Phosphate Buffer Saline (0.14 M NaCl, 0.02498 M KH_2PO_4, 0.00907 M K_2HPO_4) in 1:60 volume: volume ratio. A stock solution of 5000 µL was prepared by mixing 4198 µL of PBS solution with 82 µL of whole blood. The solution was well mixed by swirling and inverting the mixing vial to avoid shearing erythrocytes via micropipette tips prior to sample loading into the microdevice.

3.1.3 Experimentation

First the microdevice was thoroughly cleaned with e-pure water (Millipore Simplicity purification system, resistance = 18 Ohms), and inspected under the microscope for any debris. The microdevice was then rinsed with PBS solution. The diluted blood suspension was introduced into the microdevice via sample ports labeled in Figure 3.1 and drawn across the Hybriwell chamber using tissue at the opposite sample port. The blood suspension was drawn across the chamber 5 times to ensure that all the Phosphate Buffer Saline was displaced with a uniform blood concentration throughout the hybriwell chamber. The filled microdevice was positioned on the microscope stage, and alligator clips were used to connect the

platinum electrodes to the waveform generator. The waveform generator was programmed with a sinusoidal AC frequency of 1 MHz. The electric field strength was maintained at 0.025 V/micron, which results from an applied voltage of 5 V_{pp} over an electrode gap of 200 microns. Since the distance between electrodes varies in our devices between 150 microns and 200 microns, the applied voltage was adjusted using the following relation to obtain a constant electric field:

$$\mathbf{E}= \frac{V}{d} \mathbf{= 0.025\ Vpp/micron\ = Constant} \tag{3.1}$$

where V is the peak to peak voltage of the field (volts) and d is the distance between the electrodes (microns).

The blood suspension in the microdevice was allowed to settle for 10 min while the microscope was focusing and video capture settings were adjusted. The output from the waveform generator was turned on and 5 seconds later, the video microscopy recording was started. The movement of the erythrocytes was recorded via video microscopy at 10-second intervals for 4 min. These images were compiled and subsequently analyzed to quantify cell motion. A set of images for all four positive blood types taken after 120 seconds of field application are given in Figure 3.2.

The day when the blood was drawn was referred to as day 0 and subsequent days as 1, 2, 3, etc. In order to check for consistency in data, experiments were performed for 3 different days and two runs were conducted each day, resulting in 6

data sets for each condition set. Step wise procedure for experimentation is given in Appendix B.

3.1.4 Image analysis

The images were processed to get X/Y position, cell radius, cell area, bound width and bound height of the cells using Zeiss AXIOCAM 4.5 software. Based on the difference in optical intensity of the cells and the background in the image, this edge recognition software selected cells or cell conglomerates. The software was then able to disregard objects that were not cells (either too big or too small). Manual selection of any missed cells occurred with a circle selection tool. For every selected object, the software recorded a variety of properties including X/Y position, radius, bound height and width in a spread sheet. The cell count on each time-stamped image was also recorded. The images were analyzed for characteristic differences in their movement every 30 seconds up to 120 seconds. A step wise procedure for Image analysis is given in Appendix C.

3.1.5 Data analysis

The total number of cells in each image was counted and the data was tabulated as % change of total number of cells at a given time compared to the total number of cells at time 0 seconds (before the field was applied) (see Appendix K). This analysis showed that the total number of cells did not decrease by much after 120 seconds of field application. Mostly the % change of total number of cells after

120 seconds of field application compared to time 0 seconds (before the field was applied) was above 70% for all blood types. There was an interesting trend observed for average % changes. For A+ and B+ blood types, there was a continuous loss of cells from time 0 seconds (before the field was applied) until 120 seconds. AB+ had almost the same number of cells in the field throughout. O+ had a decrease in total number of cells up to 50 seconds and then had an increasing trend. This difference between the blood types for % change of total number of cells with time is a primary indication for the impact of ABO blood types on the dielectrophoresis of erythrocytes.

The X/Y data obtained during *Image Analysis* was analyzed for variations with respect to blood type. The first analysis done was a Sextant Analysis. In this, the images were divided into 6 equal sized regions or sextants using MATLAB. The regions were made by diving the image vertically into two by distance between electrodes and then horizontally into three parts. Cell count was analyzed in each region. However, the sextant approach proved not to be sensitive enough to quantify observed differences in motion; the regions were too large to show specific differences in the dielectrophoretic movement of each blood type.

For this reason a wedge analysis was developed. Using a MATLAB program, the image was divided into 10-15 equally sized wedges, in a manner such that they approximated electric field lines (Figure 3.3). These wedge lines originate at the high field electrode and terminate at the low field electrode and were calculated from an information file containing the size of the high field electrode, the distance between

the electrodes, resolution of the image, the positioning of the high field and low field electrode. Wedge size was determined by spacing the wedge lines 20 microns apart at the low field electrode. Figure 3. 4 (b), (d), (f) shows these lines drawn on the same plot as the X/Y cell positions (Figure 3.4 (a), (c), (e)). Average movement of cells in the vertical direction (up the wedges) as well as horizontally across the wedges was tabulated for 0 (before the application of field), 30, 60, 90 and 120 seconds. Data from the MATLAB program was also compiled for all blood types into a spreadsheet where average trends and corresponding standard errors were calculated. Even though the experiments were performed for 3 different days, the analysis was done by taking the average over all the days, assuming that the 5 day period in which the experiments were done was too small to show age dependency on the data. This was consistent with the fact that the cell properties like cell rigidity do not change significantly until after 6 days [50].

The dielectrophoretic movement of erythrocytes was two-dimensional as can be seen from Figure 3. 2. Hence, three specific parameters were developed to capture the overall movement of the cells; *Average Vertical Movement* (AVM), *Mean Fractional Horizontal Movement* (MFHM) and *Mean Normalized Horizontal Movement* (MNHM).

Average Vertical Movement (AVM) of the cells captures the movement of the cells vertically, between the high field electrode and the low field electrode. To determine *Average Vertical Movement* (AVM) of cells, the total length of each wedge was calculated (w_i). Then the average cell distance, from the high-field electrode, in

each wedge was calculated. This value was normalized by the total length of the wedge resulting in a bounded number between 0 and 1, where 0 places the cell next to the high field electrode while 1 reflects cells aggregating at the low field electrode (negative dielectrophoresis) (see Figure 3.5 (d)). Each wedge yields a normalized vertical movement value, from which a mean across all wedges was calculated to give average vertical movement. This data was plotted as a function of time for all blood types (Figures 3.6 (a), (b)). Average vertical movement captures the vertical movement of erythrocytes up or down the wedges, in a dielectrophoretic field. In equation form:

$$AVM = \frac{\sum_{i=1}^{N} \frac{\sum_{j=1}^{j=n} \frac{c_j}{w_j}}{n}}{N} \tag{3.2}$$

where n is the total number of cells in wedge 'j', c_j is the distance of the cell to the high field electrode along the wedge, w_j is the length of the wedge and N is the total number of wedges.

The *Mean Fractional Horizontal Movement* (MFHM) of cells captures their horizontal movement away from midfield relative to the image dimensions. It was determined as a horizontal distance from midfield. This midfield reference line was determined as a vertical line between high field electrode center to the low field electrode (Figure 3.3). The length from this centerline to the image edges on either side (D_L on the left side and D_R on the right side) was recorded. Then the average horizontal distance of all the cells from this midfield was calculated separately for the

left hand side (d_L) and the right hand side (d_R) (Figure 3.5 (b)). The total number of cells on either side of the centerline (N_L on the left side and N_R on the right side) were calculated. Then the sum of the distances of all the cells on either side of the center line were normalized by dividing their respective length of the image on that side of midfield line and their respective total number of cells. The mean of these values was calculated to give *Mean Fractional Horizontal Movement* (MFHM) and were plotted for each blood type as a function of time (Figure 3.7 (a)). Fractional horizontal movement helps in assessing the horizontal movement of the cells with respect to the image. In equation form:

$$MFHM = \frac{\frac{\sum_{i=1}^{N_L} d_L}{N_L \bullet D_L} + \frac{\sum_{i=1}^{N_R} d_R}{N_R \bullet D_R}}{2} \tag{3.3}$$

The third parameter studied was the *Mean Normalized Horizontal Movement* (MNHM), which captures the time-based horizontal movement of cells. The average horizontal distance (AHD) at each time was divided by the AHD at time 0 seconds (before the application of field) to give the Mean normalized horizontal movement (Figure 3.5 (c)). This captures the time-based horizontal movement of the erythrocytes in a dielectrophoretic field (Figure 3. 7). In equation form:

$$MNHM = \frac{1}{2}\left(\frac{\left(\frac{\sum_{i=1}^{N_L} d_L}{N_L} \right)_{time=t\,\sec}}{\left(\frac{\sum_{i=1}^{N_L} d_L}{N_L} \right)_{time=0\,\sec}} + \frac{\left(\frac{\sum_{i=1}^{N_R} d_R}{N_R} \right)_{time=t\,\sec}}{\left(\frac{\sum_{i=1}^{N_R} d_R}{N_R} \right)_{time=0\,\sec}} \right) \quad (3.4)$$

where d_L and d_R are the horizontal distances of the cells from the midfield line which are positioned to the left and right of it respectively. N_L and N_R are the total number of cells on the left and right of the midfield line respectively, and t is the time at which time dependent horizontal movement is being calculated. The time dependent horizontal movement describes the horizontal movement of the erythrocytes relative to their initial position at time zero. This is in contrast to fractional horizontal movement, which captures their movement with respect to the geometry of the figure. The micro electrodes are not precisely in the same place in each experiment. Hence fractional horizontal movement tries to overcome this problem by normalizing the distance of the cells on either side of the midfield by the actual distance. The time dependent horizontal movement does not have this, but is normalized based on time. It should be again noted here that the variables were chosen specifically to ascertain the dependency of dielectrophoresis of erythrocytes on their blood type. A synopsis of the MATLAB program which calculates average vertical movement, fractional

horizontal movement and time dependent horizontal movement is given in Appendix E.

3.2 Results and Discussion

The qualitative and quantitative responses for all four positive blood types (A+, B+, AB+, O+) in a 0.025 V_{pp}/micron electric field are presented in this work. The dielectrophoretic movement of each of these blood types was seen to follow different trends with time. *Average Vertical Movement* (AVM), *Mean Fractional Horizontal Movement* (MFHM) and *Mean Normalized Horizontal Movement* (MNHM) were used to capture the vertical, horizontal and time based movements of the erythrocytes in a dielectrophoretic field. The variables were precise enough to capture the difference in the dielectrophoretic response of the erythrocytes based on their blood types.

Raw images of the dielectrophoretic movement of all four positive blood types are shown in Figure 3.2 at 120 seconds. As can be seen, the erythrocytes respond in less than 2 minutes to the nonuniform AC field. This rapid cell motion makes it challenging to quantify. However, on a preliminary qualitative observation, the A positive blood type had a drastic horizontal and vertical movement in the field while O+ blood type showed a milder response to the field. The B+ and AB+ blood types showed a response movement which was somewhere in between the A+ and O+ extremes. It can be seen that the response is less drastic for the O+ blood type in both

directions compared to all the rest of the positive blood types (A+, B+, AB+). The time-based qualitative images are presented in Figure 3.4(a) for O+ along with its corresponding wedge line representation in Figure 3.4(b).

The vertical movement of each blood type was captured by the variable Average Vertical Movement (AVM). The results of vertical movement as a function of time for all blood types are shown in Figure 3.6. In general, the values at 120 seconds are between 0.53 and 0.58, showing that the dielectrophoresis of erythrocytes is not distinctly positive dielectrophoresis (value near 0) or negative dielectrophoresis (value near 1). Qualitative images suggest that the O+ has a milder dielectrophoretic response than the other blood types, and this is confirmed by the fact that the vertical movement values for O+ are less than the other blood types with values between 0.48 and 0.53 at all observed times (see Figure 3.6 (a)). The vertical movement values follow a nonlinear trend with time for all blood types (see Table 3.1).

The AB+, B+, O+ values follow a quadratic trend in time with a reasonable accuracy of R-squared values of greater than 0.9. The same vertical movement values are shown in Figure 3.6 (b) along with their corresponding standard error bars. It can be noted that these errors are reasonable with values between 0.003 to 0.01 and are expected given that these are biological, micrometer scale experiments. It can be seen that O+ is has distinct values from the rest, starting from 30 seconds. All four blood types are most distinct at 60 seconds where only B+ and AB+ slightly overlap (Figure 3.6 (b)). Hence the trend in vertical movement with time was studied up to 60 seconds by fitting linear trend lines to the data (Figure 3.6 (c)). The regression values

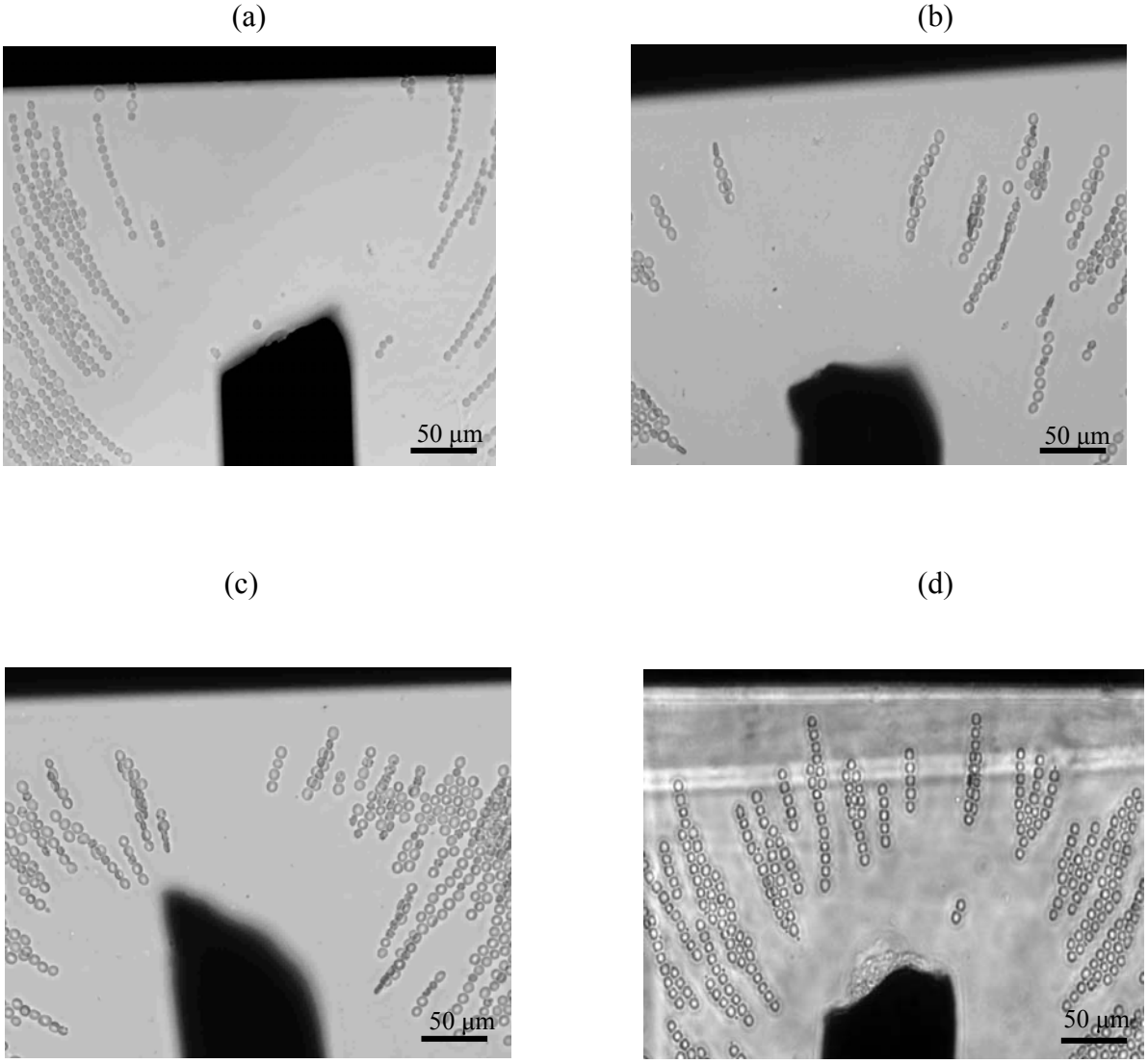

Figure 3.2 Comparison of the dielectrophoretic response of all four positive blood types after 120 seconds of field application

(a) Represents A+ (b) represents B+ (c) represents AB+ (d) represents O+. A+ and B+ have less number of cells, AB+ has conglomeration of cells and O+ has high number of cells on their respective images.

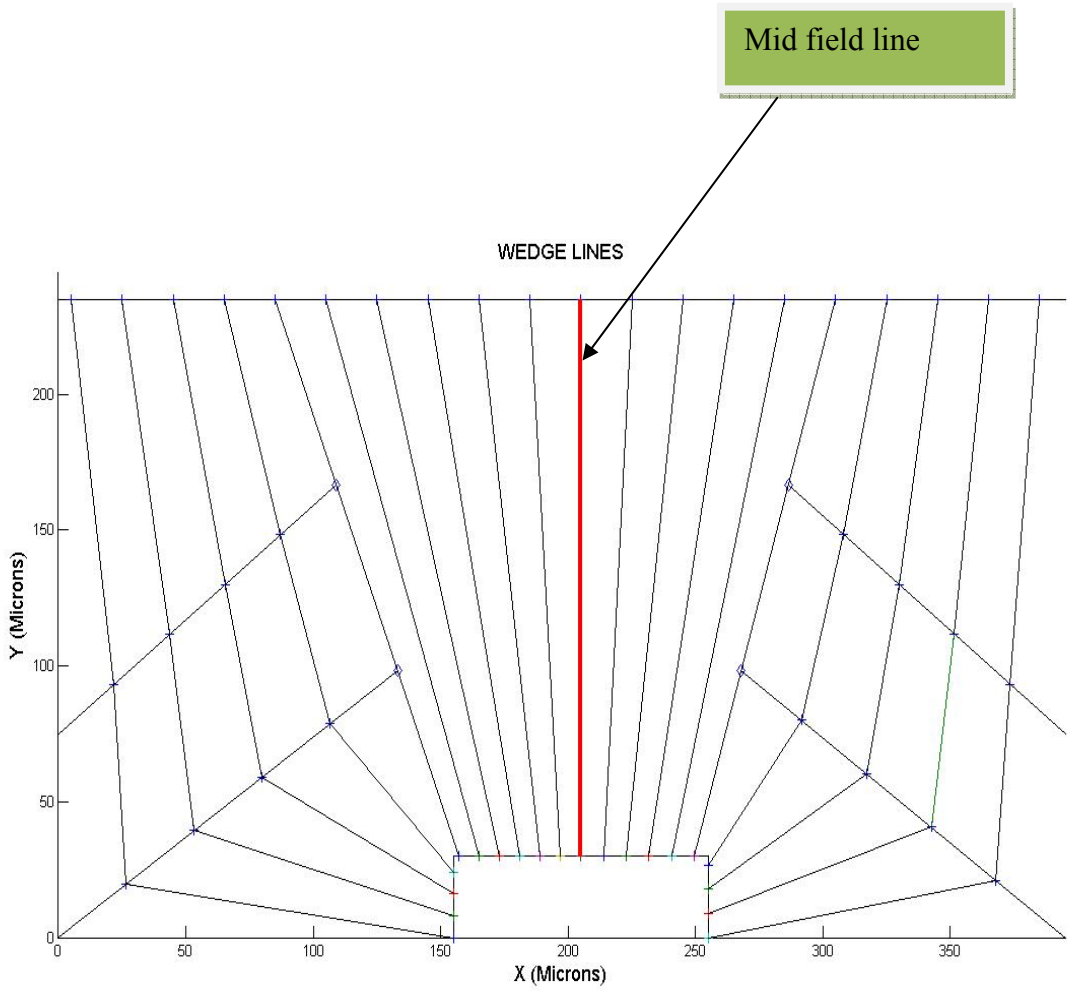

Figure 3.3 MATLAB output showing wedgelines with midfield line indicated

Mid field line is shown on the image with an arrow. It is used as a basis for horizontal movement calculations.

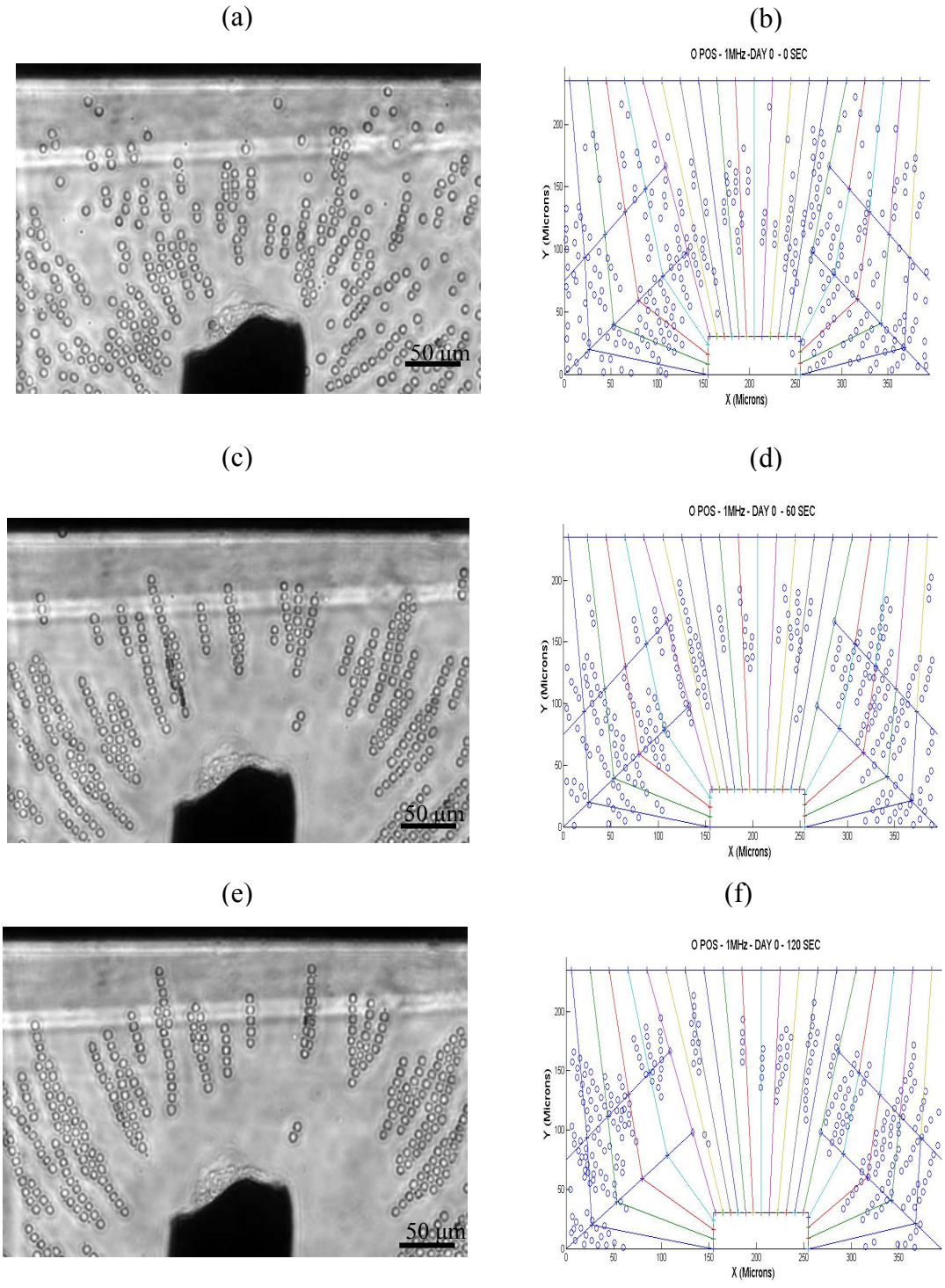

Figure 3.4 Comparison of the dielectrophoretic response of O+ blood type at time 0 (a, b), 60 (c, d), 120 seconds (e, f) and their corresponding MATLAB representations with wedgelines.

(a) (b) (c)

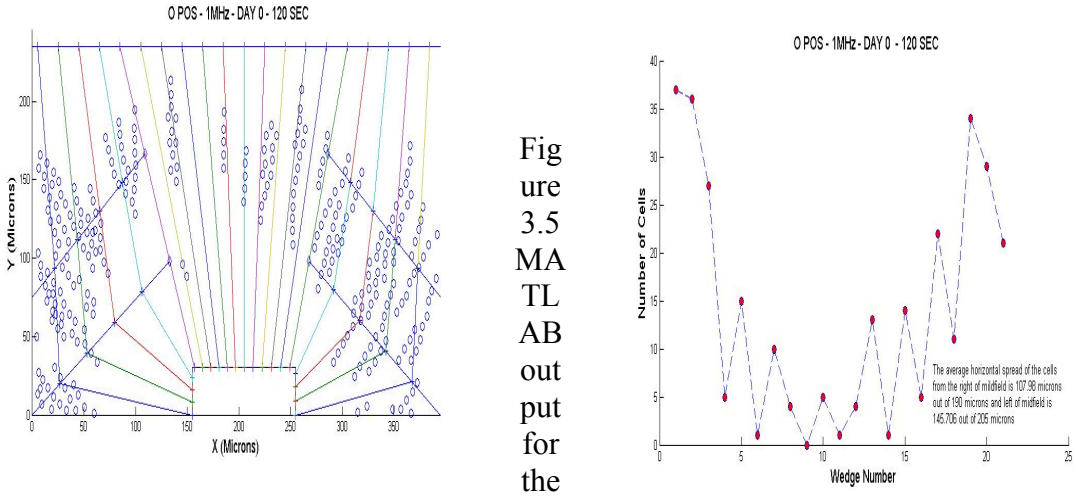

Figure 3.5 MATLAB output for the dielectrophoretic response analysis for O+ after 120 seconds of field application

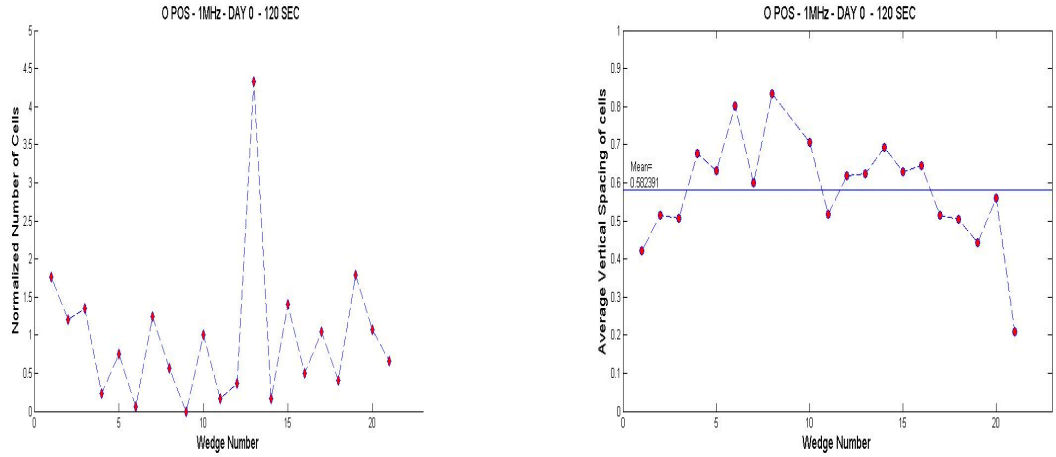

(a) MATLAB representation of the image, (b) number of cells in each wedge, (c) normalized number of cells in each wedge over time 0 seconds, (d) average vertical spacing of cells in each wedge

are given in Table 3.1. It can again be observed that the O+ has completely different slope and intercept from all the rest of the blood types. A+, B+ and AB+ have identical slopes and only a slightly varying intercepts. There is a nonlinear trend in

vertical movement with time for all blood types with an R-squared value less than 0.9. O+ is quite distinct (Table 3.1).

The parameter used to assess the horizontal movement of the cells is Mean Fractional Horizontal Movement (MFHM). The variation of fractional horizontal movement with time is shown in Figure 3.7. It can again be seen that the fractional horizontal movement values for O+ are considerably less than all the other blood types. Initially the A+ and B+ blood types have nearly the same values, but they separate with time and A+ has higher values (Figure 3.7 (a)). This again shows the drastic nature of the dielectrophoretic response of A+ blood type. The AB+ has values which are less than B+ and higher than O+ blood types. It is clearly seen that O+ has distinct values from the rest of the blood types at 30, 50 and 60 seconds (Figure 3.7(b)). Among all the time periods tested, 90 seconds shows most distinction between all the blood types. Though the standard error bars overlap at 90 seconds, the average values are apart whereas at other time points there are at least two of them which are too close. Linear regression lines were fit to the data up to 90 seconds (Figure 3.7 (b)).The regression data is given in Table 3.2. All the blood types follow a linear trend of fractional horizontal movement with time having R-squared values of greater than 0.9. A+, B+ and AB+ have identical slopes (Table 3.2). O+ has a zero slope (with 3 significant digits) showing strong stability with time. This suggests that O+ has milder response with a dielectrophoretic field compared to the rest of the blood types.

The horizontal movement with respect to time is captured by the variable Mean Normalized Horizontal Movement (MNHM) (see Figure 3.8). This variable assesses the horizontal movement with respect to the initial random positioning of the erythrocytes in dielectrophoretic field at time 0 seconds (before the application of field). Up to 60 seconds after the field is applied, it can be noted that, A+, B+, and AB+ blood types have similar time dependent horizontal movement values. After 90 seconds, however, the three blood types' time dependent horizontal movement values become distinct. At 120 seconds, again B+ and AB+ blood types show similar values. Once again, this variable also captures the fact that A+ has the most drastic dielectrophoretic response with the highest time dependent horizontal movement values while O+ has the milder response with the least values at all times. O+ has a distinct time dependent horizontal movement value from the rest of the blood types taking the error bars into consideration (Figure 3.8 (b)). Comparing all the tested time periods, 90 seconds has all blood types separated apart. In all the rest of the time periods at least two blood types are close to each other. Hence linear regression was performed on time dependent horizontal movement data up to 90 seconds (Figure 3.8 (c)). All blood types have R-squared value of 0.9 for linear regression. A+, B+ and AB+ have identical slopes but O+ has a distinct slope which is less than that of the others, This suggests a milder dielectrophoretic response for O+ which might due to

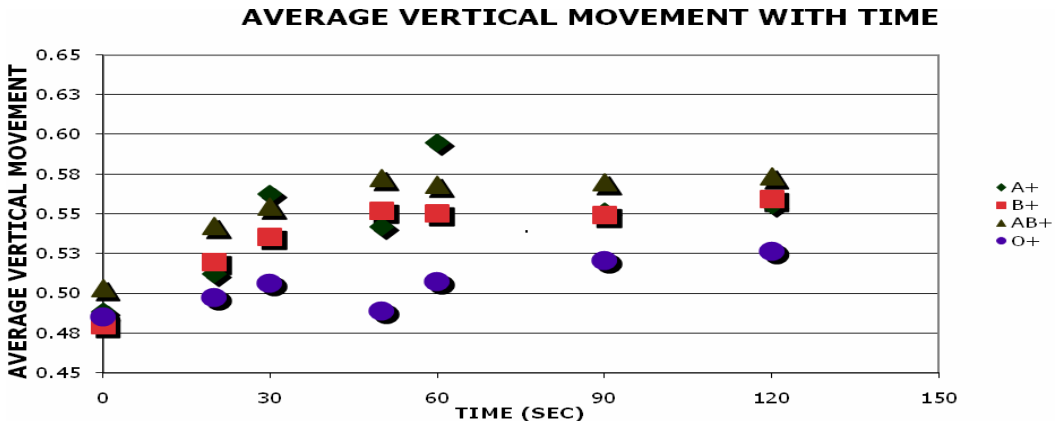

(a)

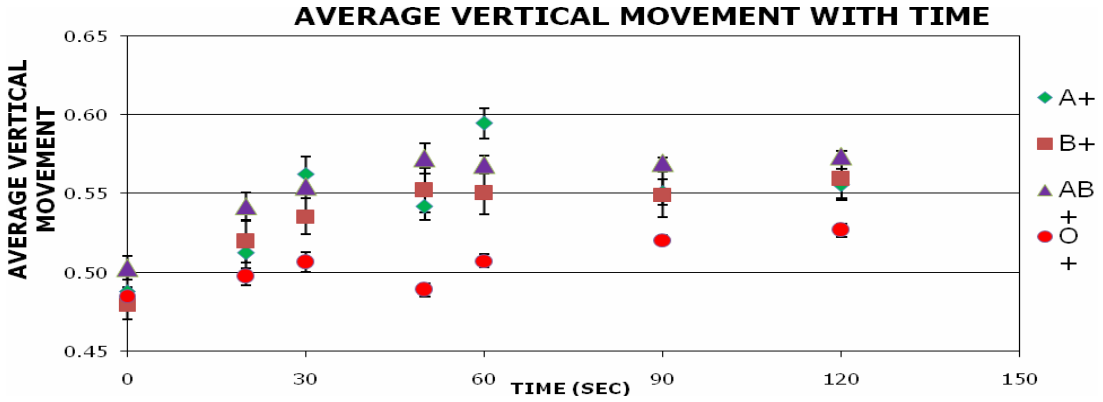

(b)

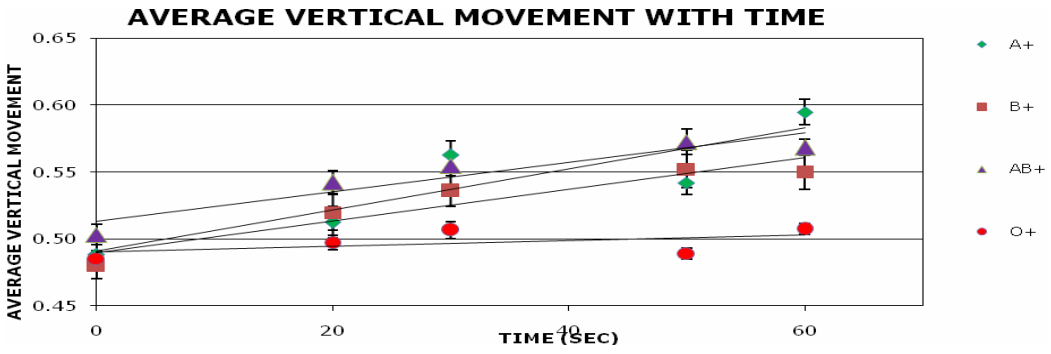

(c)

Figure 3.6 Average Vertical Movement (AVM) plots with time for positive blood types (A+, B+, O+, AB+)

All the above graphs show the same data having (a) without error bars (b) with error bars (c) with linear regression lines

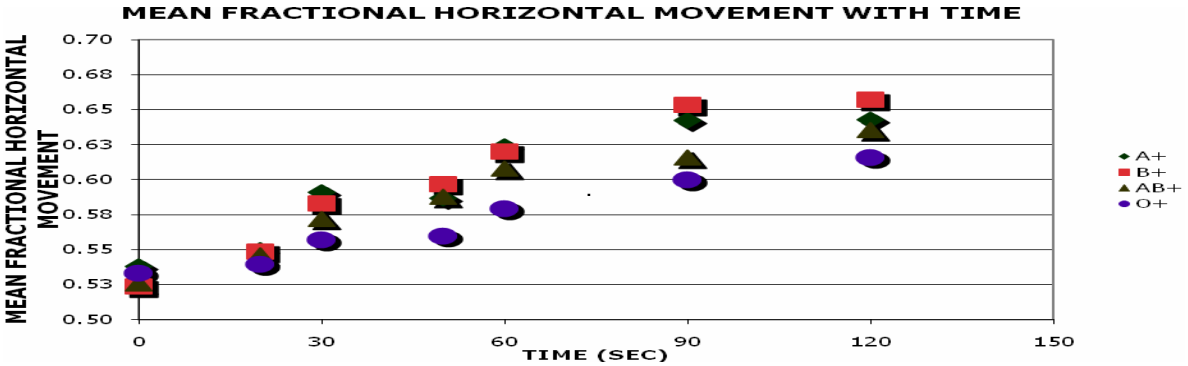

(a)

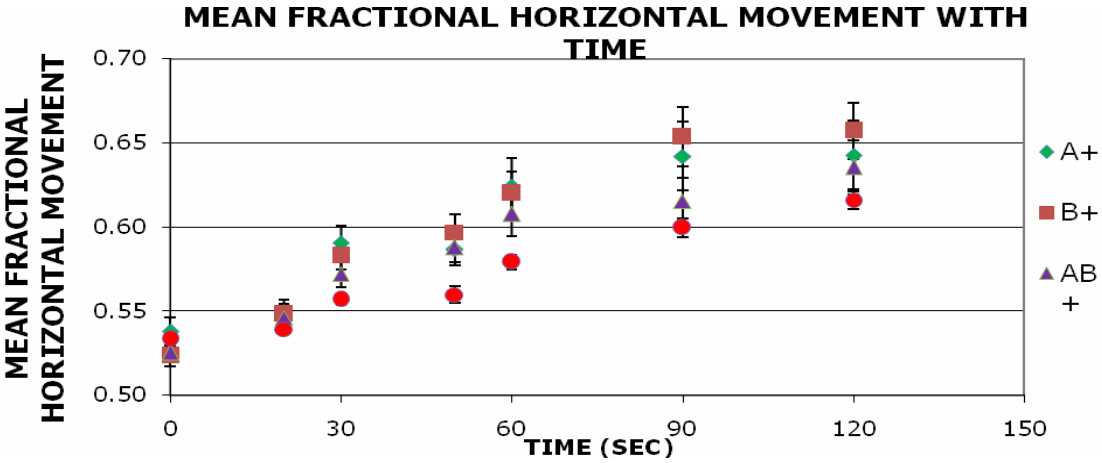

(b)

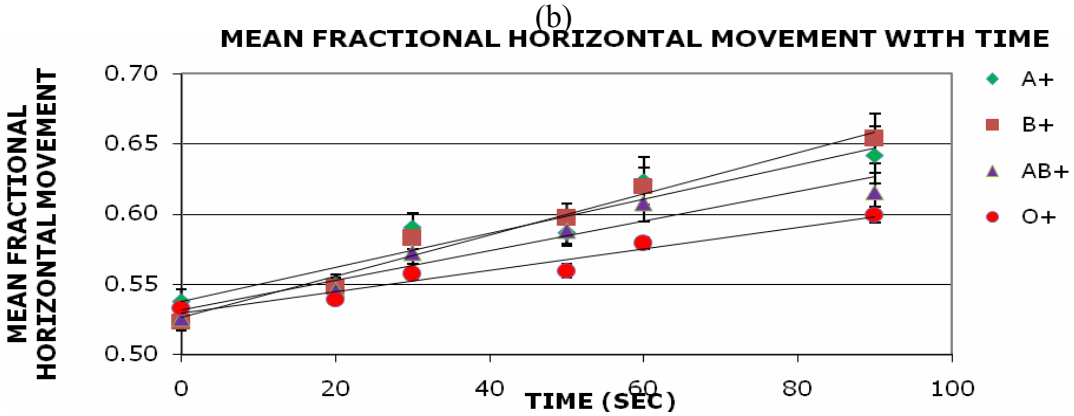

(c)

Figure 3.7 Mean Fractionalized Horizontal Movement (MFHM) plot with time (A+, B+, AB+ and O+)

All the above graphs show the same data having (a) without error bars (b) with error bars (c) with linear regression lines

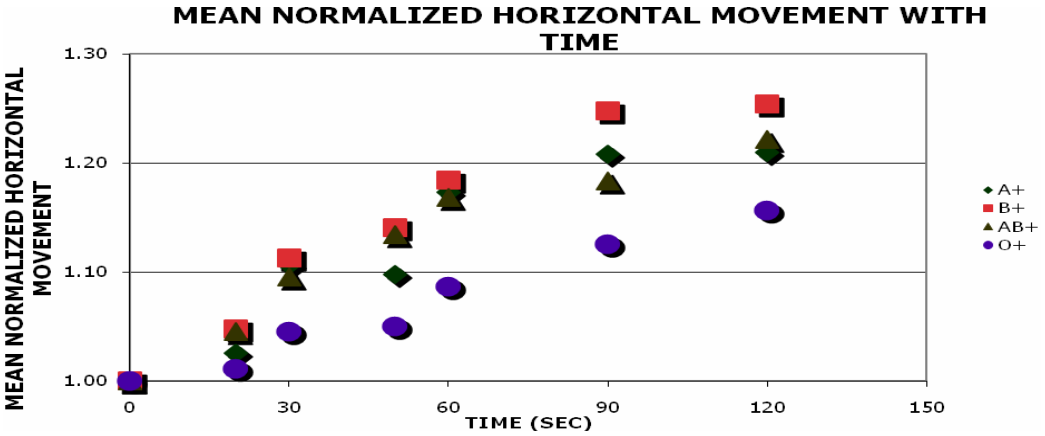

(a)

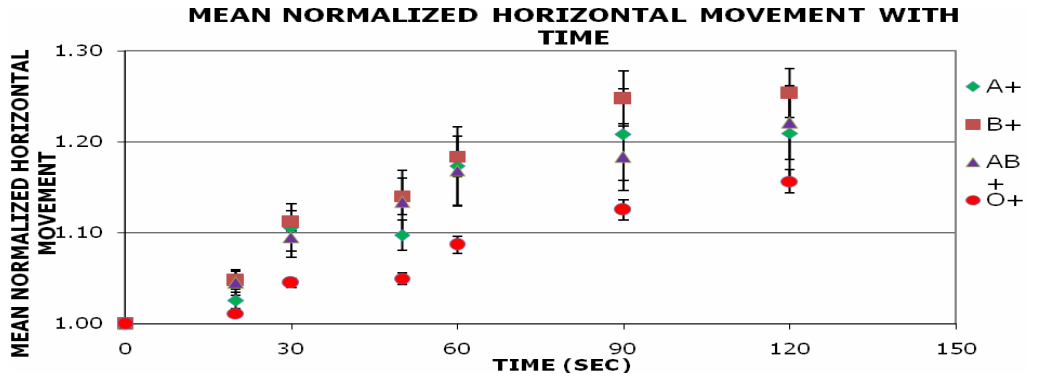

(b)

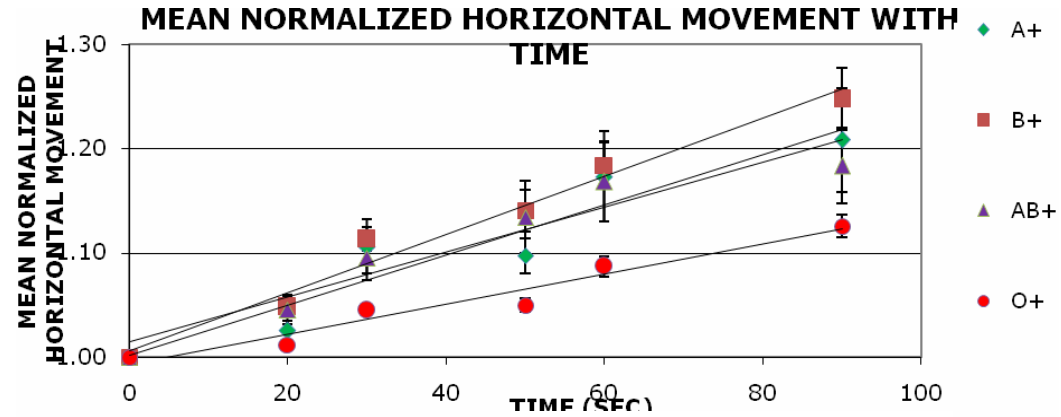

(c)

Figure 3.8. Mean Normalized Horizontal Movement (MNHM) plot with time for positive blood types (A+, B+, AB+, O+)

All the above graphs show the same data having (a) without error bars (b) with error bars (c) with linear regression lines

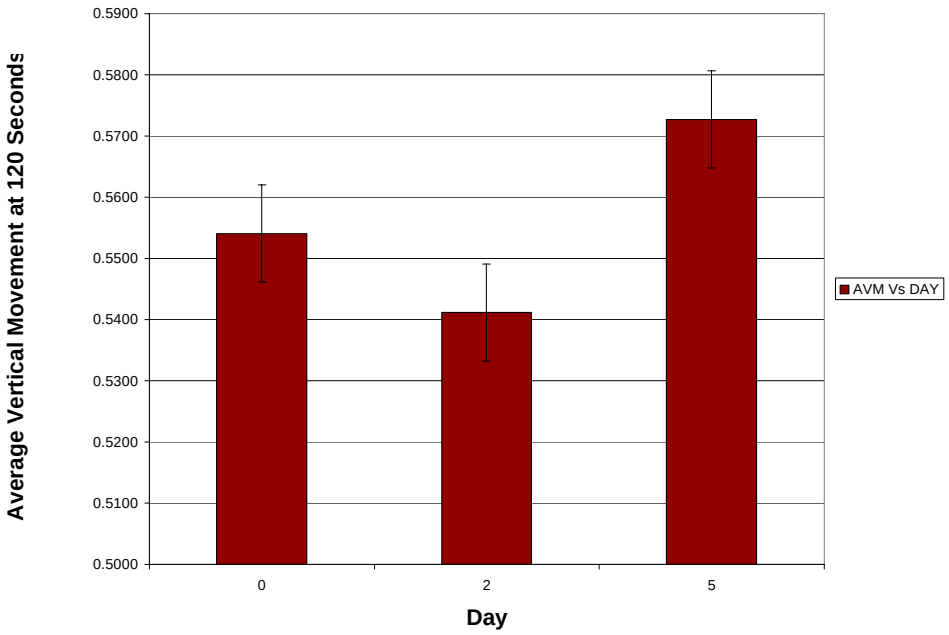

Figure 3.9 Average Vertical Movement at 120 seconds data for O+ for experiments performed with blood on day 0, 2 and 5.

Table 3.1 Average Vertical Movement (AVM) trends analysis with coefficients for a line

Blood type	slope	intercept	R^2 value
A+	0.001	0.49	0.776
B+	0.001	0.489	0.895
AB+	0.001	0.513	0.885
O+	0	0.49	0.275

Table 3.2 Mean Fractional Horizontal Movement (MFHM) trends analysis with coefficients for a line

Blood type	slope	intercept	R^2 value
A+	0.001	0.538	0.906
B+	0.001	0.526	0.974
AB+	0.001	0.531	0.926
O+	0	0.529	0.952

Table 3.3 Mean Normalized Horizontal Movement (MNHM) trends analysis with coefficients for a line

Blood type	slope	intercept	R^2 value
A+	0.002	1.001	0.905
B+	0.002	1.006	0.975
AB+	0.002	1.014	0.922
O+	0.001	0.993	0.952

the fact that O+ has no ABO antigens.

The overall pattern of the dielectrophoretic movement of erythrocytes depends on their blood type. The O+ blood type showed the least of all the responses likely due to the absence of the two antigens. It is also noteworthy that the behavior of O+ is not similar to either A+ or B+ unlike AB+. On variables, it can be clearly seen that A+, B+ and AB+ keep together while O+ has a trend that is separate from them. This might be due to the fact that A+, B+ and AB+ have antigens on their surfaces and that the A antigen is not too dissimilar structurally from the B antigen [25]. In horizontal movement, the AB+ has fractional horizontal movement and time dependent horizontal movement values which are between those shown by A+, B+ and O+. This is to be expected given the fact that AB+ has both the antigens of A+ and B+.

The standard error was also calculated across the 5 days of experimentation since it is known that membrane fluidity of the erythrocytes do not change for 6 days of storage outside the body. It was found to be quite small and it is presented for vertical movement data (see Figure 3.9).

3.3 Statistical Analysis

Analysis of variance (ANOVA) andlLeast significance difference multiple comparisons (LSD – MC) were performed on all vertical movement, fractional horizontal movement and time dependent horizontal movement data. ANOVA was performed to assess the primary effects (Day, Time, Repetitions, Blood type) and the

interaction effect (Day*Time, Day * Type and Time* Type). Hence the model used for performing the tests is as follows in Equation 3.5

Y = DAY TYPE TIME REPETITION DAY*TIME DAY*TYPE TIME*TYPE; (3.5)

Y can be vertical movement, fractional horizontal movement or time dependent horizontal movement. Also it should be noted for all further discussion that DAY has 3 levels 0,2 and 5; TYPE has 4 levels A, B, AB and O; TIME has 7 levels 0, 20, 30, 50, 60, 90 and 120 (TIME for time dependent horizontal movement does not have 0 level); REPETITION has 2 levels R1 and R2.

As discussed in section 3.2, there was reasonable separation between all blood types for vertical movement at 60 seconds, for fractional horizontal movement and time dependent horizontal movement at 90 seconds. ANOVA and LSD – MC were performed for data at these specific times also. Here the model statement in Equation 3.5 was adjusted to remove interaction effects as seen in Equation 3.6.

Y = DAY TYPE TIME REPETITION (3.6)

Y can be vertical movement, fractional horizontal movement or time dependent horizontal movement.

3.3.1 Average vertical movement

The model in Equation 3.5 fit well for vertical movement data for all times with a P value of less than 0.0001. Hence an alpha of 0.05 was chosen to study the ANOVA results. At this confidence level of 95 % (corresponding to an alpha of

0.05), it was seen that all primary effects of day, blood type, repetitions and time had significant effect on the vertical movement data. There was significant interaction between day and blood type. There was no evidence to suggest that there was interaction between (day and time) and (time and type). LSD – MC at an alpha of 0.05 suggested that O had a significantly low mean vertical movement compared to all the rest of the blood types. At this alpha value there was no evidence to suggest that there was a difference between A+, B+ and AB+ blood types. Results of LSD – MC at other alpha values are given in Table 3.4. The vertical movement data only for 60 seconds was also analyzed. The model in Equation 3.6 fit the data at a P value of 0.1172. Hence an alpha of 0.15 (confidence level of 85 %) was chosen for analysis. At this alpha value for 60 seconds vertical movement data, there was significant influence of blood type and repetitions on the data. There was no influence of day on 60 seconds vertical movement data. At alpha of 0.15, LSD – MC showed O to be significantly different from A+ and AB+ but not from B+. There was no evidence to suggest that A+, B+ and AB+ were significantly different from each other. The LSD-MC on day suggested that day 5 was significantly different from days 0 and 2. The results are discussed in a more conclusive manner in chapter 6 and recommendations based on statistical analysis are given in chapter 7.

3.3.2 Mean fractional horizontal movement

ANOVA and LSD – MC were performed on Mean fractional horizontal movement data and the model in Equation 3.5 fit the data to a P value less than

0.0001. An alpha of 0.05 was chosen to perform the analysis. At this alpha value, the parameters day, blood type, repetition and time had significant influence on fractional horizontal movement data. Also based on fractional horizontal movement, there was significant interaction between (day and blood type), (day and time) and (blood type and time). LSD – MC of day showed that day 0 was significantly different from 2 and 5. The repetitions R1 and R2 were significantly different from each other. The time periods 0, 90, 120 were significantly different from the rest. LSD – MC on blood type showed that O was significantly different from A+ and B+ but not from AB+. There was no evidence to suggest that A+, B+ and AB+ were significantly different from each other. Results of LSD – MC at other alpha values are given in Table 3.5. It can be noted from section 3.2 that 90 seconds had fractional horizontal movement of all 4 blood types apart. Hence ANOVA and LSD – MC were performed on 90 seconds fractional horizontal movement data. The model in Equation 3.5 fit the data only to a P value of 0.2718. This is a reasonably poor fit and hence the conclusions were not very robust. At an alpha of 0.3, there was no evidence to suggest that day or blood type were significantly influencing the fractional horizontal movement values. There was significant influence by repetitions. At this alpha value all blood types showed the same on LSD – MC test. Conclusions based on the results are given in chapter 6 and recommendations in chapter 7.

3.3.3 Mean normalized horizontal movement

Mean normalized horizontal movement data was fit to the model given in Equation 3.5 to perform ANOVA and LSD – MC analysis. The model fit well to a P value of 0.0001. An alpha of 0.05 was chosen to perform the analysis. At this alpha, the parameters day, blood type, time, repetitions significantly influenced the time dependent horizontal movement data. Also (day and blood type) and significantly interact with each other. (Day and time) and (blood type and time) do not significantly interact with each other. LSD –MC test at alpha of 0.05 showed that O was significantly different from the rest of the blood types. There was no sufficient evidence to suggest any difference between A+, B+ and AB+. Results of LSD – MC on blood type for some other values of alpha are shown in Table 3.6. The LSD –MC on day showed that day 0 was significantly different from days 2 and 5. The repetitions R1 and R2 are significantly different from each other. The time periods 90 and 120 seconds are significantly different from the rest. As discussed in section 3.2, 90 seconds had the best separation between all the blood types based on Figure 3.8 (a). Hence ANOVA and LSD – MC were performed on time dependent horizontal movement data at 90 seconds. The model in Equation 3.6 was fit to the data but it resulted in a P value of 0.2885. Hence this poor fit made the results not robust. At an alpha of 0.3, it was observed that day and blood type did not have significant influence on time dependent horizontal movement data. Repetitions strongly influenced the data. LSD – MC on blood type at an alpha of 0.3 showed that all the

blood types were the same. The conclusions made based on the results in chapter 6 and recommendations in chapter 7.

3.4 Conclusion

This chapter discussed the results of dielectrophoretic blood typing part of the research. The hypothesis tested was the dielectrophoresis of erythrocytes with time depends on ABO blood type. The results confirmed the hypothesis with O+ having a significantly different dielectrophoretic response compared to other blood types. This of significance since O+ is a universal donor for blood transfusion. It was also discussed that A+, B+ and AB+ had slightly similar response due the fact that A and B antigens are not very dissimilar.

Table 3.4 Multiple comparison results for Average Vertical Movement (AVM)

Alpha Value	Confidence level	Results (AVM)
0.05	95%	O+ is significantly different from the rest
0.15	85%	O+ is significantly different from the rest and AB is significantly different from B.
0.35	65%	AB+ and O+ are significantly different from each other and from the rest
0.44	56%	All four blood types are significantly different

Table 3.5 Multiple comparison results for Mean Fractional Horizontal Movement (MFHM)

Alpha Value	Confidence level	Results (MFHM)
0.05	95%	O+ is significantly different from A and B
0.15	85%	O+ is significantly different from the rest
0.25	75%	AB+ and O+ are significantly different from each other and from the rest
0.92	8%	All four blood types are significantly different

Table 3.6 Multiple comparison results for Mean Normalized Horizontal Movement (MNHM)

Alpha Value	Confidence level	Results (MNHM)
0.05	95%	O+ is significantly different from the rest
0.35	65%	O+ and B+ are significantly different from each other and from the rest.
0.85	15%	All four blood types are significantly different

CHAPTER 4

FREQUENCY DEPENDENCY

An alternating current changes (alternates) with respect to the direction of the electric field potential at a given rate. This rate is called the frequency of the electric field and is measured in Hertz (Hz) which is equivalent to cycles/second. The frequency of the electric field determines the Clausius Mossotti factor, which is critical in determining the dielectrophoretic force strength. The real part of Clausius Mossotti factor α, is given by the following equation

$$\alpha = \mathrm{Re}\left\{\frac{\tilde{\varepsilon}_p - \tilde{\varepsilon}_m}{\tilde{\varepsilon}_p + 2\,\tilde{\varepsilon}_m}\right\} \qquad \text{(From 1.2)}$$

where $\tilde{\varepsilon}_p$ denote complex permittivity of the particle (erythrocyte) and $\tilde{\varepsilon}_m$ denotes the complex permittivity of the medium in which the cells are suspended. The complex permittivity, $\tilde{\varepsilon} = \varepsilon - i\sigma/\omega$, depends on the frequency of the field, ω, the electrical conductivity. Hence, the Clausius Mossotti factor is a strong function of the frequency of the field. Adjusting frequency to get a desired effect has already been

shown useful as in the case of naoparticles [56 – 59]. Maintaining a frequency of up to 100 MHz, carbon nanotubes were deposited on to predefined electrodes [91]. Several frequency dependent dielectrophoretic studies were made like for the case of electrowetting of electromechanical mechanisms to better understand the underlying processes [92].

From Equation 1.1, it can be seen that the dielectric force depends on the Clausius Mossotti factor. Hence it is necessary to study the dielectrophoretic behavior of the erythrocytes as a function of the frequency to bring out the differences in the blood type responses. As per our hypothesis, each blood type results in a different dielectrophoretic response with a change in electric field frequency (see chapter 2). A major portion of this chapter will be submitted for publication [93].

4.1 Materials and Methods

The main emphasis on the set of experiments discussed here is the frequency of the AC field. Experiments were performed at 0.5, 1, 2, 3, 4 and 5 MHz while keeping the electric field strength constant. The experiments were conducted for all the four positive ABO blood types at day 0.

A detailed description of the experimentation, microdevice fabrication and data analysis was given in the materials and methods section of chapter 3. The same method was adopted for experimentation, microdevice fabrication and data analysis. The main difference is the design of experiments and the frequency parameter was

systematically changed. Nevertheless, a brief summary of the experimentation, microdevice fabrication and data analysis is presented below.

Whole blood was obtained from volunteers and stored at 3^{o}C. The blood was taken out just before performing the experiments. A microdevice was fabricated by placing 2 platinum wires between a self-adhesive hybriwell slide and a microscope glass slide (see Figure 3.1). The blood was first diluted in a 1:60 ratio using a phosphate buffer saline (PBS). The diluted blood solution was introduced into the microdevice chamber via sample ports after thorough washing of the microdevice with first Millipore purified water and then with PBS solution. The blood solution was introduced by placing few drops of it (approx. 62 µl) on one of the sample ports and by drawing the suspension across the device by placing a kimwipe tissue paper on the other sample port. This creates a suction in the chamber and draws the blood solution into the device.

The microdevice filled with the blood solution was placed on the microscope stage and the device was attached to an AC waveform generator via alligator clips (see Figure 3.1). Based on the distance between the electrodes the electric potential to be applied was calculated using the Equation 3.1. By changing the settings on the waveform generator, the specified voltage and frequency were adjusted. The whole setup was connected to a computer via video microscopy. The electric field is applied and movement of the erythrocytes was observed and recorded on the computer. The video microscopy recorded the images as snapshots taken every 10 seconds and then compiled them into a video. Experiments were performed for 0.5, 1, 2, 3, 4, 5 and 6

MHz frequencies for each blood type. The experiments were repeated 3 times on 3 different days using fresh blood each time.

The images collected from the video microscopy were analyzed using the software AXIOCAM 4.5. For frequency dependency analysis, the images taken at 0 seconds (just before application of the electric field) and at 120 seconds after application of the electric field were analyzed. The software circles the erythrocytes based on the difference between their optical intensity and that of the background. The software gives the X/Y position of the cells on the image. The data is processed to calculate the Average Vertical Movement (AVM), Mean Fractional Horizontal Movement (MFHM) and Mean Normalized Horizontal Movement (MNHM) values. These parameters are discussed in detail in Chapter 3.

4.2 Results and Discussion

The data was analyzed to obtain the same parameters used for blood typing analysis – Average Vertical Movement, Mean Fractional Horizontal Movement and Mean Normalized Horizontal Movement (Equations 3.2, 3.3, 3.4). The data was plotted as scatter plots to analyze the trend and bar graphs to analyze the corresponding standard errors.

Vertical movement analysis was conducted to quantify positive vs negative dielectrophoretic movement; the vertical movement data can be seen in Figure 4.1 (a). The data shows a nonlinear trend for all blood types. Based on only the scatter plot, it can be said that the best separation is at 1 MHz. If error bars are taken into

consideration (see Figure 4.1 (b)), there is very little difference between all the blood types at any frequency with respect to the vertical movement of erythrocytes. However, there are differences between specific blood types at particular frequencies. At 0.5 MHz, there is no statistical difference between all the blood types. At 1 MHz, A+, AB+ and O+ blood types are distinguishable from each other. B+ is not distinguishable from any of them. At 2 MHz, only B+ stands apart from all the rest of the blood types at a maximum value. At 3 MHz also, B+ is the most distinguishable but this time with the least value. At 4 MHz, O+ is the most distinguishable with the maximum value. At 5 MHz all the values are within standard errors as per the histogram in Figure 3.2, taking the error bars into consideration.

Average vertical movement increases with frequency for all blood types in a nonlinear trend. O+ is not linear at all, with a R^2 value of 0.11 for a linear fit. For A+ the trend is cubic with a R^2 value of over 0.95. All the other blood types do not fit to a polynomial of up to the 3rd degree with a R^2 value of over 0.95. There is no blood type with a general maximum or minimum over all the frequencies and there is a different blood type having a maximum or minimum value for each frequency. The coefficients of the polynomials fit and the corresponding R^2 values are shown in Table H.1 in appendix H.

Mean fractional horizontal movement analysis was conducted to assess movement of the cells toward or away from the midfield line. The fractional horizontal movement values are shown in Figure 4.2. As far as the scatter plot was concerned, there is a good difference between the blood types at 2 MHz for fractional

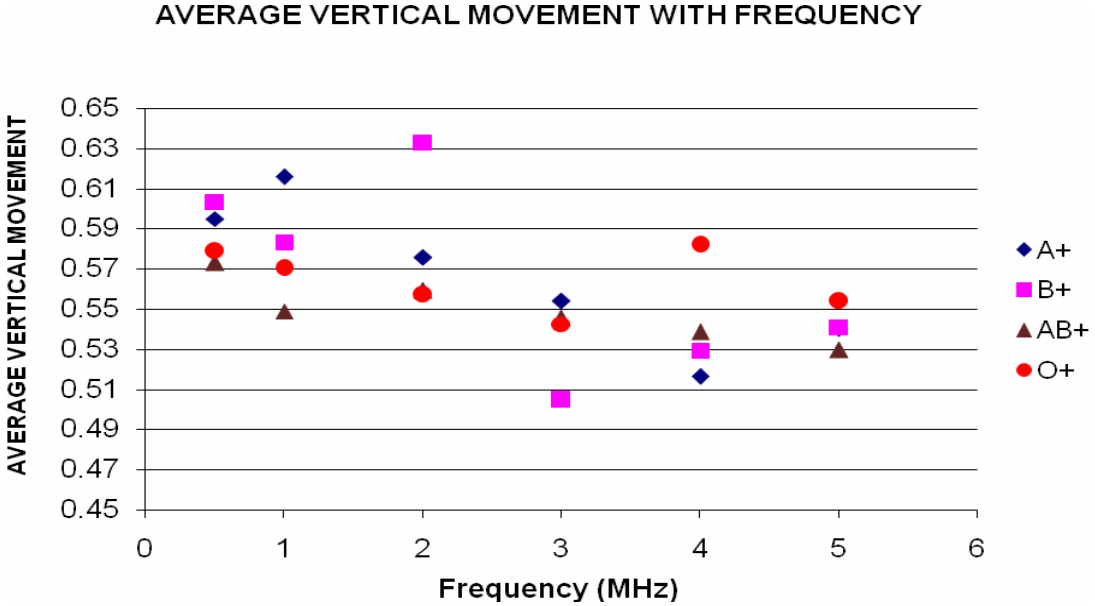

(a)

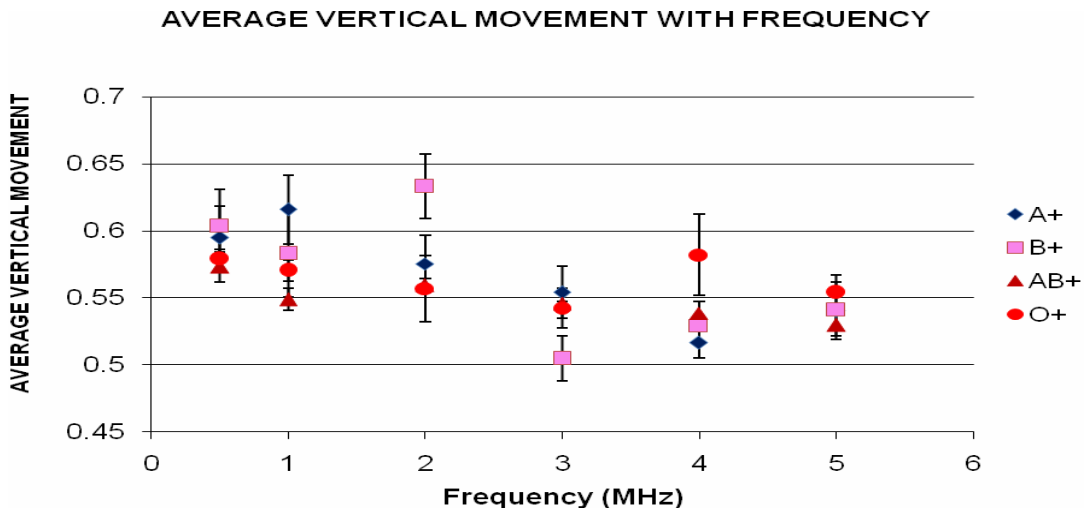

(b)

Figure 4.1 Plot of Average Vertical Movement (AVM) with changing frequency for positive ABO blood types.

Both plots above represent the same data. (a) without standard error bars (b) with standard error bars.

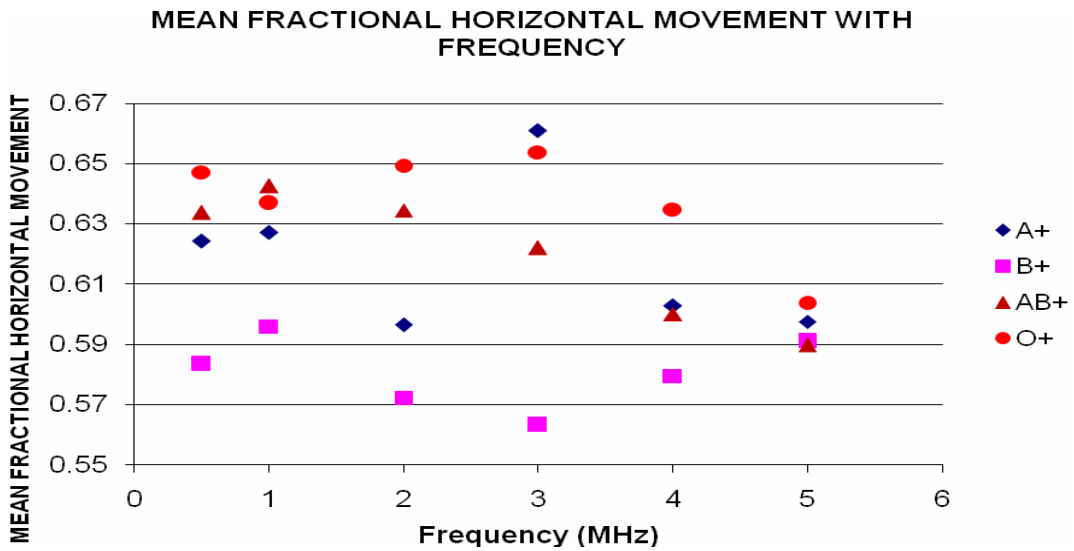

(a)

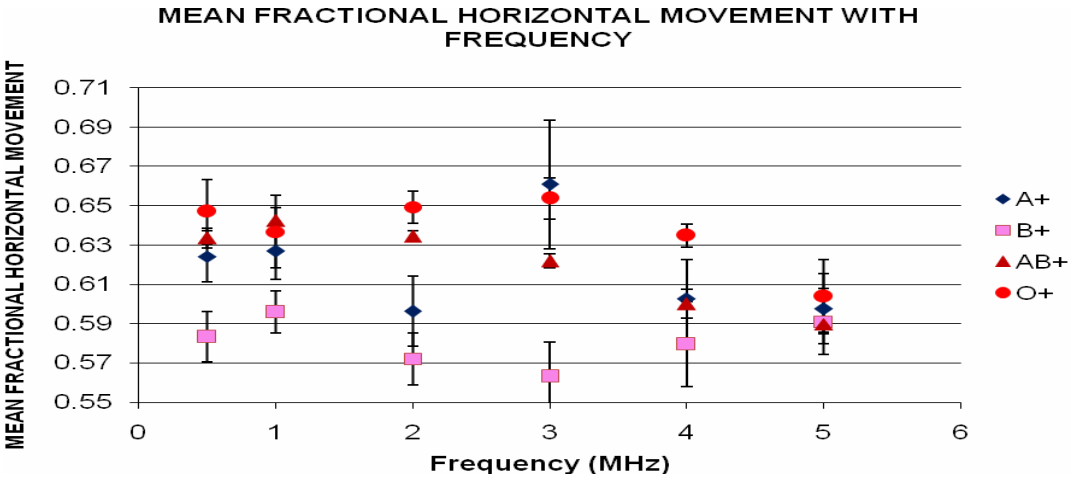

(b)

Figure 4.2 Plot of Mean Fractionalized Horizontal Movement (MFHM) with changing frequency for positive ABO blood types.

Both plots above represent the same data. (a) without standard error bars (b) with standard error bars.

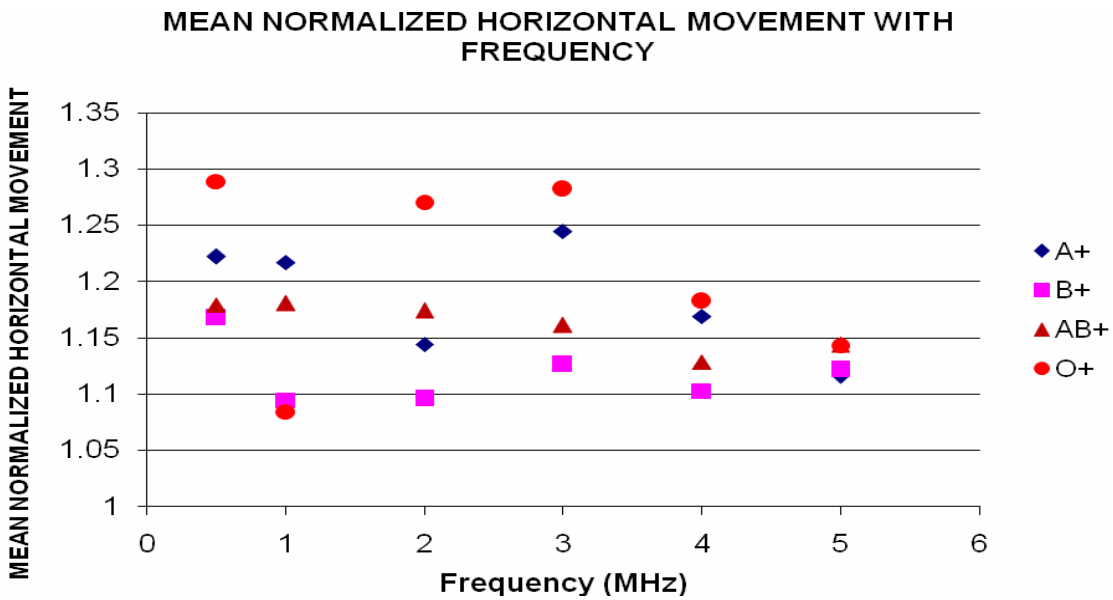

(a)

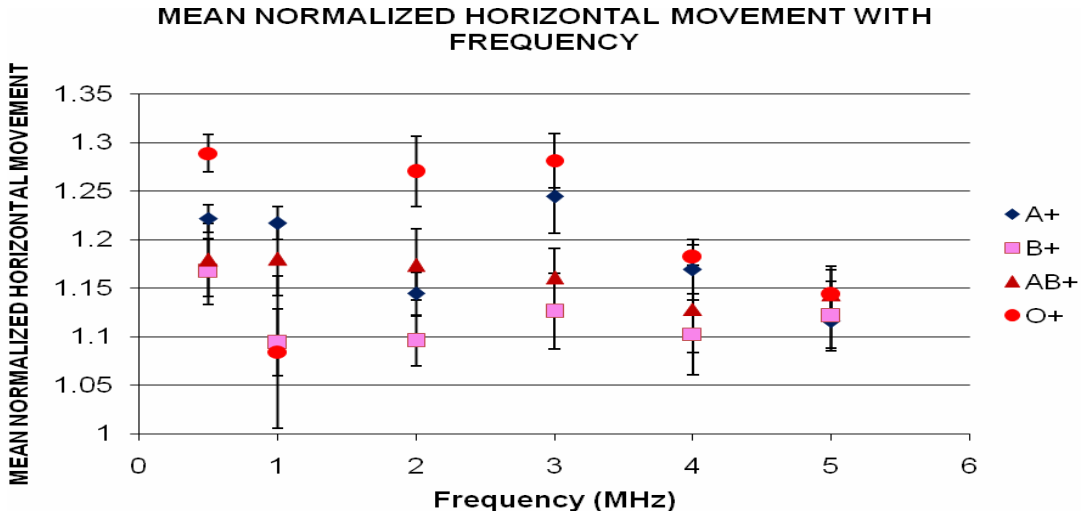

(b)

Figure 4.3 Plot of Mean Normalized Horizontal Movement (MNHM) with changing frequency for positive ABO blood types.

Both plots above represent the same data. (a) without standard error bars (b) with standard error bars.

horizontal movement values. If the error bars are also considered, then at 2MHz, A+ and B+ are not distinguishable. At 0.5 MHz and 1 MHz, only B+ is distinguishable from the rest of the blood type having the least value. At 3 MHz, B+ and AB+ are distinguishable from others and between themselves. At 4 and 5 MHz, all the blood types have statistically similar values.

Fractional horizontal movement for all blood types shows a nonlinear trend over all the examined frequencies. O+ has the maximum value of fractional horizontal movement at all frequencies except at 3 MHz where A+ has the maximum value. B+ almost always has the minimum fractional horizontal movement value. Also B+ is very nonlinear compared to other blood types with a R^2 value of 0.007 for a linear fit. AB+ has a quadratic trend of fractional horizontal movement with increasing frequencies with a R^2 value of over 0.95. A+ has a cubic trend with an R^2 value of just over 0.95 (Table H.2.).

Mean normalized horizontal movement analysis was performed to assess the time dependent horizontal movements of the cells. The time dependent horizontal movement values are shown in Figure 4.3 (a). The scatter plot shows that 2 MHz is a good frequency to separate all blood types, but taking the error bars into consideration (Figure 4.3 (b)), it can be seen that A+ and AB+ are not very distinguishable. At 0.5 MHz, only O+ exhibits a unique highest value. At 1, 3, 4 and 5 MHz, all the blood types have statistically similar values.

The time dependent horizontal movement values also have a nonlinear trend with frequency. O+ had a high time dependent horizontal movement value at all

tested frequencies. B+ has least value for all frequencies except at 1 MHz where O+ has the least time dependent horizontal movement value. O+ is the most nonlinear of all the tested blood types with a R^2 value of 0.05. A cubic polynomial with a R^2 value of 0.938reasonably approximates AB+ frequency dependence. All the blood types showed R^2 values less than 0.95 for polynomial trend lines up to the 3rd degree (see Table H.3. in Appendix H).

4.3 Statistical Analysis

Analysis of variance (ANOVA) and Least significance difference – Multiple comparisons (LSD – MC) were performed on vertical movement, fractional horizontal movement and time dependent horizontal movement data obtained from frequency dependency data. Frequency, blood type, time and Repetitions could have an influence on the data so the model statement was given as follows (Equation 4.2), The interaction between the frequency and blood type was also tested.

Y = FREQUENCY TYPE TIME REPETITION FREQUENCY * TYPE; (4.2)

Where Y can be vertical movement, fractional horizontal movement and time dependent horizontal movement. The parameters have the following levels: FREQUENCY has 6 levels - 0.5, 1, 2, 3, 4 and 5 MHz; TYPE has 4 levels - A, B, AB and O; Time has 2 levels – 0, 120 (for time dependent horizontal movement time has only one level – 120, hence TIME is removed from the model statement), REPETITION has 3 levels – R1, R2 and R3.

4.3.1 Average vertical movement

The model in Equation 3.2 fit well for average vertical movement data giving a P value of less than 0.0001. Hence an alpha value of 0.05 is chosen for analysis. At this alpha value, there was no sufficient evidence to suggest that frequency and blood type have a significant influence on the vertical movement data. There was significant influence by time and repetitions on the data. ANOVA also revealed that there was no significant interaction between frequency and blood type. LSD –MC showed that all the levels of \blood type were same at an alpha = 0.05. Frequencies of 2 MHz and 4 MHz were significantly different from each other and from the rest of the frequencies.

4.3.2 Mean fractional horizontal movement

Fractional horizontal movement data were fit to the model in Equation 3.2 and it resulted in a good fit with P value of less than 0.0001. An alpha of 0.95 was considered for analysis. At this level, frequency did not significantly affect the fractional horizontal movement values. Blood type, time, repetition significantly affected fractional horizontal movement. ANOVA also suggested that there was no interaction between frequency and blood type. LSD – MC on blood type suggested that B+ was significantly different from O+ and AB+. There was no sufficient evidence to suggest that A+, B+ and AB+ were statistically different at an alpha of 0.05. LSD – MC on frequencies suggested that 1 MHz was significantly different from 4 and 5 MHz but the rest of the frequencies were not significantly different.

4.3.3 Mean normalized horizontal movement

The model statement in Equation 3.2 was used to fit Mean normalized horizontal movement data and it resulted in a P vale of 0.5129. This is a low P value and hence the results obtained from it are not very robust. Nevertheless, the results are discussed here with an alpha of 0.55. At this level, blood type and repetitions have a significant influence on the time dependent horizontal movement data. There is insufficient evidence to suggest that frequency has a significant influence on time dependent horizontal movement data. Also, there was no sufficient evidence to suggest that there was significant influence between frequency and blood type. LSD – MS on blood type at alpha of 0.55 showed that all blood types were significantly different from each other. LSD –MS on frequency at the same alpha level showed that 0.5, 3 MHz were significantly different from the rest but not from each other.

Conclusions were drawn based on the discussion above and are presented in chapter 6 and recommendations in chapter 7.

4.4 Conclusion

This chapter discussed the frequency dependency of dielectrophoresis of erythrocytes. The hypothesis tested was that the ABO blood type of the erythrocytes has an effect on their dielectrophoretic response to varying frequencies. This was confirmed by the fact that trend of vertical and a horizontal movement of erythrocytes at different frequencies were different for each blood type. It was also tested to find an optimal frequency for differentiating all 4 positive ABO blood types but the picture did not

emerge clearly. There were certain frequencies where a few blood types were different from each other based on their dielectrophoretic response. But there was no frequency among those tested where all the blood types were different from each other.

CHAPTER 5

F IELD DEPENDENCY

The movement of the erythrocytes in a dielectrophoretic field is dependent on the strength of the electric field gradient. The dielectrophoretic field force is nonlinear with respect to electric field strength as seen from the squared term in the equation below.

$$F = \frac{1}{2} \alpha v \nabla |E_e|^2 \qquad \text{(From 1.1)}$$

Where α is the real part of Clausius Mossotti factor, v is the volume of the cell and E_e is the electric field.

The presence of the quadratic field gradient term in the Dielectrophoresis force expression makes it strongly dependent on the field intensity. Hence field strength was varied and its impact on the dielectrophoretic behavior of erythrocytes was studied for each blood type. The main hypothesis tested was that the increase in field strength has a different impact for all the blood types (see chapter 2). Also, the impact of the electrode geometry was also studied. Hence, instead of varying the

electric potential, the distance between the electrodes was varied keeping the electric potential constant.

The whole project was performed using a microdevice with platinum wire electrodes that were manually cut and positioned. As a result of this construction technique, the electrodes had irregular edges. The effect of electrode shape on the dielectrophoresis was also studied using COMSOL simulation. A dielectrophoretic field with perfectly square electrodes and that with slanted tipped electrodes were simulated and contrasted. A major portion of this chapter will be submitted for publication [93].

5.1 Materials and Methods

The same materials and methods were employed for field dependency (see chapters 3 and 4). The main distinction with field dependency comes in the design of experiments and data analysis. The same variables as in previous chapters – Average vertical movement, Mean fractional horizontal movement and Mean normalized horizontal movement were used to study the dielectrophoretic response of the erythrocytes but now as a function of field strength. The field strength was varied in each experiment by changing the distance between the electrodes from 80 microns to 225 microns while keeping the voltage constant at 6 V_{pp} (see Equation 1.1.).

A microdevice was made by arranging 2 platinum wires in a perpendicular electrode configuration. The electrodes were placed on an adhesive hybriwell slide

and a microscopic slide was attached to it to form a sealed microdevice chamber. The distance between the electrodes was adjusted using a plastic hybriwell strip cut from the edge of a hybriwell slide. This was done by inserting the strip into the microdevice chamber through a sample port and then by sliding the strip sideways to push the electrodes around to get the required distance between the tip of one electrode and the face of another electrode. The distance was measured using measurement software real time with video microscope. The field strength in the dielectrophoretic field was varied by varying the distance and the influence on dielectrophoresis of erythrocytes was studied.

Whole blood was mixed with a phosphate buffer saline (PBS) in a ratio of 1:60. The solution was introduced into the microdevice after washing it 5 times each with pure water and then with PBS solution. The distance between the electrodes was also adjusted values between 80 and 225 microns before filling the device with blood. The blood solution was sucked into the device by placing a few drops of blood solution on a sample port and pressing kimwipe tissue paper on the other port to create suction. After the microdevice was filled with the blood solution, it was once again placed on the microscope stage and a waveform generator was connected via alligator clips. The applied voltage in all experiments was 6 V_{pp} and 1 MHz frequency. The current was applied and the motion of erythrocytes in the device is recorded by video microscopy. The microscope was programmed to take images every 10 seconds for a period of 240 seconds.

The images taken at 0 seconds (before the electric field was applied) and 120 seconds after the field was applied were analyzed using AXIOCAM 4.5. This software after image processing produces an output which contains the X/Y coordinates of the position of each cell. This data was processed in a MATLAB program which gives the parameters of interest – Average vertical movement, Mean fractional horizontal movement and Mean normalized horizontal movement. These are the same as those discussed in Chapter 3.

The experiments were designed to perform 5 different distances between the electrodes in the range of 100 to 200 microns. Since the distance between the electrodes had to be adjusted manually, the range was difficult to be precisely maintained at 100 to 200 microns. Hence, the distances performed in the experiment ranged between 80 and 225 microns. The experiments were repeated 3 times with a newly donated blood sample. These experiments were performed for all four different positive blood types of the ABO blood type system: A+, B+, AB+, O+. The experiments could not be repeated for the precise distance between the electrodes but care was taken to conduct an experiment approximately every 20 microns. Hence when the final analysis was performed, the vertical movement, fractional horizontal movement and time dependent horizontal movement data could not be averaged over the 3 data sets since they did not precisely correspond to the same distance between the electrodes. All the data from each dataset was processed using a MATLAB program written for this purpose and a least squares fit in both the X/Y directions was made to this data. Conclusions were made using this least squares fit data.

5.2 Results and Discussion

5.2.1. Average vertical movement

Vertical movement analysis was performed to assess the positive vs negative dielectrophoresis of erythrocytes. The vertical movement of the erythrocytes was analyzed using average vertical movement (Equation 3.2) parameter. The vertical movement data was fit to a linear regression subject to the least squares conditions by a MATLAB program. The output of the data is shown in Figure 5.1 for each blood type separately. The linear regression data is shown in Table 5.1. The slopes of all blood types are negative showing a decreasing trend. Except for A+, all the intercepts are comparable. The data is most linear for A+ compared to the rest of the blood types. AB+ and B+ have high scatter and has a R-squared value of less than 0.1. A point (field strength = 0.075, AVM = 0.635) for AB+ was a suspected outlier (Figure 5.1). Hence Q – test was performed on it to ascertain whether it had to be retained. The observed Q value Q_{obs}, was calculated using equation 5.2 and was found to be 0.1643.

$$Q = \frac{SuspectValue - NearestValue}{Largest Value - SmallestValue} \tag{5.2}$$

The critical Q value from standard tables at 95% confidence level for a dataset with 15 observations is 0.384. Since the observed Q is less than the critical Q value, the suspect outlier of AVM = 0.635 has to be retained.

5.2.2. Mean Fractional horizontal movement

Mean fractional horizontal movement analysis was conducted to assess the movement of the cells horizontally across the dielectrophoretic field (equation 3.3). The horizontal movement of the cells relative to image dimensions was studied by the variable fractional horizontal movement. The data was also fit to a linear least squares regression for all the 4 positive blood types (Figure 5.2). The data showed a similar increasing trend for all blood types. A+ has the steepest increasing trend with the highest positive slope (Table 5.2). B+ and AB+ have similar slopes. O+ has the least slope showing a slower response of AVM with increasing field strength. The intercepts of all 4 blood types were comparable. A+ had the best linear fit of all (Table 5.2). O+ data is the most scattered with a linear R-squared value of less than 0.1.

5.2.3. Mean normalized horizontal movement

Mean normalized horizontal movement analysis was performed to understand the time based horizontal movement of the dielectrophoresis of erythrocytes with increase in field strength (equation 3.4). A linear least squares fit was made to this data and is illustrated in Figure 5.3. The regression lines show increasing trend for all blood types. Like for fractional horizontal movement, A+ has the steepest increase with the highest slope compared to the rest of the blood type. O+ has the lowest slope of all suggesting a milder response of time dependent horizontal movement to

increasing field strength. B+ and AB+ have similar slopes like for fractional horizontal movement. O+ has the most scattered data of all with a linear R- squared value of less than 0.1 (Table 5.3). The intercepts of all the blood types are comparable with O+ having the highest.

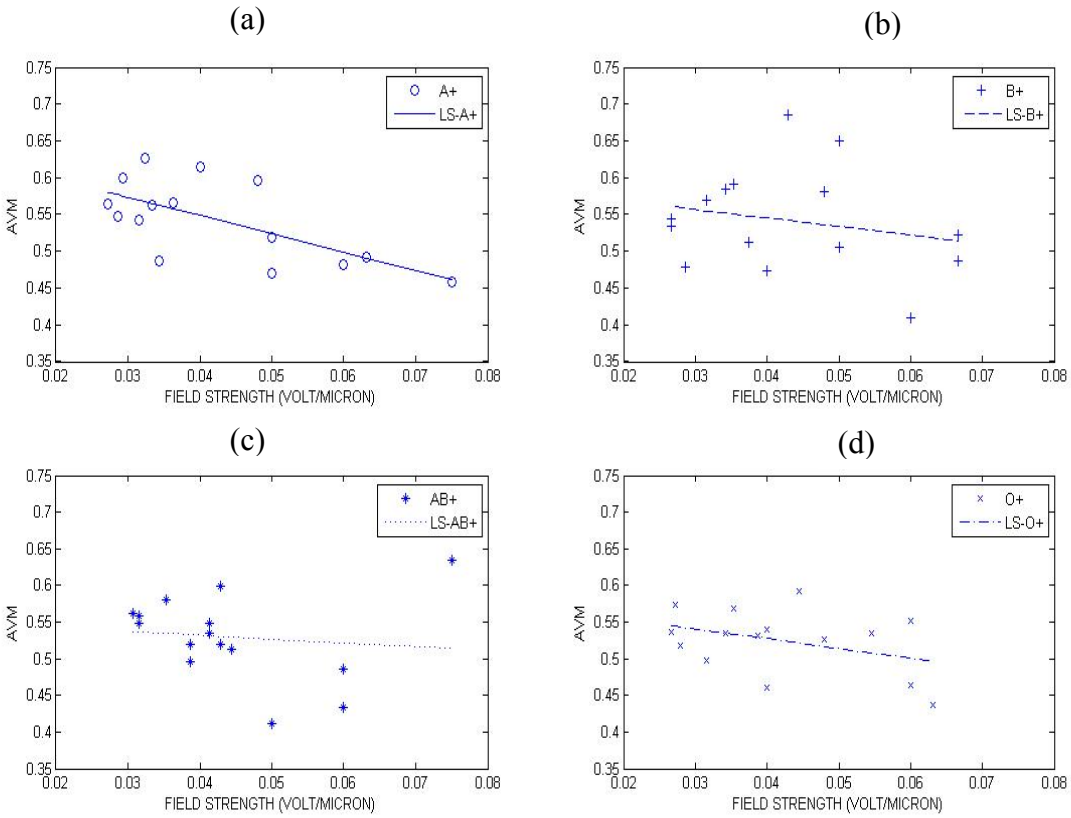

Figure 5.1 MATLAB output showing Average Vertical Movement (AVM) data with varying field strength for all positive ABO blood types

All blood types have a decreasing trend of vertical movement with increase of field strength. A+ has the steepest descent. The figure shows vertical movement trend for (a) A+, (b) B+, (c) AB+ and (d) O+

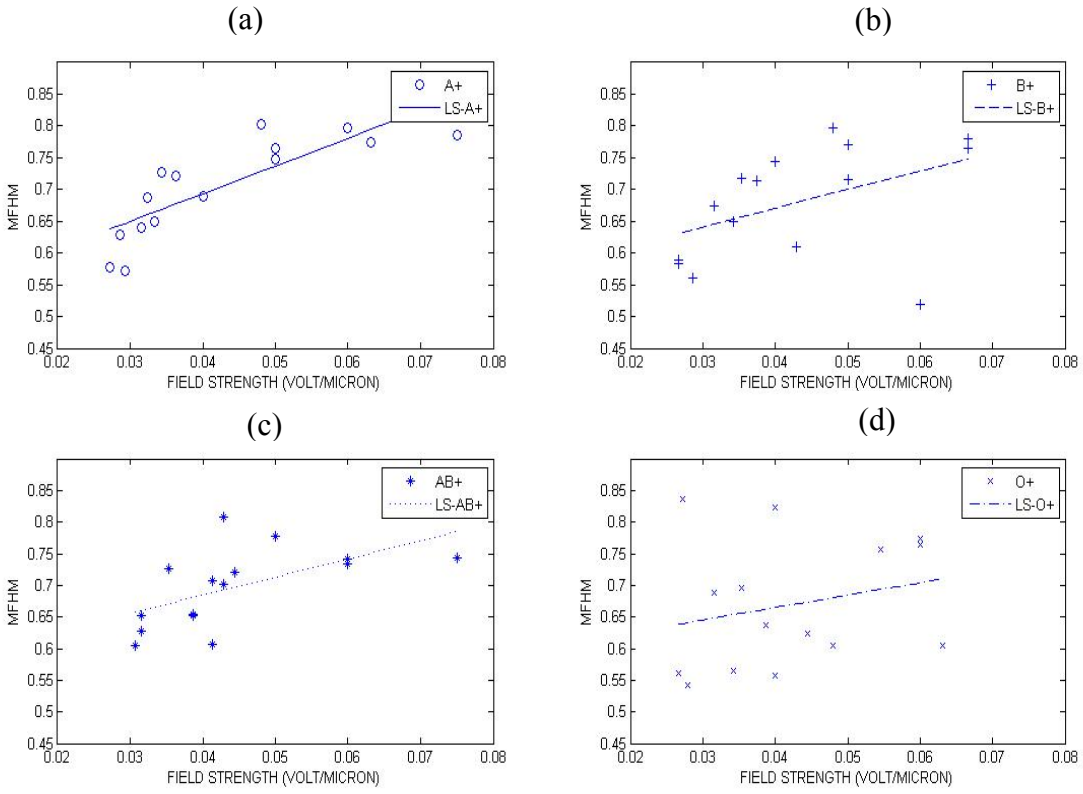

Figure 5.2 MATLAB output showing Mean Fractionalized Horizontal Movement (MFHM) data with varying field strength for all positive ABO blood types

All blood types have an increasing trend of vertical movement with increase of field strength. A+ has the steepest ascent and O+ has the least ascent. The figure shows vertical movement trend for (a) A+, (b) B+, (c) AB+ and (d) O+

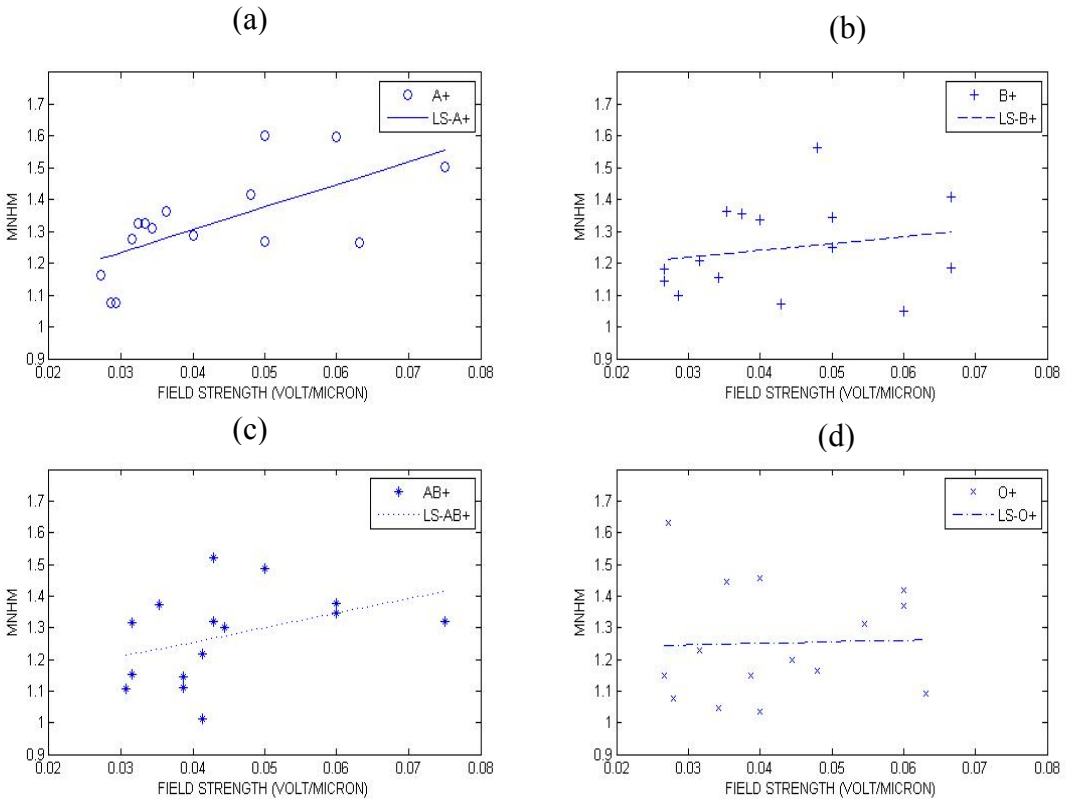

Figure 5.3 MATLAB output showing Mean Normalized Horizontal Movement (MNHM) data with varying field strength for all positive ABO blood types

All blood types have an increasing trend of vertical movement with increase of field strength. A+ has the steepest ascent and O+ has the least ascent. The figure shows vertical movement trend for (a) A+, (b) B+, (c) AB+ and (d) O+

Table 5.1 Linear regression values for Average Vertical Movement (AVM) for field strength dependence

BLOOD TYPE	SLOPE	INTERCEPT	R-squared (AVM)
A	-2.4810	0.6478	0.4344
B	-1.1616	0.5916	0.0490
AB	-0.4897	0.5514	0.0163
O	-1.3539	0.5814	0.1528

Table 5.2 Linear regression values for Mean Fractional Horizontal Movement (MFHM) for field strength dependence

BLOOD TYPE	SLOPE	INTERCEPT	R-squared (MFHM)
A	4.3716	0.5181	0.6762
B	2.9329	0.5531	0.2013
AB	2.8763	0.5697	0.3344
O	1.9713	0.5858	0.0595

Table 5.3 Linear regression values for Mean Normalized Horizontal Movement (MNHM) for field strength dependence

BLOOD TYPE	SLOPE	INTERCEPT	R-squared
A	7.1519	1.0192	0.4302
B	2.1782	1.1541	0.0422
AB	4.6033	1.0701	0.1536
O	0.4881	1.2305	0.0012

5.3 Simulation results

It is important to understand the local electric field characteristics to better explain the movement of particles in it. Hence COMSOL multi physics™ was used to simulate a typical nonuniform AC electric field. dielectrophoresis as explained in chapter 1 is a nonuniform electric field. A simulation was conducted as a one half-cycle DC field since the AC field is aligned in a fixed orientation at any given instant. The voltage was 6 V_{pp} and the electrodes were placed in a perpendicular configuration. The voltage was maintained slightly higher at 6 V_{pp} in comparison to 5 V_{pp} taken for blood typing analysis experiments. This was done to study slightly higher field strengths as well.

First, the distance between the electrodes was varied to study the effect of distance between the electrode and field strength. A distance between the electrodes of 100 microns and 200 microns were studied (Figure 5.4). The images show the electric potential at each region on the image. The red region suggests greatest intensity of the potential and blue the other extreme with low field intensity. The figure with 100 microns distance between the electrodes (Figure 5.4 (a)) showed a greater gradient between the electrodes than that of the simulated image with 200 microns between the electrodes (Figure 5.4 (b)). The image with 200 microns between the electrodes showed a greater region in blue, which suggests a large region with low intensity of field. Similarly, the image with 100 microns distance between the electrodes has a large region with red color (Figure 5.4 (a)) suggesting a greater area of high field intensity to that of having 200 microns between the electrodes (Figure 5.4 (b)). This is

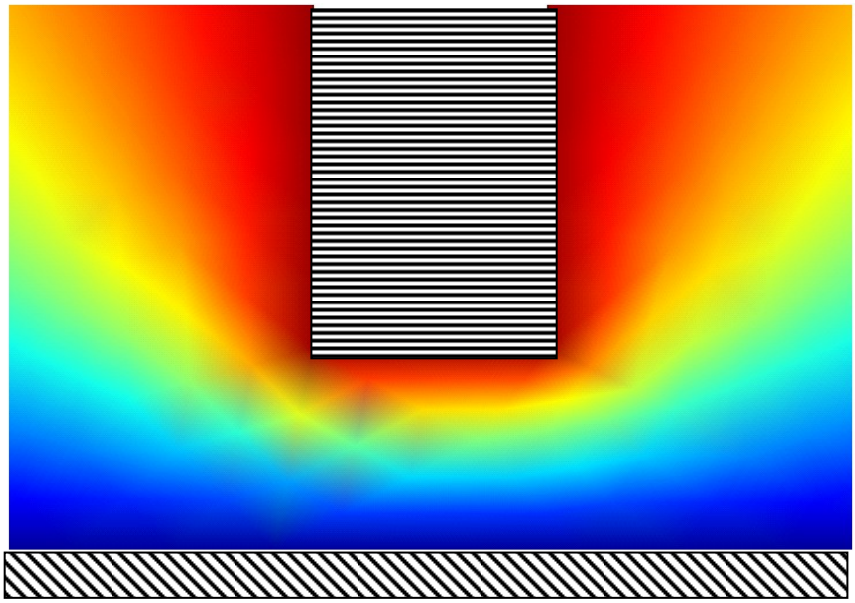

(a)

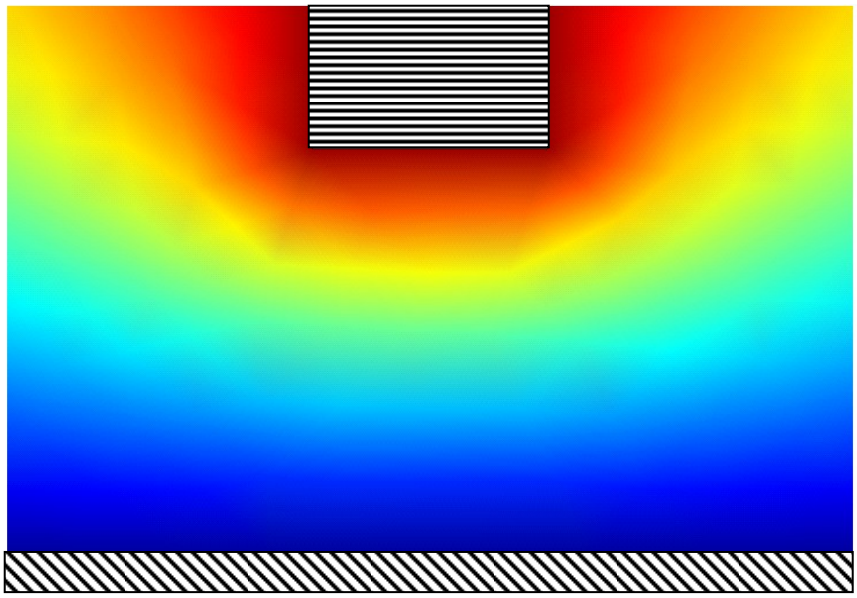

(b)

Figure 5.4 COMSOL simulation of a dielectrophoretic field with (a) 100 microns (b) 200 microns distance between the electrodes and with flat electrode edge

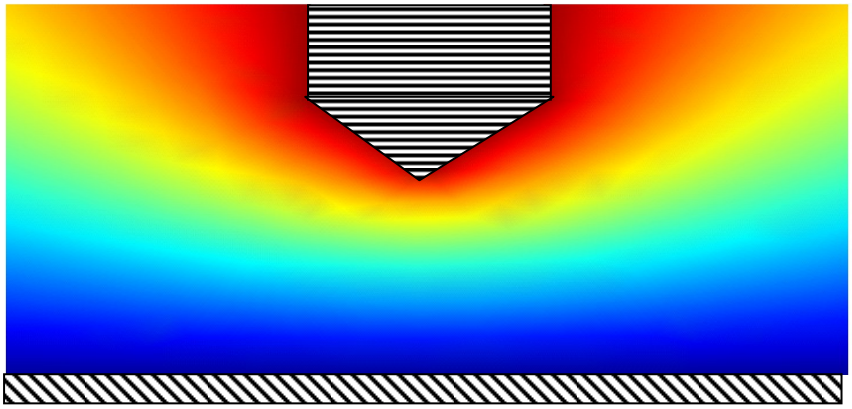

(a)

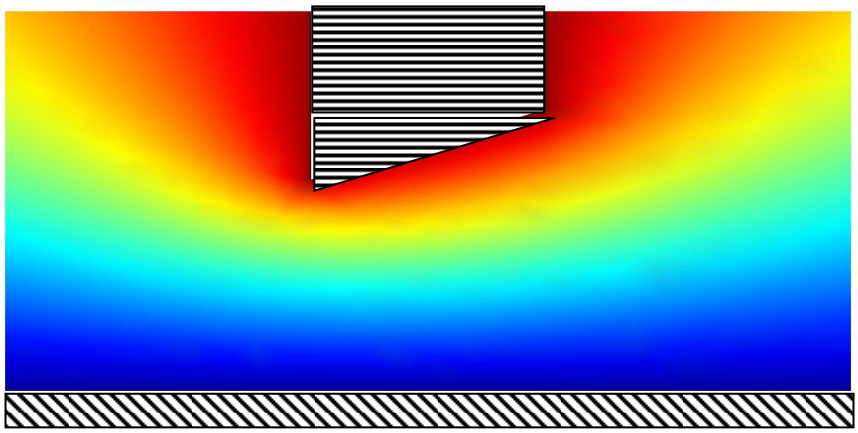

(b)

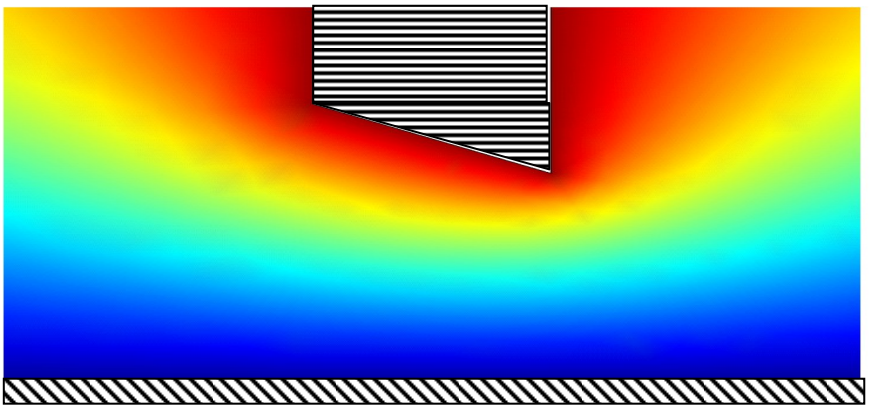

(c)

Figure 5.5.COMSOL simulation of a dielectrophoretic field with 175 microns distance between the electrodes and pointed edge of the electrode

(a) Pointed edge at center (b) pointed edge on far left (c) pointed edge on far right

There is a rapid change in field density for 100 microns distance between the electrodes consistent with the fact that the electric field is greater if the distance between the electrodes is smaller. As expected, intensity changes more rapidly in the spatial dimension when the electrodes are 100 microns apart.

Next, another set of simulations were run where the shape of the high field electrode was varied and the resulting electric field intensity distribution was studied. This is because our custom microdevice without wire preprocessing did not have perfect rectangular edges as suggested (Figure 5.4). Hence an electric field with sharp-edged high field electrode was simulated with a magnitude of 6 V. The distance between the flat electrode and the pointed tip was 150 microns. The tip was designed on a right triangle showing dimensions of 25 microns on the extending leg (Figure 5.5 (a)). Three cases were studied – the sharp edge being at the center, at the far left and the far right sides on the top of the high field electrode. The simulated images are presented in Figures 5.5 (a), (b), (c). The field is observed to be penetrated at the sharp point. There is slightly less blue region (low field) below the pointed region. As expected this penetration is in the centre of the high field electrode near the sharp point. Also the red region (high field) is slightly greater around the pointed electrodes.

In order to understand the difference between the regular rectangular shaped high field electrode and the pointed edged ones, a MATLAB program was developed to read these images as pixel arrays subtract those arrays and convert the subtracted

array into an image. The pixel number is based on its color. If both the pixels being subtracted are of the same color, then the subtracted value is zero. When this number is converted back to an image it will show as black. This subtraction of images was done for all 3 cases of pointed electrodes where the pointed region was at the center of the high field electrode, at the far left and at the far right (Figures 5.6 (a), (b), (c) respectively). The results showed that the difference was milder and mostly confined to the area of the pointed region. The region with a larger difference between the images was colored red and then green followed by blue. The region of colors, for example, in the image with a central pointed edge was confined to the center of the image. It was noteworthy to see that the edges of the image had no effect. It was the same in the case of the pointed regions being at the corners of the electrode. The region of colors was at the corresponding corners. The coloration was also slight showing less difference between the images with regular rectangular edged electrode and the ones with pointed edges. The conclusion that the field density is lower at flat electrodes and that the field becomes weaker at greater distances from the electrodes has already been studied and this simulation reaffirms this fact. [93 -98].

5.4 Conclusion

This chapter discussed the effect of changing field strength on dielectrophoresis of erythrocytes based on their ABO blood types. The hypothesis was that the ABO blood type would have an effect on the response of erythrocytes on changing field strength. The results confirmed this since the linear regression trend of the horizontal

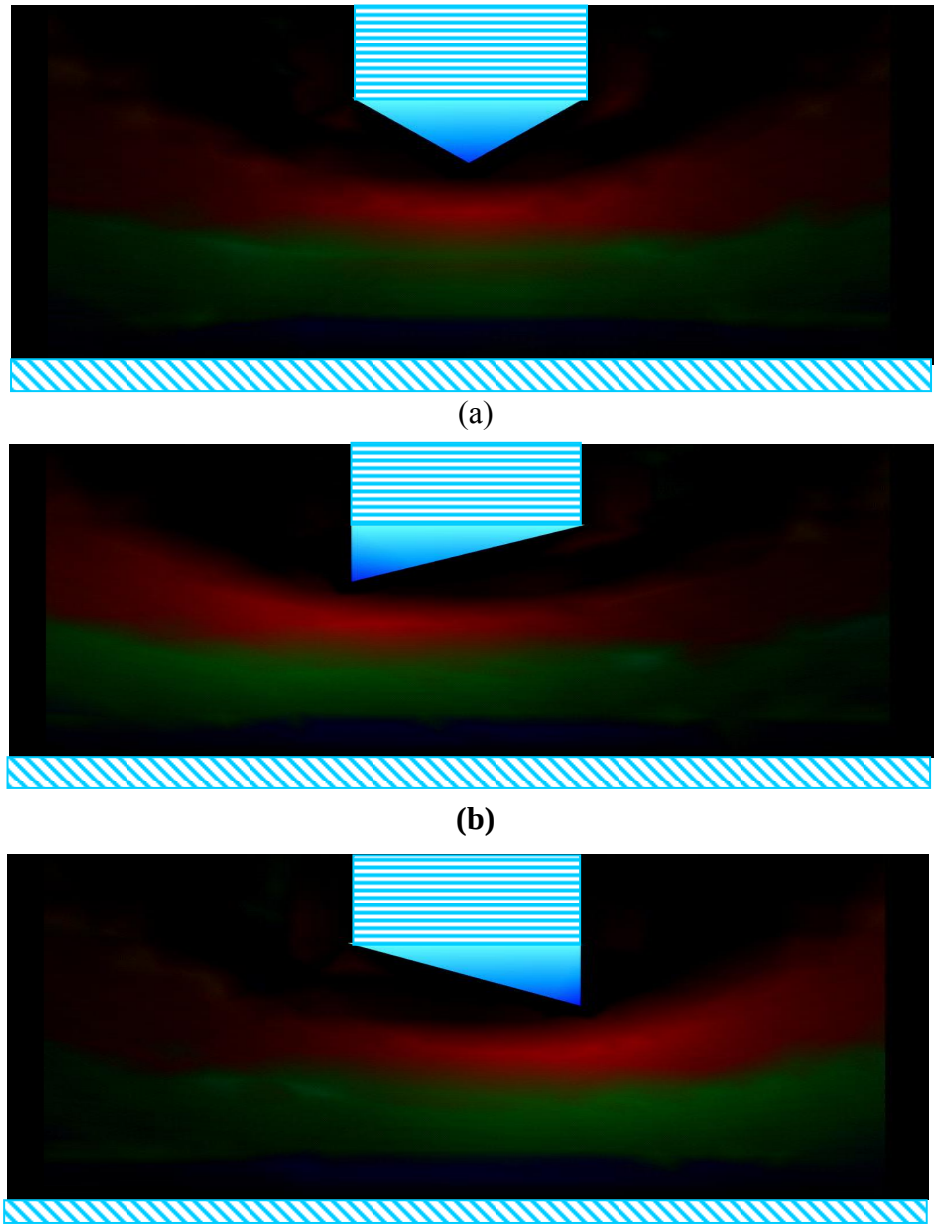

Figure 5.6. The difference in the dielectrophoretic fields of a flat electrode geometry to that of a pointed edge.

(a) Pointed edge at center (b) pointed edge on far left (c) pointed edge on far right

and vertical movements of erythrocytes was different based on their blood type, Particularly the slope of the linear trend line was significantly different for O+ from the other blood types. Dielectrophoretic field was simulated to test the effect of electrode geometry on the field. It was seen that there was higher field density for lesser distance between the electrodes and pointed edge of electrode created a higher field density around it.

CHAPTER 6

OVERALL DISCUSSION AND CONCLUSIONS

This project sought to study the role of blood types in dielectrophoresis of erythrocytes which could lead to an inexpensive, easy-to-use, electrical blood typing instrument. The project showed considerable success, particularly in showing that the dielectrophoresis of erythrocytes depends on blood type. It has been thought that erythrocytes of any blood type could be used interchangeably in their dielectrophoretic experiments. The results shown in this work have proven otherwise. A broad discussion of the results in light of the motivation for the work is discussed below. Also, the field and frequency dependency on the dielectrophoretic behavior of erythrocytes is discussed. The efficacy of using custom made microdevice was studied and it was found that these microdevices were more reliable than originally presumed. A major part of this chapter will be submitted for publication [1, 91].

6.1 Blood typing

The use of microdevices for blood typing can help increase the speed of emergency medical diagnosis. Dielectrophoresis appears to be a potential tool for this purpose. The main hypothesis tested in this part of research was that, dielectrophoresis of erythrocytes depends on their ABO blood type (see chapter 2.

Accordingly, this work has validated the capacity of dielectrophoresis as an analytical tool to differentiate positive blood types without pretreatment or cell modification. The three variables selected, Average Vertical Movement (AVM), Mean Fractional Horizontal Movement (MFHM) and Mean Normalized Horizontal Movement (MNHM) have captured the differences in the dielectrophoretic movement of the erythrocytes based on their blood types. Particularly, the low values of O+ were correlated with the fact that it had no ABO antigens on its surface. Also, the ANOVA and LSD –MC results suggested that blood type strongly influenced the dielectrophoresis of erythrocytes. In particular, LSD – MC suggested that O+ was significantly different from other blood types for both vertical movement and time dependent horizontal movement data at an high confidence level of 95 %. Other blood types were influenced to varying degrees. This suggests that the dielectrophoresis as a phenomenon is influenced by the expression of the antigen molecules on the surface of cells. This has significant ramifications in the future study of the dielectrophoretic behavior of biological cells. The results have shown good accuracy with reasonably small standard errors. LSD – MC results also suggested that day of experimentation was influencing the data. Hence future experiments should be done on the same day. It was interesting to note that for both vertical movement and time dependent horizontal movement, day interacted significantly with blood type. This shows that the way blood degenerates with days of storage depends on it blood type. As expected, the time of dielectrophoresis significantly influenced the values of vertical movement, fractional horizontal movement and time dependent horizontal

movement. While the fact that repetitions significantly influenced the data was a matter of concern, it brought into light that more parameters like gender of the blood donors, their race, health, food intake might be influencing the dielectrophoresis of their erythrocytes. These suspected parameters need to be isolated and studied in future experiments. Also, since a custom made microdevice was used, the electrodes were not exactly perpendicular and hence there was variability in the field as COMSOL simulation suggested. However, the method has shown enough robustness to differentiate dielectrophoretic movement of erythrocytes based on blood types. Overall, it was found that 60 seconds for vertical movement and 90 seconds for fractional horizontal movement and time dependent horizontal movement were better times to further explore the separation of cells. It was also seen that the values of vertical movement, fractional horizontal movement and time dependent horizontal movement come converge to similar values after 90 seconds. This was suspected being due to loss of cells in the microscope field of view, but analysis did not support this (Appendix K).

6.2 Frequency dependency

Frequency of the AC field is an important parameter in the dielectrophoresis of the erythrocytes as it controls the Clausius Mossotti factor and hence the dielectrophoretic force. This is the first body of work to study how the frequency varies with each blood type with a hypothesis that ABO blood type has an impact on the way frequency effects dielectrophoresis of erythrocytes (see chapter 2). Though

the Clausius Mossotti factor was not measured quantitatively for each blood type, it is understood from dielectrophoretic force equation that the frequency dependency of dielectrophoresis arises from this factor. Our experiments showed that the movement of erythrocytes is not the same with each blood type with a change in frequency of the field. There were frequencies where the difference was minimal in either vertical movement of cells or horizontal, and there were frequencies where there was a difference between the motion of the particles based on at least a few blood types (see Chapter 4). Of particular interest is the difference between the O+ and AB+ as these are universal donor and universal receptor for blood transfusions respectively. The differences between these particular blood types should also be understood in the light of the fact that O+ does not have any of the ABO antigens while AB+ has both A and B. Hence at 1 MHz these two blood types are distinguishable, and at 4 MHz, O+ is distinguishable from the rest of them. At 3 and 4 MHz, the fractional horizontal movement of the cells is distinguishable for AB+ and O+. At 0.5, 2 and 3 MHz these blood types could be distinguished based on the normalized horizontal movement. It was observed that there was no single frequency at which all the blood types were different based on all three parameters. The important observation was that there were few instances where there were different blood types showed a different response based on the frequency of the AC field. Hence it can be concluded that the blood type of the erythrocyte should be taken into consideration while studying the frequency dependence on erythrocyte dielectrophoresis. Overall, A+ and B+ showed close dielectrophoretic behavior since they A and B antigens have similar structure

differing by a galactose addition for B while A has a N-acetylgalactosamine (Figure 1.2).

While quite a few interesting observations were made based on the graphs, the ANOVA test did not agree that frequency at 95% confidence level was significantly affecting the parameters at – vertical movement, fractional horizontal movement and time dependent horizontal movement. The main reason for this could be that the frequencies tested are of few MHz range (from 0.5 to 5). Further experiments might be recommended to be performed in 10's or 100's of MHz range to see the influence of frequency in more substantial manner. LSD –MC picked up a few instances where one or two frequencies were different from a few others. The picture was not clear because of the limited range of frequencies tested. It should also be noted that frequency dependency data was tested only at 0 seconds and 120 seconds. Research in Dielectrophoretic Blood typing presented in chapter 2 revealed that 60 seconds for vertical movement and 90 seconds for fractional horizontal movement and time dependent horizontal movement might be better time periods to study. A study at those time periods might reveal new insights. Repetitions had a significant influence on the data. As discussed in the case of blood typing in section 5.1, the parameters influencing the blood donors like age, race, gender, food should be isolated and studied. A detailed discussion of the results is presented in chapter 5.

6.3 Field dependency

The electric field applied to the erythrocyte suspension provides energy for their movement. The hypothesis tested here was that dielectrophoretic response of erythrocytes to a change in field strength depends on their ABO blood type (see chapter 2). Hence the influence of this parameter was studied by varying the distance between the electrodes. The field strength was mapped using a COMSOL Multiphysics^{TM} simulation. The results of all three parameters: vertical movement, fractional horizontal movement and time dependent horizontal movement, were analyzed using a linear least squares program on MATLAB. The trend of the parameters with increasing field strength showed O+ to have a more distinct trend than all others (Chapter 5). A+ showed a distinguishable trend from others with the steepest behavior in all cases. O+ had the least slope and A+ the highest slope for all parameters. The low slope of O+ indicating least sensitivity to field strength might be due to the fact that it does not have A or B antigens on its surface. On the other end, the high slope values of A+ indicating a higher response to a change in field strength might have to do with the N-acetylgalactoseamine ending of the A+ antigen. In general, O+ had the most scattered data with least linear R- squared values. These observations again underline how the erythrocytes respond differently to field parameters based on their blood type due to the presence of different surface antigens.

COMSOL simulation showed that field density is maximum near the high field electrode and decreases with distance from it. It also showed that the pointed edges have high field concentration near them compared to the flat electrodes, which

is a verification of the concept known in literature. The pointed edged simulation images were subtracted from the flat electrodes imaged to delineate the difference clearly using a MATLAB program. Though output from this program showed that the difference is mainly concentrated near the pointed edge and localized for a small distance around it. While this clearly points to the fact that the microdevices used for the experiments in this work have room for improvement, it also showed that the difference was not too high for a preliminary assessment of the role of blood types in the dielectrophoresis of erythrocytes. A detailed discussion of the results is presented in chapter 5.

6.4 List of conclusions

6.4.1 Blood typing

- The main outcome of the research is that presence or absence of ABO antigens on erythrocyte surface significantly affects the dielectrophoretic behavior of erythrocytes.
- O+ is significantly different from all other blood types at a confidence level of 95%.
- The methods used in the present research could not show significant differences between A+, B+ and AB+ at a confidence level of 95%.

- O+ showed milder response to dielectrophoretic field probably due to lack of any ABO antigens on its surface
- Day and blood type significantly interact with each other. This suggests that the way blood degrades over storage is influenced by its blood type.
- Repetitions were significantly influencing the data. This suggests that some parameters like gender, race, health, age, etc. of the donors influence the dielectrophoresis of their erythrocytes.

6.4.2 Frequency dependency

- In the tested range of 0.5 MHz to 5 MHz, there was no significant influence of frequency of the field on the data.
- From the graphs, some frequencies like 1MHz and 3MHz showed separation of at least one blood type based on standard errors.
- Frequency dependency was tested by analyzing data for 0 seconds (before the application of field) and 120 seconds after field application but 60 seconds and 90 seconds may prove more beneficial.

6.4.3 Field dependency

- As the field strength was increased, vertical movement (AVM) was decreased. This might be due to the fact that as field strength becomes sufficiently large, the cells would quickly form into chains and start moving horizontally.

- The horizontal data suggest that as field strength is increased, the horizontal movement also increases.
- A+ is affected most by an increase in field strength and O+ the least.
- Data is quite scattered for O+ showing very low linear R-squared values.
- Simulation data suggested that field intensity changes rapidly in spatial direction for less distance between the electrodes
- Simulation revealed that there is concentration of field at pointed edges of electrodes.
- The irregularity of the field due to irregular shaped electrodes was confined to a small area.

CHAPTER 7

FUTURE WORK

7.1 Fabrication of microdevices

The COMSOL simulation results presented in the Chapter 5 showed that there are slight field variations due to irregular edges of the electrodes. Also, the electrodes are not always exactly perpendicular and hence there is some associated error. The custom microdevices used in this work create some practical problems. The main one is that the electrodes are free to move inside the microdevice chamber and hence the electrodes could change their position during the device positioning on the microscope stage or while attaching the alligator clips to the AC generator. The distance between the electrodes is adjusted to be approximately 150 – 200 microns and hence if the electrodes move by more than 25 microns, the electrode position is to be adjusted again. Sometimes, it was observed that after loading the device with the blood sample, the electrodes changed their position and hence the electrode had to be cleaned up, the distance adjusted and the experiment restarted. In spite of all these challenges, the custom microdevices were successfully used for making an assessment of the dielectrophoresis of erythrocytes based on their ABO blood types. The idea was to use inexpensive, nonfabricated device for the study.

Addressing the need for a fabricated microdevice for future work, a preliminary design was developed for fabrication on a glass wafer. The device would have a length of 46 mm and breadth of 5 mm. The device would have a microdevice chamber depth of 50 microns. Each device would have 8 dielectrophoretic field areas characterized by a perpendicular configuration of electrodes (Figure 7.1, 7.2). The high field electrode is 100 microns wide and 6.625 mm long projecting into the chamber (Figure 7.2). In Figure 7.3, the high field electrode project into the chamber and these are set 3.5 mm apart. The high field electrodes are attached to a metal base which is connected to the AC electric supply. Also, flat electrode region across the high field electrode acts as a low field electrode to setup a dielectrophoretic field.

The microdevice is cut out of a 3 inch glass wafer and the electrodes are implanted on it. First a 50 micron depth chamber is cut out of the glass and the electrodes, preferably platinum, are electro-depositioned on it. Then another glass slide is drilled with sample ports and laid on the patterned glass wafer to form a sealed microdevice. The layout of the device on the wafer is shown in Figure 7.4. The layout was made and dimensions adjusted in order to have a maximum number of devices made from each glass wafer.

The main challenges in making these devices are the etching of glass and electroplating of the electrodes. Normally microdevices are made from silica wafer using standard procedures. In the work presented here, the erythrocytes are observed under a microscope and the images analyzed using software which recognizes cells

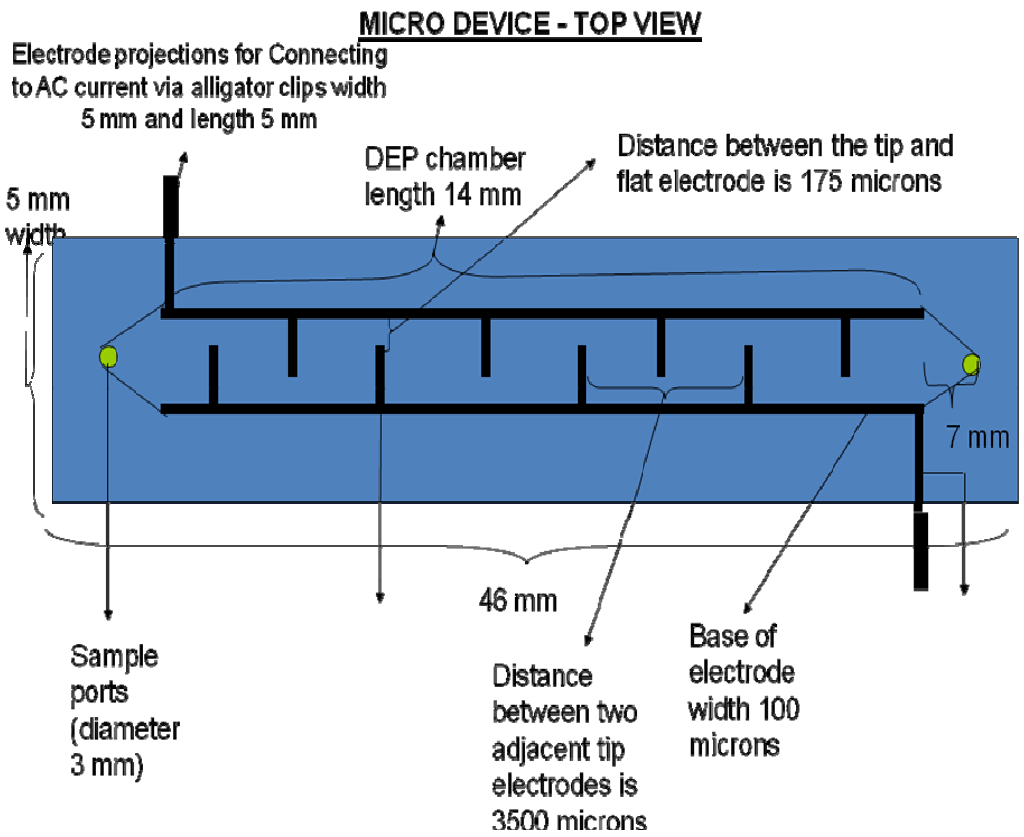

Figure 7.1 Top view of the proposed microdevice layout

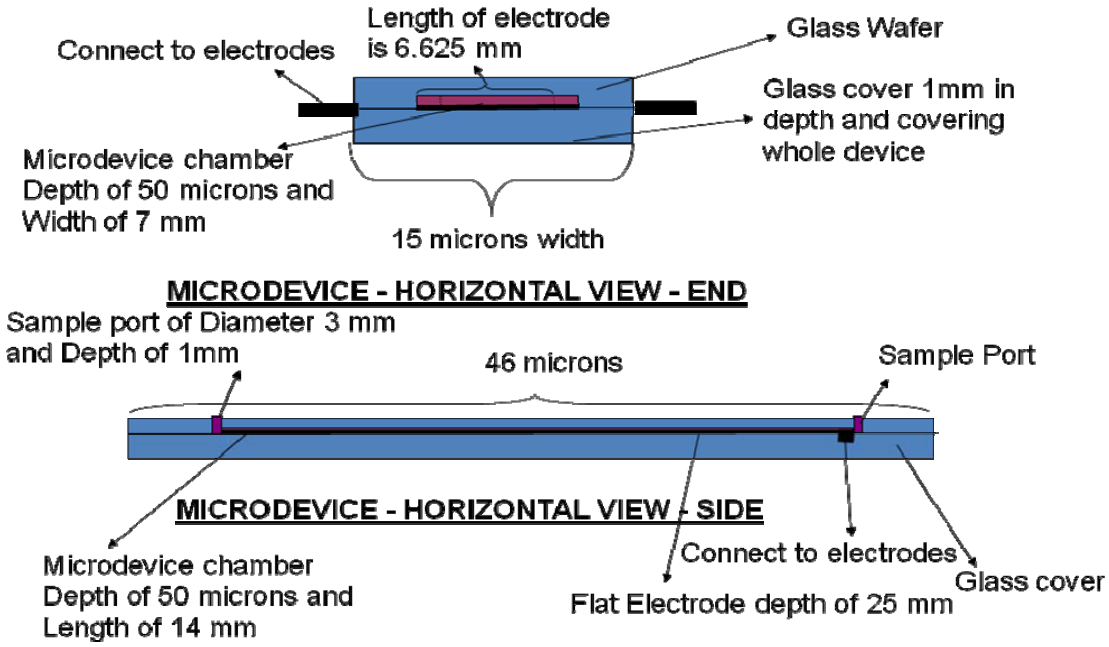

Figure 7.2 Horizontal views of the proposed microdevice layout

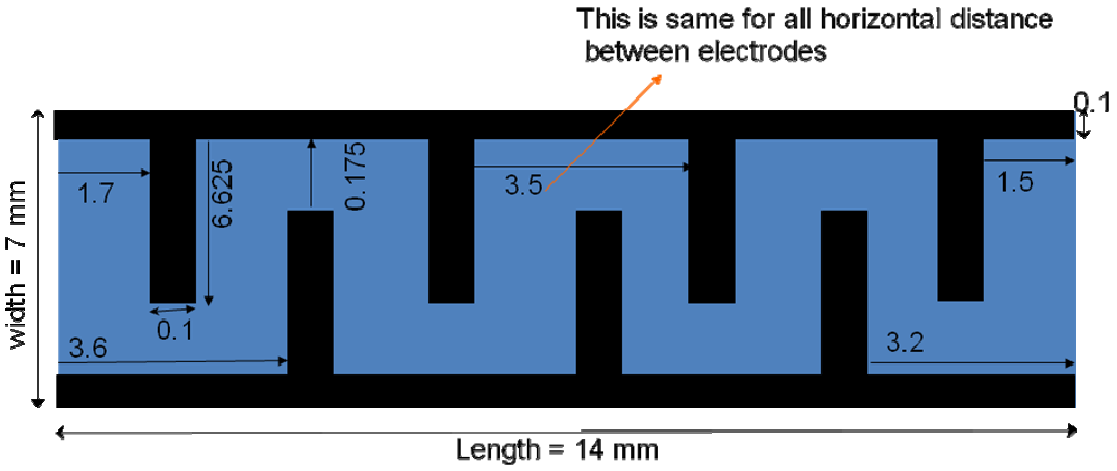

Figure 7.3 Details of the interdigitated microdevice structure

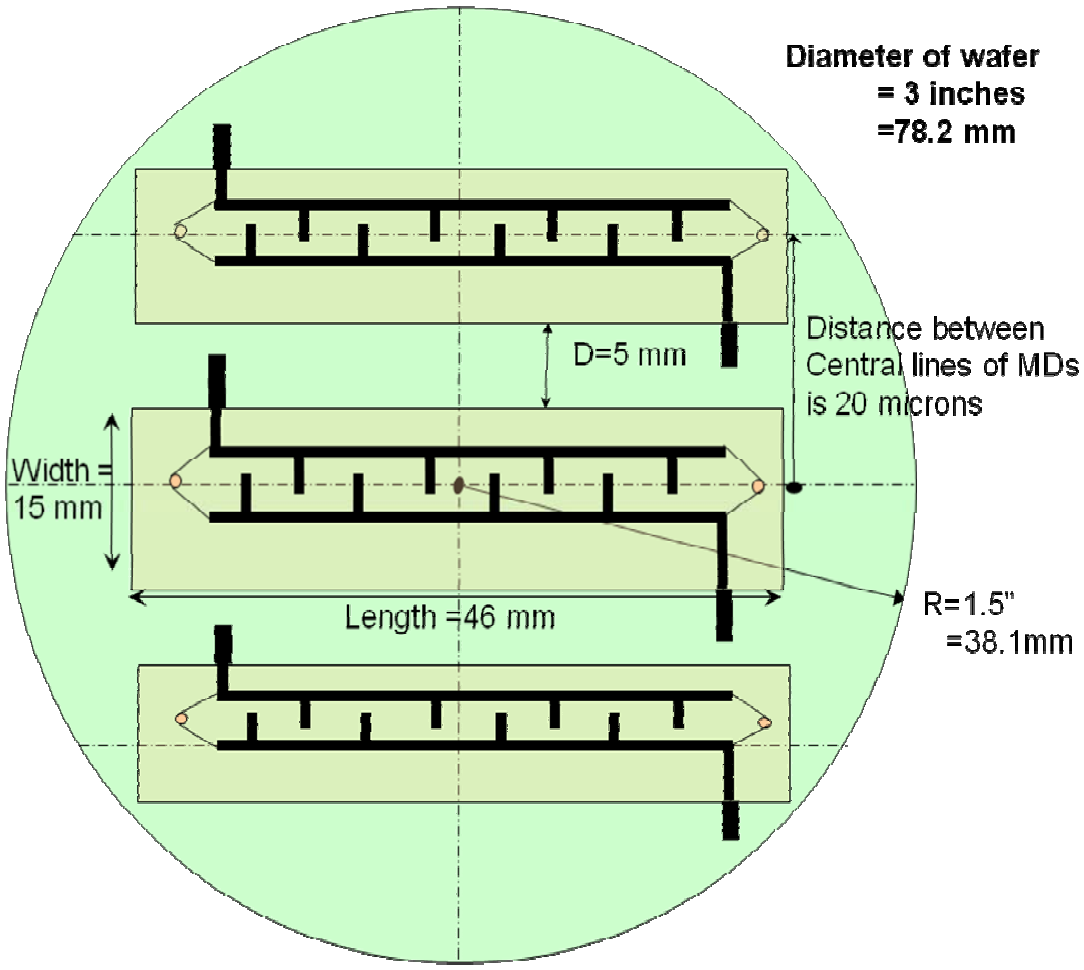

Figure 7.4 Top view of the proposed microdevice layout on a 3 inch circular glass wafer

based on the optical intensity difference of cells with respect to the background, the microdevice needs to be transparent at all wavelengths. It is unusual to fabricate microdevices from glass and hence the procedure is not well developed. The etching of glass could also lead to its frosting and hence decreasing the transparency. The electrodes plated in microdevices are only a few microns thick unlike the 100 microns thick wire used in the experiments presented in this work. Hence all these parameters need to be studied and analyzed before fabricating a new microdevice. A preliminary assessment of the devices was made as seen from the Figures 7.1 – 7.4. The detailed calculations for the fabrication of these devices are given in Appendix J.

7.2 Further experimentation

ABO blood type antigens differ only by a slight modification of the base H substance. Hence the results that show that the dielectrophoresis of erythrocytes depends on their blood type is quite interesting. Further experiments should be performed to fully quantify the differences between blood types. Options include tagging the erythrocytes with relevant chemical species or nano particles that would attach only to a specific type of the ABO blood type when mixed with the blood solution and not to others and have a significant impact on the dielectrophoretic behavior of the erythrocytes. Such materials are to be studied in detail. These materials need to be easy to use since the ultimate goal of this research is to come up with a microdevice which can perform blood typing instantly without a laboratory environment.

ABO antigens are a type of sugar present on the surface of erythrocytes along with many other sugars. Methods can be explored which " wash away" all the sugars on the blood surface and hence make the erythrocytes surfaces of all blood types similar; the dielectrophoretic behavior of such cells can then be studied. This would provide a baseline for on the dielectrophoretic behavior of a basic erythrocyte without the influence of ABO antigens. Selective cleaning of sugars on a erythrocyte surface would allow the dielectrophoretic behavior of each ABO antigen to be studied independently. These experiments would help understand the mechanism by which the antigens are influencing the dielectrophoretic behavior of the erythrocytes.

The method by which the dielectrophoresis of erythrocytes is analyzed is by taking images at regular intervals and processing them using AXIOCAM 4.5 which records the X/Y position of cells. This software recognizes the cells by the difference in optical intensity of the cells from the background. Hence it would be useful to increase the contrast of the cells either by fluorescence or by tagging them with nano particles. Erythrocytes are not auto-fluorescent and hence they need to be tagged with some particles which would help in fluorescence. These particles need to be nontoxic and must not change the natural dielectrophoretic behavior of the erythrocytes. The whole analysis of the dielectrophoresis of erythrocytes is by image analysis, using a MATLAB program and plotting graphs. Analysis must be simplified and streamlined for a microdevice produced for blood typing. These can be later integrated into the device for easy use by a physician to ascertain the blood type of the patient easily.

Also only positive ABO blood type behavior was studied in this work. The dielectrophoresis of negative blood types also needs to be studied.

7.3 List of recommendations

- Variability in the microdevice has to be decreased by fixing the shape and position of the electrodes permanently (section 7.1).
- Reproducibility in the data should be made robust by identifying the parameters which influence the erythrocytes like the age, gender, race, health of blood donors and studying dielectrophoresis in each case separately.
- Since the present work did not show significant difference between A+, B+ and AB+ blood type, new experiments have to be designed which would enhance the difference between A and B antigens. This could solve separating A+ and B+ and perhaps, AB+ also,
- The day of experimentation should be kept constant, preferably day 0 as this research is intended in developing blood typing instrument to be used at point of care in physician's office.
- Frequency dependency on dielectrophoresis of erythrocytes has to be studied on a much wider scale possibly between, 10s of MHz to 100s of MHz to see its real effect.
- Frequency dependency and field dependency should be studied by analyzing images at 60 seconds and 90 seconds instead of 120 seconds based on the conclusions in section 6.4.1.

- A+ is more sensitive to field strength compared to B+ and AB+ hence this feature could be utilized for separation of A+ from B+ and AB+.
- Based on Figures 4.1 and 4.2, B+ has distinct vertical movement and fractional horizontal movement values at 3 MHz. This frequency can be further explored to separate B+ from A+ and AB+
- Experiments are to be performed for all negative blood types, A-, B-, AB- and O- to get a complete picture of erythrocyte dielectrophoresis.

REFERENCES

1. Nobel prize, Nobel foundation. http://nobelprize.org/educational_games /medicine/landsteiner/readmore.html, October 2000.

2. Daggolu, P.R., Minerick, A.R., Electrophoresis, (to be submitted in July 2007).

3. Lifeblood, Franklin institute. http://www.fi.edu/biosci/blood/blood.html. May 2007.

4. O'Neil, D. Blood components. http://anthro.palomar.edu/blood/ blood_components.htm. May 2007.

5. Danni, R. Blood-The fluid of life. http://www.phlebotomycert.com /phleb_blood.htm. May 2007.

6. Hematocrit. http://www.medicinenet.com/hematocrit/article.htm. October 2006.

7. Blood Facts. http://www.bloodbook.com/facts.html. October 2006.

8. http://www.biology4kids.com/extras/dtop_micro/7315_580.jpg. June 2007.

9. Olson M.L., Hill C.A., De la Vega H., et al; Transfusion Clinical Biology, 11: 33-39, 2004.

10. Williamson L.M., Vox Sang 83: 65 – 69 (Suppl 1).

11. Nobel foundation. Blood typing. http://nobelprize.org/educational_games/ medicine/landsteiner/readmore.html. May 2007.

12. Sancho M., Martinez G., Martin C., Journal of Electrostatics 57 (2003), 143 – 156.

13. Gheorghiu, E., Ann. N Y Acad Sci. 1999, 873, 262-268.

14. Sheffield P.W., Tinmouth A., Branch D.R., Transfusion Medicine reviews 19, 2005, 295 – 307.

15. Patenaude S.I., Sato N.O.L., Borisova S.N., Szpacenko A., Nature structural biology , vol 9, 2002, 685 – 690.

16. Zmuda-Trzebiatowska, E. Glycosylation. http://www.cryst.bbk.ac.uk/pps97/assignments/projects/emilia/abo.gif. May 2007.

17. Lloyd K.O., Kabat E.A., Layug E.J, et al, Immunochemical studies on blood groups, XXXIV. Biochemistry 5, 1966: 1489 – 1501.

18. Lloyd K.O., Kabat E.A., Biophys Res. Commun. 1964, 16, 385 – 390.

19. Blood typing. http://adam.about.com/encyclopedia/Blood-typing.htm. May 2007.

20. Cutler, C. Blood typing. http://www.nlm.nih.gov/medlineplus/ency/article/003345.htm. May 2007.

21. Vaughn, A. Blood type chart – ABO. http://www.vaughns-1-pagers.com/medicine/blood-type.htm. May 2007.

22. Table of blood group system. http://blood.co.uk/ibgrl/ISBT%20Pages/ISBT%20Terminology%20Pages/Table%20of%20blood%20group%20systems.htm. May 2007.

23. Landsteiner K.L.P., Proc Soc Exp Biol Med 1951, 24, 941 – 942.

24. Levine P. B., Bobbitt O., Waller R.K., Soc Exp Biol Med 1951, 77, 403 - 405.

25. Muller, T., Fielder, S., et al., Biotechnol Tech. 1996, 10, 221 – 226.

26. Radin N.S., J. Lipid Res 1984, 25, 1536 – 1540.

27. Degroote S., Wolthoorn J. Van Meer G., Semin Cell Dev Biol, 2004, 15, 375 – 387.

28. Harouse J.M., Bhat S., Spitalnik S.L., et al, Science 1991, 253, 320 – 323.

29. Bhat S., Spitalnik S.L., et al, Proc Nat Acad Sci USA 1991, 88, 7131 – 7134.

30. Mahfoud R., Mylvaganam M., et al, J. Lipid Res 2002, 43, 1670 – 1679.

31. Luban N.L., Tranfusion 1994, 34, 821 – 827.

32. Weigel-Kelley K.A.,Yoder M.C., Srivastava A., Blood 2003, 102, 3927 – 3933.

33. Goldin, C., Caprani, A., Eur Biophysics J. 1997, 26, 175-182.

34. Draper, C. J., Greenwalt, T. J., Dumaswala, U. J., Transfusion 2002, 42, 830 – 835.

35. Soper S.A., Hashimoto M., Situma C., et al, Methods 2005, 37 (1), 103 – 113.

36. Minerick, A. R., Zhou, R., Takshistov, P., Chang, H. C., Electrophoresis 2003, 24, 3703-3717.

37. Gascoyne, P., Mahidol, C., Ruchirawat, M., Satayavivad, J., et al, Lab on a Chip 2002, 2, 70-75.

38. Pethig R., Huang Y., Wang X., Burt JPH, J. Phys. D. Appl. Phys 24 (1992), 881 – 888.

39. Crews, N., Darabi, J., et al, Sensors and Actuators, (accepted on 27 February 2007).

40. Pham, P., Texier, I., et al, Journal Electrostatics, (accepted on 24 November 2006).

41. Choi, S., Park, J., Lab on a Chip 2005, 5, 1161 – 1167.

42. Yantzi, J.D., Yeow, J.T.W., Abdallah, S.S., Biosensors and Bioelectronics 2006, 22, 2539 – 2545.

43. Castellarnau, M., Zine, N., et al, Sensors and Actuators B 2007, 120, 615 – 620.

44. Cheng J, Sheldon E.L., Wu L., Uribe A. et al, Nature Biotechnology 16, 1998, 541-546.

45. Markx, G.H., Pethig, R., Biotechnol., Bioeng. 1995, 45, 337 – 343.

46. Helmke B.P., Minerick A.R., Proceedings of the National Academy of Science, April 25, 2006, vol 103, 6419 – 6424.

47. Benguigui, L., Shalom, A.L., Lin, I. J., J. Phys. D:Appl. Phys. 1986, 19, 1853 – 1861.

48. Xu, C., Wang, Y., Cao, M., Lu, Z., Electrophoresis 1999, 20, 1829 – 1831.

49. Yuang J., Huang, Y., Wang, X, -B., Becker, F.F., Gascoyne, P.R.C., Anal. Chem. 1999, 71, 911 – 918.

50. Huang, Y., Ju, S., et al, Anal. Chem. 2002, 74, 3362 – 3371.

51. Ichiki, T., Shinbashi, S., Ujie, T., Horiike, Y., J. Polym. Sci. Tech. 2002, 15, 487 – 492.

52. Li, H., Bashir, R., Actuators B 2002, 86, 215 – 221.

53. Rankin biomedical corporation. http://websites.labx.com/rankin/listings.cfm?show=1&catid=1282. October 2006.

54. Bentwich, Z. Plos Medicine. http://medicine.plosjournals.org/perlserv/?request=get-document&doi=10.1371/journal.pmed.0020214. June 2006.

55. The body. http://www.thebody.com/gmhc/issues/novdec01/cheaper.htm. June 2006.

56. Ugaz, V. M., Brahmasandra, S. N., Burke, D. T., Burns, M. A., Electrophoresis 2002, 23, 1450 - 1459.

57. www.marchofdimes.com/professionals/681_1221.asp. October 2006.

58. Beutler, E., Shull, F. Sickle cell Anemia Association. http://www.ascaa.org/comm.htm. October 2006.

59. https://www2.carolina.com/webapp/wcs/stores/servlet/ProductDisplay?memberId=-1002&productId=47047&langId=-1&storeId=10151&catalogId=10101. June 2006.

60. Forestry suppliers Inc. http://www.forestry-suppliers.com/product_pages/View_Catalog_Page.asp?mi=2136. June 2006.

61. Gershtein, S., Gershtein, A. Minim conversion chart. http://www.convert-me.com/en/convert/units/volume/volume.minim.en.html. May 2007.

62. Pohl, H. *Dielectrophoresis*. New York, NY: Cambridge University Press, 1978.

63. Pethig, R., Crit. Rev. Biotech. 1996, 16, 331-348.

64. Vrinceanu, D., Gheorghiu, E., Bioelectrochem. Bioenerg. 1996, 40, 167-170.

65. Gheorghiu, E.,Asami, K., Bioelectrochem. Bioenerg 1998, 45, 139-143.

66. Becker, F. F., Wang, X. B., Pethig, R., Gascoyne, P. R. C., et al, J. Phys. D Appl. Phys 1994, 27, 2659-2662.

67. Becker, F. F., Wang, X. B., Pethig, R., Gascoyne, P. R. C., et al, Proc. Natl. Acad. Sci. USA 1995, 92, 860 – 864.

68. Gascoyne P., Pethig, R., Satayavivad, J., Becker, F. F., Ruchirawat, M., Biochemica et Bio Physica Acta 1997, 1323, 240-252.

69. Borgatti M., Altomare L., Baruffa M., Fabbri E., et al., International Journal of Molecular Medicine 15, 913 – 920, 2005.

70. Coley, H.M., Labeed, F.H., et Al, Biochemica et Biophysica Acta 2007, 1770, 601 – 608.

71. Haab, B.B., Proteomics 2003, 3, 2116 – 2122.

72. Speicher, M.R., Carter, N.P., Nat. Rev. Genet. 2005, 6, 782 – 792.

73. Wheeler, D. B., Carpenter, A., E., Sabitini, D.M., Nat. Genet. 2005, 37, S25 – S30.

74. Washizu, M., Techaumnat, B., Journa of Electrostatics, (accepted 24 december 2006).

75. Yang, M., Lim, C.C., et al, Biosensors and Bioelectronics 2007, 22, 1688 – 1693.

76. Broche, K.M., Bhadal, N., et al, Oral Oncology 2007, 43, 199 – 203.

77. Labeed, F.H., Coley, H.M., Hughes, M.P., Biochim Biophys Acta 2006, 1760, 922 – 929.

78. Labeed, F.H., Coley, H.M., Hughes, M.P., Thomas, H., Biophys J 2003, 85 (3), 2028 – 2034.

79. Gascoyne, P.R. C, Ruchirawat, M., Ratanachoo, K., Biochim. Biophys. Acta 2002, 1564, 449 – 458.

80. Lapizco-Encinas, B. H., Simmons B. A., et al., Electrophoresis 2004, 25, 1695 – 1704.

81. Yuang J., Wang X., Becker F.F., Gascyone P.R.C., Biophysical Journal 78, 2000, 2680 – 2689.

82. Sun, J., Guo, Z., et al., Chemphyschem 2005, 6, 2485 – 2488.

83. Jones, T.B., IEEE Eng. Med. Bio. 2003, 22, 33 – 42.

84. Zhou, H., White, L.R., Tilton, R.D., Journal of Colloid and Interfacial Science 2005, 285, 179 – 191.

85. Durr, M., Kentsch, J., Muller, T., et al., Electrophoresis 2003, 24, 722 – 731.

86. Kadaksham, A. T. J., Singh, P., Augury, N., Electrophoresis 2004, 25, 3625 – 3632.

87. Zheng, L., Li, S., Brody, J. P., Burke, P. J., Langmuir 2004, 20, 8612 – 8619.

88. Martinsen, O., Grimmes, S., Schwan, H., Encyclopedia of Surface and Colloid Science, 2002, (Dekker, New York).

89. Definition of mean cell volume. http://www.medterms.com/script/main/art.asp?articlekey=9990. May 2007.

90. Kunkel, P. Volume of torus. http://whistleralley.com/torus/torus.htm May 2007.

91. Zhang, Z.B., Liu, X.J., Campbell, E.E.B., Zhang, S.L., Journal of applied Physics 2005, 98, 056103.

92. Jones, T.B., Wang, K.L., Yao, D.J., Langmuir 2004, 20, 2813 – 2818.

93. Daggolu, P.R., Minerick, A.R. Electrophoresis (to be submitted in May 2007).

94. Gascoyne, P.R.C, Vyjoukal, J., J., Electrophoresis 2002., 23, 1973 – 1983.

95. Gimsa, J., Wachner, D., BioPhys. J. 1998, 75, 1107 – 1116.

96. Ramos, A., Morgan, H., Green, N., et al., J.Phys D.:Appl. Phys. 1998, 31, 2338 – 2553.

97. Hughes, M.P, Nano technology 2000, 11, 124 - 132.

98. Green, N., Ramos, A., Morgan, H., J. Phys. D: Appl. Phys. 2000, 33, 632 – 641.

APPENDIX A

PROCEDURE FOR CUSTOM MICRODEVICE FABRICATION

1. Take 2 platinum wires of about 3 centimeters each. Make them straight by gently pulling them from one end to the other.
2. Turn one of them into a “L” shape by bending it.
3. Peel off the plastic cover from the hybriwell slide and place the platinum wires on the slide.
4. Press the wires onto the slide where the adhesive is present.
5. Place a microscopic slide on top of this and press it hard. This forms the microdevice chamber.
6. Turn the platinum wires projecting out of the chamber along the edge of the microdevice chamber.
7. Wrap the electrodes seen outside with aluminum foils on each side.
8. Paste aluminum foils onto the microdevice with an adhesive electric tape.

APPENDIX B

PROCEDURE FOR CONDUCTING EXPERIMENTS

1. Take 3 small 50 ml beakers and fill one of them with pure water and another with PBS buffer solution.
2. Clean the microdevice by placing a drop of water one of the sample ports and placing the kimwipe tissue paper on the other sample port.
3. Press the tissue paper to create suction in the chamber and the water moves to the other end. Repeat this for 5 times.
4. Clean the microdevice with Phosphate Buffer Saline (PBS) solution by following the same procedure as for cleaning with water.
5. Make a blood solution in the third beaker by mixing 4.918 ml of PBS and 82 µl of Blood. Mix the solution gently with the micropipette tip.
6. Place the microdevice filled with PBS solution on the microscope bench and adjust the distance between the electrodes to the desired value.
7. The distance between the electrodes can be adjusted by inserting a thin plastic strip into the microdevice chamber via a sample port and then moving the strip sideways to adjust the placement of the electrodes. Also, small distances can be adjusted by gently tapping on the microdevice near the electrode area.
8. Then fill the microdevice with the blood solution following the same procedure as for cleaning it with water or PBS.
9. Place the microdevice on the microscope bench and connect it to the wave form generator via alligator clips.

10. Open the AXIOCAM 4.5 software on the computer to adjust the parameters for video microscopy.
11. Set the computer so as to record the motion of particles for 240 seconds with an interval of 10 seconds.
12. Adjust the parameters on the waveform generator, like frequency of the AC electric field and the electric potential to desired values.
13. Turn on the video microscopy recording and start the waveform generator.
14. After 240 seconds, stop the waveform generator and save the motion of particles as both video file (.zvi) and image files (.jpg).
15. Clean the microdevice with PBS solution and then with water.

APPENDIX C

PROCEDURE FOR DATA ANALYSIS

1. Open AXIOCAM 4.5 program
2. Open the image to be analyzed.
3. Go to MEASURE →RUN PROGRAM (Figure C.1).
4. Click open image and select the program to be run.
5. Turn off the "append" option on the screen and change the file name of the analysis to be formed to the desired file name – e.g. "A+d0t120s"
6. Click "execute".
7. On the next window, the program selects the cells based on the light intensity difference between cells and the image background (Figure C.2).
8. If the selection is not satisfactory, i.e. most cells are not selected of some parts of the image which are not cells are also selected, then click RESET and then click one of the cells. This will make the program select the cells of the same light intensity as the one clicked. This usually results in selection of most cells. Click NEXT.
9. On the next window, There are options to separate, delete or add cell on the left side of the window (Figure C.3). Use these options o select only the cells and not any of the parts of the image. Click NEXT
10. On this window, there is information of the cells on the image including the X/Y position of the cells (figure C.4). Click FINISH.
11. Now on the main window there appear two files- one with data of each cell on the image (with .regs extension) (Figure C.5) and other with total number of cells on the image (with .fld extension) (Figure C.6). Then save the file.

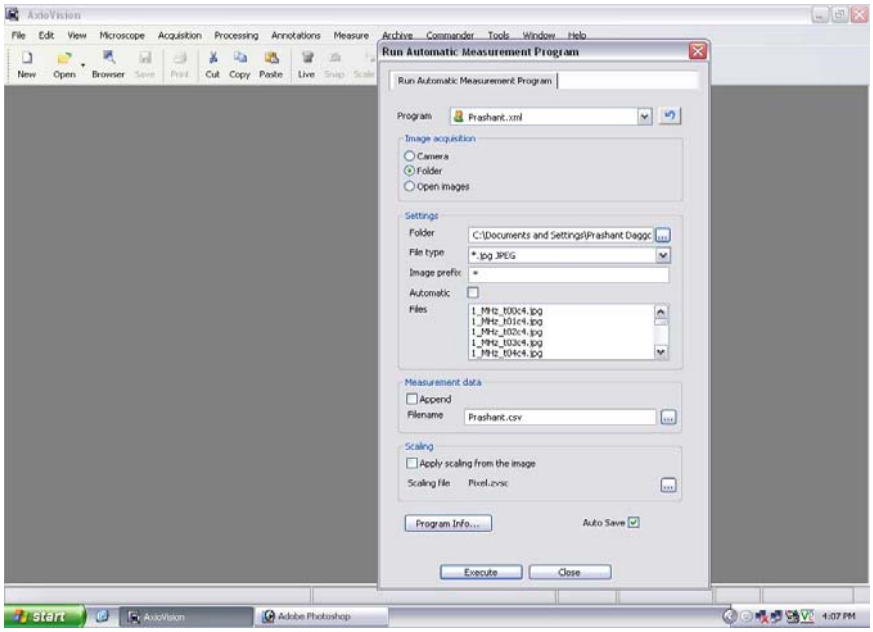

Figure C.1 Menu to choose the images to be analyzed on AXIOCAM 4.5

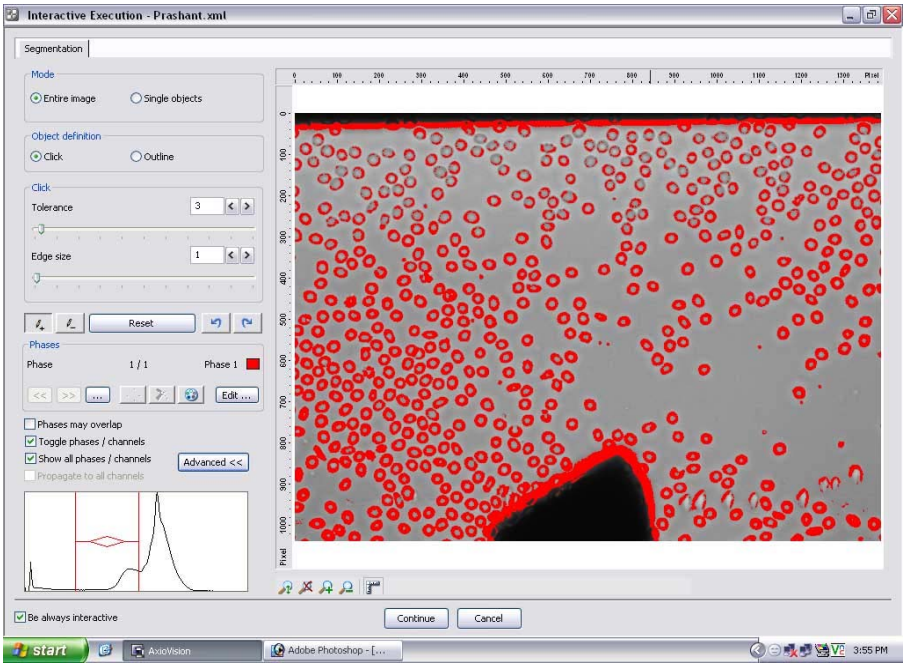

Figure C.2 Program automatically selects some cells based on the optical intensity difference between the cells and the background

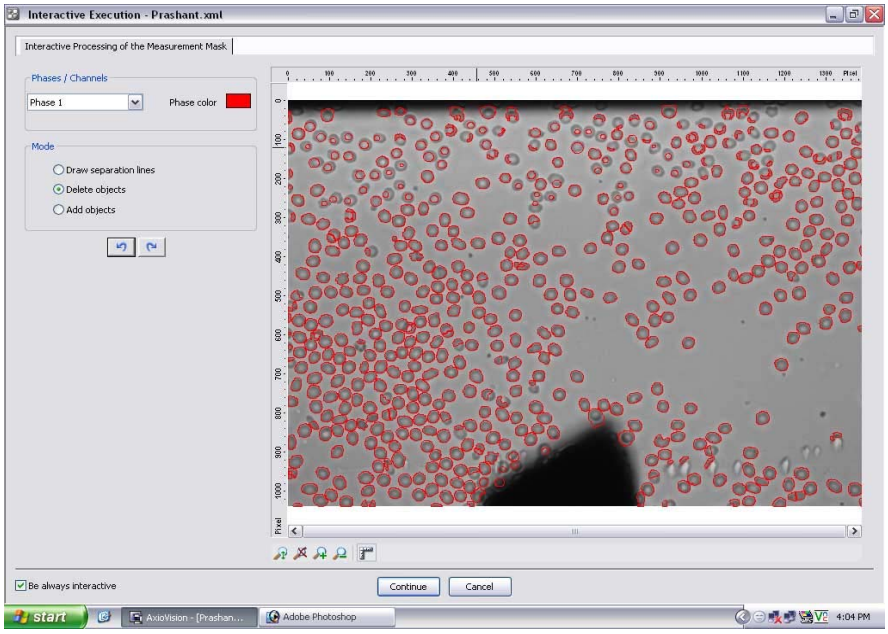

Figure C.3 Menu to edit the automatic cell selection made by the program

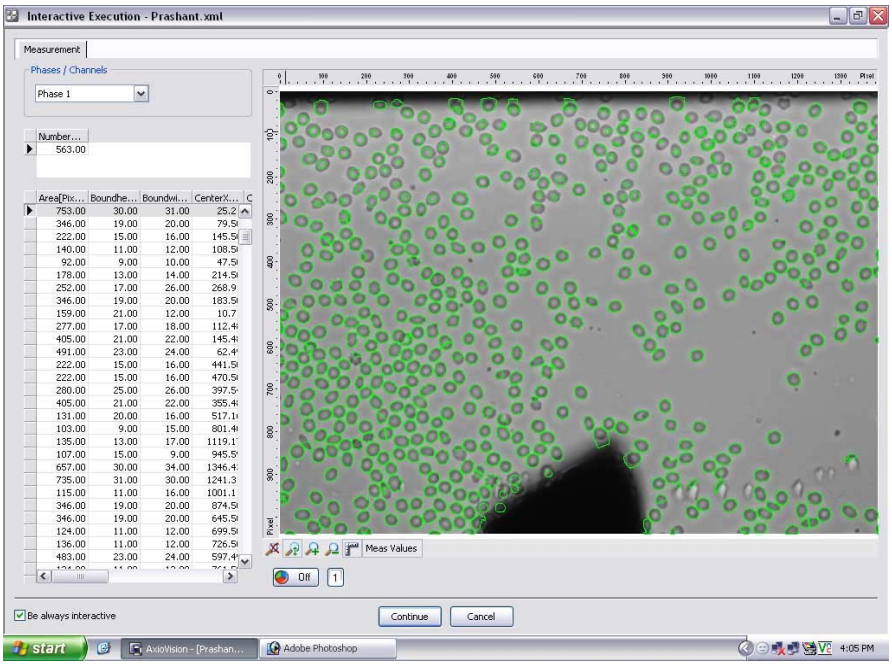

Figure C.4 Window showing the results of the image analysis

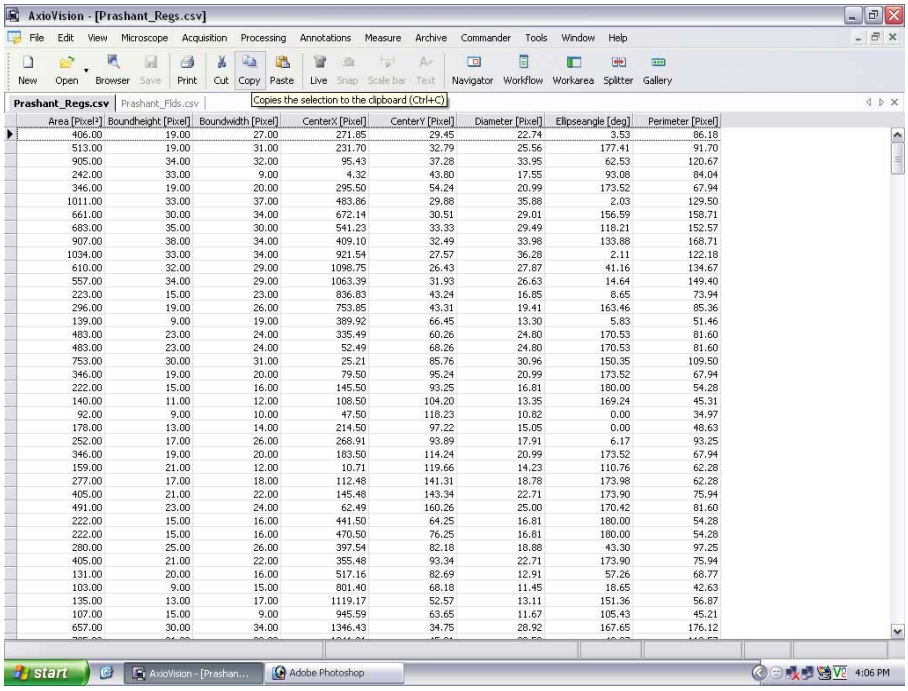

Figure C.5 Window showing the output of the analysis with X/Y position of the cells as a table

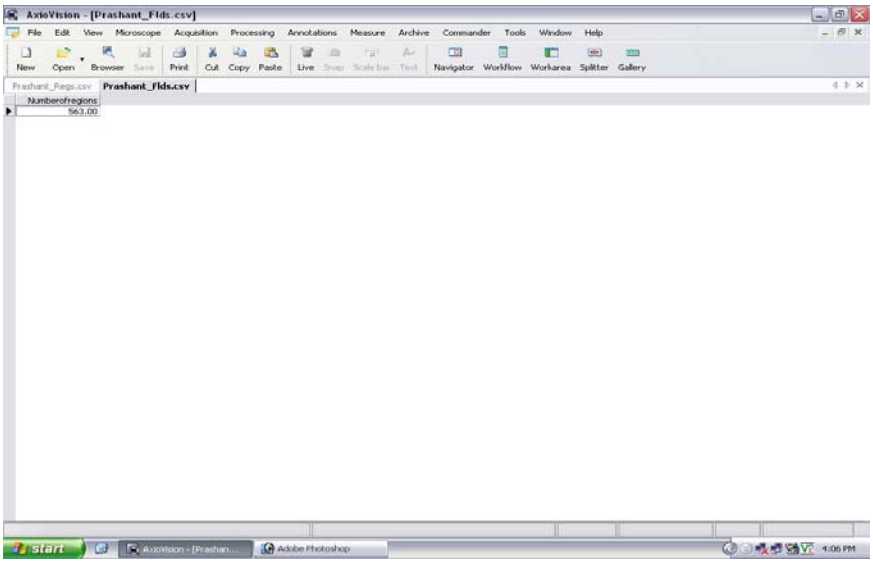

Figure C.6 Window showing the total number of cells on the image

APPENDIX D

MATLAB INPUT FILE FOR WEDGE ANALYSIS PROGRAM

The MATLAB program for wedge analysis requires a input file named ‘info. txt”. This file should contain the information about the geometry of the figure and they have to be in a specific order. The information to be provided is listed below in the required order.

- Origin (set to 0)
- Distance between the electrodes
- Length of the electrode tip
- Position of the tip electrode (left point)
- Position of the tip electrode (Right point)
- Position of the flat electrode (Left point)
- Position of the flat electrode (Right point)
- Resolution of the image (X)
- Resolution of the image (Y)
- Resolution of the cells. (X)
- Resolution of the cells. (X)

Sample file;

0,100,110,100,200,55,70,365,275,365,275

APPENDIX E

SYNOPSIS OF WEDGE ANALYSIS PROGRAM

E.1. Reading the data

```
clear;
% LOAD CELL DATA FROM DATA ANLYSIS
data= csvread('C:\Documents and Settings\All Users\Documents\Prashant\Data Anlysis\field dependency2\AB+\155microns120 seconds_Regs.csv',2,0);
% LOAD INFO FILE WITH WIDTH OF THE ELECTRODE, DIDTANCE BETWEEN THEM, RESOLUTION OF THE IMAGE ETC
inf= csvread('C:\Documents and Settings\Prashant Daggolu\Desktop\matlabresults\field dependency 2\AB+\155microns\info.txt',0,0);
ti='  AB POS - 155 MICRONS - 1 MHz  - 120 SEC'; % TITLE

cd('C:\Documents and Settings\Prashant Daggolu\Desktop\matlabresults\field dependency 2\AB+\155microns');

% LOAD CELL DATA FROM DATA ANLYSIS

% LOAD INFO FILE WITH WIDTH OF THE ELECTRODE, DISTANCE BETWEEN THEM, RESOLUTION OF THE IMAGE ETC

asw=12;
l=length(data);
y=data(1:l,5);
x=data(1:l,4);
% y=inf(11)-y;
x=inf(10)-x;
%CONVERT THE CELL DATA TO MICRONS
f1=inf(8)/inf(10);
f2=inf(9)/inf(11);
x=x*f1;
y=y*f2;

%MAX AND MIN Y AND X
ym=inf(9);
xm=inf(8);
xn=0;
yn=0;
% Y VALUES OF FLAT ELECTRODE
yl=ym-inf(6);
yr=ym-inf(7);
% x=xm-x;
ym=inf(9);
xm=inf(8);
yr=ym-inf(6);
```

```
yl=ym-inf(7);
```

E.2. Construction of the electrodes

```
je=xa+w;
js=je-100;
jm=(js+je)/2;
lx1=jm:20:xm;
lx2=jm:-20:-0.1;
lx2=fliplr(lx2);
ltx1=length(lx1);
ltx2=length(lx2);
ltx=ltx1+ltx2;
for i=1:ltx2
lx(i)=lx2(i);
i=i+1;
end;
j=2;
for i= (ltx2+1):(ltx-1)
lx(i)=lx1(j);
j=j+1;
i=i+1;
end;
ly=((lx-xn)*k)+yl;
alpha=figure;
line(a,b); % FLAT ELECTRODE
title(ti);
hold on;
plot(lx,ly,'+');
hold on;
rectangle('position',[xa 0 w h]);%TIP ELECTRODE
hold on;
```

E.3. Construction of wedge lines

```
plot(xa,tyl,'+');%POINTS ON TIP ELECTRODE
hold on;
plot(je,tyr,'+');
hold on;
plot(tx1,h,'+');
hold on;
plot(xv1,yv1,'d');%CUTOFF POINTS
hold on;
```

```
plot(xw1,yw1,'d');
hold on;
plot(xv2,yv2,'d');
hold on;
plot(xw2,yw2,'d');
hold on;
line(xo1,yo1);%HELP LINES TO DRAW CURVATURE
hold on;
line(xo2,yo2);
hold on;
line(xp1,yp1);
hold on;
line(xp2,yp2);
hold on;
plot(xlb,ylb,'+');%POINTS ON HELP LINE FOR DRAWING CURVATURE
hold on;
plot(xlt,ylt,'+');
hold on;
plot(xrb,yrb,'+');
hold on;
plot(xrt,yrt,'+');
hold on;
xlb=xlb';
ylb=ylb';
xlt=xlt';
ylt=ylt';

xrb=xrb';
yrb=yrb';
xrt=xrt';
yrt=yrt';

for i=1:lty1
xlb(2,i)=js;
i=i+1;
end;

for i=1:lty2
xrb(2,i)=je;
i=i+1;
end;

for i=1:lty1
ylb(2,i)=ty1(i,1);
```

```
i=i+1;
end;
ty2=fliplr(ty2);
for i=1:lty2
yrb(2,i)=ty2(1,i);
i=i+1;
end;

for i=1:lty1
xlt(2,i)=xlb(1,i);
i=i+1;
end;


for i=1:lty2
xrt(2,i)=xrb(1,i);
i=i+1;
end;

for i=1:lty1
ylt(2,i)=ylb(1,i);
i=i+1;
end;

for i=1:lty2
yrt(2,i)=yrb(1,i);
i=i+1;
end;

for i=1:lty1
xx(2,i)=xlt(1,i);
yy(2,i)=ylt(1,i);
i=i+1;
end;
line(xrt,yrt);
hold on;
llx=length(xx);
j=1;
lxrt=length(xrt);
k=lxrt;
for i=(del+1):llx
xx(2,i)=xrt(1,k);
yy(2,i)=yrt(1,k);
i=i+1;
```

```
j=j+1;
k=k-1;
end;

line(xlb,ylb);
hold on;
line(xlt,ylt);
hold on;
line(xx,yy);
hold on;
line (xrb,yrb);
hold on;
axis([0 xm 0 ym]);
```

E.4. Program to check the psotion of the cells in each wedge on left curvature

```
% ANALYSIS OF LEFT CURVATURE

j=1;
f=1;
for i=1:l %l is the total number of cells
if    (((y(i,1)-(slop(j,1)*x(i,1))-cmat(j,1))<0)&&((y(i,1)-(mlt*x(i,1))-clt)>0))||(((y(i,1)-
(mlt*x(i,1))-clt)<0)&&((y(i,1)-(mlt1(j,1)*x(i,1))-clt1(j,1))<0)&&((y(i,1)-
(mlb*x(i,1))-clb)>0))||(((y(i,1)-(mlb*x(i,1))-clb)<0)&&((y(i,1)-(mlb1(j,1)*x(i,1))-
clb1(j,1))<0))
count=count+1;% COUNT CELLS
xcell{1,j}(1,f)=x(i,1);
ycell{1,j}(1,f)=y(i,1);
f=f+1;
end;
i=i+1;
%       t=t+1;
end;

ncells(j,1)=count;
j=2;
count=0;
f=1;
for j=2:lty1 %lty1 is the number of lines which have curvature on the left
t=j-1;

for i=1:l %l is the total number of cells
```

```
if    (((y(i,1)-(slop(j,1)*x(i,1))-cmat(j,1))<0)&&((y(i,1)-(mlt*x(i,1))-clt)>0))||(((y(i,1)-
(mlt*x(i,1))-clt)<0)&&((y(i,1)-(mlt1(j,1)*x(i,1))-clt1(j,1))<0)&&((y(i,1)-
(mlb*x(i,1))-clb)>0))||(((y(i,1)-(mlb*x(i,1))-clb)<0)&&((y(i,1)-(mlb1(j,1)*x(i,1))-
clb1(j,1))<0))
if x(i,1)<js
if    (((y(i,1)-(slop(t,1)*x(i,1))-cmat(t,1))>0)&&((y(i,1)-(mlt*x(i,1))-clt)>0))||(((y(i,1)-
(mlt*x(i,1))-clt)<0)&&((y(i,1)-(mlt1(t,1)*x(i,1))-clt1(t,1))>0)&&((y(i,1)-
(mlb*x(i,1))-clb)>0))||(((y(i,1)-(mlb*x(i,1))-clb)<0)&&((y(i,1)-(mlb1(t,1)*x(i,1))-
clb1(t,1))>0))
count=count+1;% COUNT CELLS
xcell{1,j}(1,f)=x(i,1);
ycell{1,j}(1,f)=y(i,1);
f=f+1;
end;
end;
end;

i=i+1;
end;


ncells(j,1)=count;%CELLS OF ONLY THE WEDGE
sum=count;
count=0;
%  xc1{1,j}=xcell{1,j}(1,find(xcell{1,j}>0));
%  yc1{1,j}=ycell{1,j}(1,find(ycell{1,j}>0));
j=j+1;
f=1;
end;
```

E.5. Making plots

```
avcells=avcells';
avcells1=avcells1';
mav=mean(avcells1);
mapx(1,1)=0;
mapy(1,1)=mav;
mapx(2,1)=lnc+2;
mapy(2,1)=mav;
scncel1=scncel';

beta=figure;
title(ti);
```

```
ylabel ('NUMBER OF CELLS');
xlabel ('WEDGE NUMBER');


line(u2,ncells,'Marker','o','MarkerFaceColor','r');

annotation1 = annotation(...
'textbox',...
'Position',[0.125 0.2 0.29 0.1],...
'FitHeightToText','on',...
'LineStyle','none',...
'String',{'The average horizontal spread of the cells','from the left of mildfield
is',horavl,'microns out of',jm,'microns'});

annotation2 = annotation(...
'textbox',...
'Position',[0.65 0.2 0.29 0.1],...
'FitHeightToText','on',...
'LineStyle','none',...
'String',{'The average horizontal spread of the cells','from the right of mildfield
is',horavr,'microns out of',(xm-jm),'microns'});

gamma=figure;
line(u2,scncel1,'Marker','d','MarkerFaceColor','r');
mscn=max(scncel1);
mcn=ceil(mscn);
if mcn==1
mcn=2;
end;
axis([0 (lnc+2) 0 mcn]);
title(ti);
ylabel ('NORMALIZED NUMBER OF CELLS');
xlabel ('WEDGE NUMBER');


delta=figure;
plot(u1,avcells1,'o','MarkerFaceColor','r','LineStyle','--');
title(ti)
line(mapx,mapy,'LineStyle','-');
annotation1 = annotation(...
'textbox',...
'Position',[0.1396 0.3364 0.122 0.07129],...
```

```
'String',{'Mean=',mav},...
'LineStyle','none',...
'FitHeightToText','on');
ylabel ('AVERAGE VERTICAL SPACING OF CELLS');
xlabel ('WEDGE NUMBER');
axis([0 (lnc+2) 0 1]);

if asw==0

ncells1=ncells';
%     cd(cdw);
%     path(pw);
csvwrite('ncells0.csv',ncells1);
end;
```

APPENDIX F

MATLAB PROGRAM MAKING LEAST SQUARES FIT FOR FIELD DEPENDENCY TESTS

```
clear;
% LOAD CELL DATA FROM DATA ANLYSIS
data= xlsread('C:\Documents and Settings\All Users\Documents\Prashant\Data
Anlysis\field_data.xls');
dist_A=data(:,2);
dist_B=data(:,9);
dist_AB=data(:,16);
dist_O=data(:,23);
fs_A=data(:,3);
fs_B=data(:,10);
fs_AB=data(:,17);
fs_O=data(:,24);
avm_A=data(:,4);
avm_B=data(:,11);
avm_AB=data(:,18);
avm_O=data(:,25);
mfhm_A=data(:,5);
mfhm_B=data(:,12);
mfhm_AB=data(:,19);
mfhm_O=data(:,26);
mnhm_A=data(:,6);
mnhm_B=data(:,13);
mnhm_AB=data(:,20);
mnhm_O=data(:,27);
ls_AVM_A=polyfit(fs_A,avm_A,2);
ls_AVM_B=polyfit(fs_B,avm_B,2);
ls_AVM_AB=polyfit(fs_AB,avm_AB,2);
ls_AVM_O=polyfit(fs_O,avm_O,2);
ls_MFHM_A=polyfit(fs_A,mfhm_A,2);
ls_MFHM_B=polyfit(fs_B,mfhm_B,2);
ls_MFHM_AB=polyfit(fs_AB,mfhm_AB,2);
ls_MFHM_O=polyfit(fs_O,mfhm_O,2);
ls_MNHM_A=polyfit(fs_A,mnhm_A,2);
ls_MNHM_B=polyfit(fs_B,mnhm_B,2);
ls_MNHM_AB=polyfit(fs_AB,mnhm_AB,2);
ls_MNHM_O=polyfit(fs_O,mnhm_O,2);
coeff(1,:)=ls_AVM_A;
coeff(2,:)=ls_AVM_B;
coeff(3,:)=ls_AVM_AB;
coeff(4,:)=ls_AVM_O;
coeff(5,:)=ls_MFHM_A;
coeff(6,:)=ls_MFHM_B;
coeff(7,:)=ls_MFHM_AB;
coeff(8,:)=ls_MFHM_O;
```

```
coeff(9,:)=ls_MNHM_A;
coeff(10,:)=ls_MNHM_B;
coeff(11,:)=ls_MNHM_AB;
coeff(12,:)=ls_MNHM_O;



sfs_A=sort(fs_A);
sfs_B=sort(fs_B);
sfs_AB=sort(fs_AB);
sfs_O=sort(fs_O);
fc_AVM_A=polyval(ls_AVM_A,sfs_A);
fc_AVM_B=polyval(ls_AVM_B,sfs_B);
fc_AVM_AB=polyval(ls_AVM_AB,sfs_AB);
fc_AVM_O=polyval(ls_AVM_O,sfs_O);
fc_MFHM_A=polyval(ls_MFHM_A,sfs_A);
fc_MFHM_B=polyval(ls_MFHM_B,sfs_B);
fc_MFHM_AB=polyval(ls_MFHM_AB,sfs_AB);
fc_MFHM_O=polyval(ls_MFHM_O,sfs_O);
fc_MNHM_A=polyval(ls_MNHM_A,sfs_A);
fc_MNHM_B=polyval(ls_MNHM_B,sfs_B);
fc_MNHM_AB=polyval(ls_MNHM_AB,sfs_AB);
fc_MNHM_O=polyval(ls_MNHM_O,sfs_O);
alpha =figure;
ylabel ('AVM');
xlabel ('FIELD STRENGTH (VOLT/MICRON)');
axis ([0.02 0.08 0.35 0.75]);
hold on;
subplot(2,2,1);
plot(fs_A,avm_A,'o');
line(sfs_A,fc_AVM_A);
axis ([0.02 0.08 0.35 0.75]);
legend ('A+','LS-A+',1);
ylabel ('AVM');
xlabel ('FIELD STRENGTH (VOLT/MICRON)');
hold on;
subplot(2,2,2);
plot(fs_B,avm_B,'+');
line(sfs_B,fc_AVM_B,'LineStyle', '--');
axis ([0.02 0.08 0.35 0.75]);
legend ('B+','LS-B+',1);
ylabel ('AVM');
xlabel ('FIELD STRENGTH (VOLT/MICRON)');
hold on;
```

```
subplot(2,2,3);
plot(fs_AB,avm_AB,'*');
line(sfs_AB,fc_AVM_AB,'LineStyle',':');
axis ([0.02 0.08 0.35 0.75]);
legend ('AB+','LS-AB+',1);
ylabel ('AVM');
xlabel ('FIELD STRENGTH (VOLT/MICRON)');
hold on;
subplot(2,2,4);
plot(fs_O,avm_O,'X');
line(sfs_O,fc_AVM_O,'LineStyle','-.');
axis ([0.02 0.08 0.35 0.75]);
legend ('O+','LS-O+',1);
ylabel ('AVM');
xlabel ('FIELD STRENGTH (VOLT/MICRON)');
hold on;
% h=legend('A+','B+','AB+','O+','LS_A+','LS_B+','LS_AB+','LS_O+',2);
beta=figure;
ylabel ('MFHM');
xlabel ('FIELD STRENGTH (VOLT/MICRON)');
axis ([0.02 0.08 0.45 0.9]);
hold on;
subplot(2,2,1);
plot(fs_A,mfhm_A,'o');
line(sfs_A,fc_MFHM_A);
axis ([0.02 0.08 0.45 0.9]);
legend ('A+','LS-A+',1);
ylabel ('MFHM');
xlabel ('FIELD STRENGTH (VOLT/MICRON)');
hold on;
subplot(2,2,2);
plot(fs_B,mfhm_B,'+');
line(sfs_B,fc_MFHM_B,'LineStyle', '--');
axis ([0.02 0.08 0.45 0.9]);
legend ('B+','LS-B+',1);
ylabel ('MFHM');
xlabel ('FIELD STRENGTH (VOLT/MICRON)');
hold on;
subplot(2,2,3);
plot(fs_AB,mfhm_AB,'*');
line(sfs_AB,fc_MFHM_AB,'LineStyle',':');
axis ([0.02 0.08 0.45 0.9]);
legend ('AB+','LS-AB+',1);
ylabel ('MFHM');
```

```
xlabel ('FIELD STRENGTH (VOLT/MICRON)');
hold on;
subplot(2,2,4);
plot(fs_O,mfhm_O,'X');
line(sfs_O,fc_MFHM_O,'LineStyle','-.');
axis ([0.02 0.08 0.45 0.9]);
legend ('O+','LS-O+',1);
ylabel ('MFHM');
xlabel ('FIELD STRENGTH (VOLT/MICRON)');
hold on;
% h=legend('A+','B+','AB+','O+','LS_A+','LS_B+','LS_AB+','LS_O+',2);
gamma=figure;
ylabel ('MNHM');
xlabel ('FIELD STRENGTH (VOLT/MICRON)');
axis ([0.02 0.08 0.9 1.8]);
hold on;
subplot(2,2,1);
plot(fs_A,mnhm_A,'o');
line(sfs_A,fc_MNHM_A);
axis ([0.02 0.08 0.9 1.8]);
legend ('A+','LS-A+',1);
ylabel ('MNHM');
xlabel ('FIELD STRENGTH (VOLT/MICRON)');
hold on;
subplot(2,2,2);
plot(fs_B,mnhm_B,'+');
line(sfs_B,fc_MNHM_B,'LineStyle', '--');
axis ([0.02 0.08 0.9 1.8]);
legend ('B+','LS-B+',1);
ylabel ('MNHM');
xlabel ('FIELD STRENGTH (VOLT/MICRON)');
hold on;
subplot(2,2,3);
plot(fs_AB,mnhm_AB,'*');
line(sfs_AB,fc_MNHM_AB,'LineStyle',':');
axis ([0.02 0.08 0.9 1.8]);
legend ('AB+','LS-AB+',1);
ylabel ('MNHM');
xlabel ('FIELD STRENGTH (VOLT/MICRON)');
hold on;
subplot(2,2,4);
plot(fs_O,mnhm_O,'X');
line(sfs_O,fc_MNHM_O,'LineStyle','-.');
axis ([0.02 0.08 0.9 1.8]);
```

```
legend ('O+','LS-O+',1);
ylabel ('MNHM');
xlabel ('FIELD STRENGTH (VOLT/MICRON)');
hold on;
% h=legend('A+','B+','AB+','O+','LS_A+','LS_B+','LS_AB+','LS_O+',2);
xlswrite ('C:\Documents and Settings\Prashant Daggolu\Desktop\matlabresults\ls_coeff.xls',coeff);
```

APPENDIX G

BLOOD TYPING DATA

The following tables show the actual results of blood typing data for each blood type. The first table below shows data of Average vertical movement for each blood time for corresponding times.

Table G.1. Average Vertical Movement (AVM) data with standard errors (SE) for positive ABO blood types at 5 different time points

	A+		B+		AB+		O+	
Time (sec)	AVM	SE	AVM	SE	AVM	SE	AVM	SE
0	0.4883	0.0106	0.4799	0.0096	0.5032	0.0077	0.4853	0.0057
30	0.5628	0.0107	0.5358	0.0117	0.5549	0.0077	0.5065	0.0062
60	0.5948	0.0096	0.5504	0.0134	0.5686	0.0059	0.5074	0.0043
90	0.5513	0.0081	0.5495	0.0145	0.5699	0.0033	0.5207	0.0030
120	0.5560	0.0079	0.5594	0.0120	0.5739	0.0035	0.5268	0.0040

Table G.2. Mean Fractional Horizontal movement (MFHM) data with standard errors (SE) for positive ABO blood types at 5 different time points

	A+		B+		AB+		O+	
Time (sec)	MFHM	SE	MFHM	SE	MFHM	SE	MFHM	SE
0	0.5377	0.0084	0.5236	0.0042	0.5256	0.0086	0.5334	0.0039
30	0.5909	0.0102	0.5829	0.0081	0.5721	0.0079	0.5571	0.0036
60	0.6240	0.0170	0.6200	0.0131	0.6076	0.0133	0.5792	0.0045
90	0.6421	0.0204	0.6536	0.0177	0.6156	0.0135	0.5997	0.0055
120	0.6429	0.0206	0.6573	0.0168	0.6355	0.0159	0.6161	0.0052

Table G.3. Mean Normalized Horizontal Movement (MNHM) data with standard errors (SE) for positive ABO blood types at 5 different time points

	A+		B+		AB+		O+	
Time (sec)	MNHM	SE	MNHM	SE	MNHM	SE	MNHM	SE
0	1.0000	0.0000	1.0000	0.0000	1.0000	0.0000	1.0000	0.0000
30	1.1061	0.0263	1.1131	0.0111	1.0953	0.0218	1.0450	0.0049
60	1.1734	0.0436	1.1841	0.0221	1.1686	0.0382	1.0869	0.0094
90	1.2082	0.0501	1.2476	0.0303	1.1836	0.0365	1.1254	0.0108
120	1.2097	0.0504	1.2538	0.0272	1.2212	0.0407	1.1568	0.0125

APPENDIX H

FREQUENCY DEPENDENCY DATA

Table H.1 Average Vertical Movement (AVM) data with standard errors (SE) for positive ABO blood types at 6 different frequencies

Frequency	A+		B+		AB+		O+	
MHz	AVM	SE	AVM	SE	AVM	SE	AVM	SE
0.5	0.594942	0.023184	0.603396	0.027289	0.572942	0.01093	0.578857	0.007097
1	0.615891	0.025699	0.583161	0.032864	0.548904	0.008107	0.570403	0.007845
2	0.575455	0.021095	0.63305	0.024199	0.559209	0.005348	0.557001	0.024669
3	0.553894	0.019402	0.504734	0.016562	0.545526	0.001611	0.542418	0.014952
4	0.516481	0.011659	0.529222	0.00367	0.538424	0.008648	0.582056	0.030527
5	0.540257	0.021216	0.540859	0.004042	0.529603	0.008033	0.553988	0.013163

Table H.2 Mean Fractional Horizontal Movement (MFHM) data with standard errors (SE) for positive ABO blood types at6 different frequencies.

Frequency	A+		B+		AB+		O+	
MHz	MFHM	SE	MFHM	SE	MFHM	SE	MFHM	SE
0.5	0.624321	0.012982	0.583409	0.012856	0.633678	0.005153	0.647175	0.016357
1	0.627048	0.014427	0.595951	0.010756	0.642591	0.006592	0.636969	0.018555
2	0.59649	0.017949	0.572238	0.013202	0.6345	0.002767	0.649453	0.008222
3	0.660898	0.032613	0.563353	0.017587	0.622014	0.003622	0.653863	0.01043
4	0.602734	0.019803	0.57958	0.02164	0.60011	0.007368	0.634901	0.005723
5	0.597574	0.017878	0.591066	0.016789	0.589853	0.003956	0.603898	0.018775

Table H.3 Mean Normalized Horizontal Movement (MNHM) data with standard errors (SE) for positive ABO blood types at 6 different frequencies.

Frequency	A+		B+		AB+		O+	
MHz	MNHM	SE	MNHM	SE	MNHM	SE	MNHM	SE
0.5	1.222125	0.014149	1.167708	0.03396	1.179262	0.037942	1.289082	0.019199
1	1.217203	0.017014	1.094291	0.034495	1.180591	0.038	1.084485	0.078552
2	1.144362	0.021803	1.095857	0.025764	1.174267	0.036729	1.270418	0.036135
3	1.244569	0.038012	1.126516	0.038702	1.161261	0.030202	1.281859	0.027835
4	1.169237	0.030991	1.10275	0.041624	1.128628	0.045264	1.1825	0.012567
5	1.116319	0.027971	1.121439	0.035664	1.14396	0.029009	1.143444	0.025775

APPENDIX I

FIELD DEPENDENCY DATA

Table I.1 Average Vertical Movement (AVM), Mean Fractional Horizontal Movement (MFHM) and Mean Normalized Horizontal Movement (MNHM) data for A+ blood type at different field strengths.

SET	Distance	Field	AVM	MFHM	MNHM
#	Microns	V/micron			
1	95	0.0632	0.4918	0.7744	1.2658
1	120	0.0500	0.4705	0.7483	1.2694
1	175	0.0343	0.4877	0.7276	1.3118
1	190	0.0316	0.5427	0.6403	1.2777
1	205	0.0293	0.6004	0.5717	1.0767
2	80	0.0750	0.4584	0.7853	1.5017
2	120	0.0500	0.5197	0.7648	1.6003
2	165	0.0364	0.5660	0.7214	1.3629
2	180	0.0333	0.5627	0.6503	1.3261
2	220	0.0273	0.5644	0.5777	1.1627
3	100	0.0600	0.4826	0.7973	1.5962
3	125	0.0480	0.5956	0.8034	1.4164
3	150	0.0400	0.6154	0.6891	1.2888
3	185	0.0324	0.6257	0.6864	1.3257
3	210	0.0286	0.5473	0.6285	1.0775

Table I.2 Average Vertical Movement (AVM), Mean Fractional Horizontal Movement (MFHM) and Mean Normalized Horizontal Movement (MNHM) data for B+ blood type at different field strengths.

SET	Distance	Field	**AVM**	**MFHM**	**MNHM**
#	Microns	V/micron			
1	90	0.0667	0.5231	0.7649	1.1839
1	120	0.0500	0.5047	0.7709	1.2490
1	150	0.0400	0.4737	0.7433	1.3373
1	190	0.0316	0.5685	0.6742	1.2091
1	210	0.0286	0.4778	0.5610	1.0991
2	100	0.0600	0.4093	0.5192	1.0499
2	120	0.0500	0.6494	0.7155	1.3425
2	140	0.0429	0.6856	0.6103	1.0735
2	175	0.0343	0.5849	0.6493	1.1563
2	225	0.0267	0.5434	0.5834	1.1830
3	90	0.0667	0.4868	0.7800	1.4084
3	125	0.0480	0.5811	0.7961	1.5634
3	160	0.0375	0.5117	0.7132	1.3541
3	170	0.0353	0.5912	0.7174	1.3643
3	225	0.0267	0.5340	0.5894	1.1422

Table I.3 Average Vertical Movement (AVM), Mean Fractional Horizontal Movement (MFHM) and Mean Normalized Horizontal Movement (MNHM) data for AB+ blood type at different field strengths.

SET	Distance	Field	AVM	MFHM	MNHM
#	Microns	V/micron			
1	80	0.0750	0.6350	0.7437	1.3189
1	120	0.0500	0.4110	0.7773	1.4875
1	140	0.0429	0.5192	0.8078	1.5211
1	170	0.0353	0.5805	0.7263	1.3731
1	190	0.0316	0.5582	0.6526	1.3158
2	100	0.0600	0.4864	0.7419	1.3480
2	140	0.0429	0.5982	0.7012	1.3210
2	145	0.0414	0.5485	0.6067	1.0122
2	155	0.0387	0.4962	0.6543	1.1119
2	195	0.0308	0.5620	0.6054	1.1088
3	100	0.0600	0.4335	0.7336	1.3756
3	135	0.0444	0.5136	0.7199	1.3010
3	145	0.0414	0.5348	0.7073	1.2183
3	155	0.0387	0.5202	0.6516	1.1468
3	190	0.0316	0.5487	0.6280	1.1514

Table I.4 Average Vertical Movement (AVM), Mean Fractional Horizontal Movement (MFHM) and Mean Normalized Horizontal Movement (MNHM) data for O+ blood type at different field strengths.

SET	Distance	Field	**AVM**	**MFHM**	**MNHM**
#	Microns	V/micron			
1	100	0.0600	0.4644	0.7575	1.3102
1	110	0.0545	0.5342	0.6874	1.2295
1	150	0.0400	0.4603	0.6057	1.1625
1	190	0.0316	0.4983	0.6240	1.1983
1	220	0.0273	0.5728	0.5649	1.0478
2	100	0.0600	0.5520	0.8223	1.4551
2	125	0.0480	0.5265	0.8356	1.6300
2	155	0.0387	0.5321	0.6951	1.4461
2	170	0.0353	0.5688	0.5605	1.1480
2	225	0.0267	0.5357	0.5419	1.0778
3	95	0.0632	0.4373	0.7729	1.4182
3	135	0.0444	0.5915	0.7639	1.3672
3	150	0.0400	0.5402	0.6374	1.1495
3	175	0.0343	0.5350	0.6046	1.0903
3	215	0.0279	0.5173	0.5581	1.0357

APPENDIX J

MICRODEVICE FABRICATION SPECIFICATIONS

1. Dimensions of the microdevice:

   Length = 46 mm

   Width =15 mm (not including the projections for current connection)

   =25 mm (including the projections for current connection)

   Depth = 1 mm (glass cover) + depth of the wafer

2. Dimensions of the chamber for experiments:

   Length = 14 mm (not including the triangular region for initial flow)

   =28 mm (including the triangular region on either end of the rectangular chamber)

   Width = 7 mm

Depth = 50 microns

3. Length of the triangular region on either end of the rectangular chamber is 4 mm from the end of the sample port to the rectangle.

4. Sample ports

   Diameter =3mm

Depth = depth of the silica wafer

5. Distance between the sample ports from centre to centre =25 mm

6. Electrode tips

   Length = 6. 625 mm

   Width = 100 microns

   Depth = 50 microns

   Distance between two adjacent electrode tips = base is175 microns

Distance between the electrode tip and the flat electrode =3500 microns

7. . Electrode base

   Length = 14 mm

   Width = 100 microns

   Depth = 50 microns

   Distance between the two electrode bases = 6.800 mm

8. Metal connector to the electrode projection

   Length = 7mm

   Width = 200 microns

   Depth = 50microns

9. Electrode projection outside the device so as to connect the alligator clips

   Length = 5mm

   Width = 5mm

   Depth =4 mm

APPENDIX K

PERCENTAGE CHANGE OF TOTAL NUMBER OF CELLS

Table K.1 Percentage change of total number of cells compared to time 0 seconds for A+ blood type.

A+		% Change in number of cells from time 0					
Day	Set	Time					
		20	30	50	60	90	120
0	1	93.46	95.79	91.59	94.39	88.32	92.52
0	2	90.65	81.29	76.98	76.98	76.26	74.10
2	1	100.90	87.00	94.17	75.78	75.34	73.99
2	2	97.88	106.71	75.62	75.62	51.59	37.28
5	1	89.89	81.91	82.45	77.66	68.09	59.04
5	2	87.74	86.78	81.03	81.99	76.63	73.75
	AVERAGE	82.93	81.36	78.83	77.49	75.17	75.81

Table K.2 Percentage change of total number of cells compared to time 0 seconds for B+ blood type.

B+	% Change in number of cells from time 0						
Day	Set	Time					
		20	30	50	60	90	120
0	1	90.09	88.74	87.84	91.44	84.68	89.64
0	2	97.12	90.19	86.92	81.54	73.65	58.46
2	1	100.00	93.55	98.39	92.74	94.35	94.35
2	2	91.45	82.89	61.18	45.23	32.57	25.00
5	1	94.57	92.93	87.14	86.23	79.89	70.83
5	2	90.32	89.86	79.95	80.41	82.88	78.15
	AVERAGE	83.36	81.17	78.77	76.80	76.86	76.63

Table K.3 Percentage change of total number of cells compared to time 0 seconds for AB+ blood type.

AB+	% Change in number of cells from time 0						
Day	Set	Time					
		20	30	50	60	90	120
0	1	99.43	96.97	96.97	93.56	93.18	91.29
0	2	98.25	95.75	93.00	93.75	92.00	89.50
2	1	98.82	98.43	94.90	99.61	96.86	93.33
2	2	86.11	86.11	76.85	76.30	66.11	57.96
5	1	89.78	96.00	92.00	96.44	97.33	93.78
5	2	91.12	87.05	72.20	59.24	49.64	47.45
	AVERAGE	83.36	84.33	82.27	82.70	83.59	84.76

Table K.4 Percentage change of total number of cells compared to time 0 seconds for O+ blood type.

O+	% Change in number of cells from time 0						
Day	Set	Time					
		20	30	50	60	90	120
0	1	96.62577	96.01227	91.10429	89.57055	90.18405	90.4908
0	2	86.37771	87.9257	93.49845	89.78328	92.87926	91.95046
2	1	93.6019	92.41706	68.00948	93.6019	90.52133	92.65403
2	2	96.54255	96.2766	91.75532	99.46809	95.47872	98.93617
5	1	94.88889	93.77778	84.44444	91.77778	91.33333	89.77778
5	2	92.74924	83.83686	77.34139	75.98187	77.6435	72.65861
	AVERAGE	82.97	82.89	79.45	85.74	89.72	93.78